A novel approach for the suppression of photorespiration in C_3 plants by gene transfer

Von der Fakultät für Mathematik, Informatik und Naturwissenschaften
der Rheinisch-Westfälischen Technischen Hochschule Aachen
zur Erlangung des akademischen Grades eines Doktors der Naturwissenschaften
genehmigte Dissertation

von

Md. Rafijul Bari, MSc

aus

Faridpur, Bangladesch

Berichter:

Univ.-Prof. Dr. Fritz Kreuzaler

Univ.-Prof. Dr. Ursula B. Priefer

Tag der mündlichen Prüfung: 20.04.2004

Part of this thesis is currently published:

Bari, R., Kebeish, R., Kalamajka, R., Rademacher, T., and Peterhänsel, C. (2004). A glycolate dehydrogenase in the mitochondria of *Arabidopsis thaliana*. Journal of Experimental Botany, *in press*, DOI: 10.1093/jxb/erh079

SUMMARY

In the present study, a novel principle is proposed to increase the CO_2 concentration in the vicinity of Rubisco thereby suppressing photorespiration in C_3 plants. The pathway is derived from *E. coli* and converts the glycolate formed during photorespiration into glycerate. Three enzymatic activities are required: Glycolate dehydrogenase (GDH), Glyoxylate carboligase (GCL), and Tratronic semialdehyde reductase (TSR).

In order to establish the pathway in the chloroplast of tobacco (*Nicotiana tabacum*), all necessary genes were cloned in both prokaryotic and plant expression vectors in N-terminal translational fusion to a His-tag. The genes were first expressed in bacteria and the enzymatic activity of the constructs was shown. Transgenic tobacco plants were created containing all genes necessary for the proposed pathway by plastdial as well as nuclear transformation. Plastidial transformation was done by constructing a single polycistronic operon with five open reading frames. Nuclear transformation was performed by *Agrobacterium*-mediated transformation of single or double constructs.

Plastid transformants were checked by southern blot analysis. Many transgenic plants with a variable size of shortened transgenic sequences were detected. Moreover, many of the transgenic plants also displayed drastic chlorosis and stunted growth. However, few plants showed integration of the complete operon and the next generation of those plants is currently analysed.

Initially, transgenic plants containing TSR and GCL were created by nuclear transformation due to the lack of a suitable glycolate oxidising enzyme. Variable amounts of foreign proteins were detected in Western blots. Enzymatic assays showed that the proteins are active in *planta*. However transgenic plants containing GCL protein again showed a chlorotic phenotype.

A putative open reading frame was identified in the *Arabidopsis* genome sequence with homology to glycolate-oxidizing enzymes. The open reading frame was cloned and expressed in bacteria. Enzymatic assays and complementation tests showed that the protein is indeed a glycolate dehydrogenase. The gene is preferentially expressed in illuminated leaves and the enzyme is located inside the mitochondria. This protein forms an optimised starting point for the completion of the proposed pathway.

TABLE OF CONTENTS

1 INTRODUCTION.

1.1 Photosynthesis.

Photosynthesis is a process that converts the energy of sunlight into a chemical form of energy that can be used by biological systems. All the food we eat and all the fossil fuel we use is a product of photosynthesis. Photosynthesis also releases oxygen, which is the main source of atmospheric oxygen. Photosynthesis is often described as the most important chemical reaction on earth; it provides green plants with their complete energy requirement and most other living organisms obtain their own nutrients from these plants, either directly or indirectly. Photosynthesis is carried out by many different organisms, ranging from plants to bacteria. The best known form of photosynthesis is the one carried out by higher plants and algae, as well as by cyanobacteria and their relatives. Green plants, as the majority of autotrophic organisms, acquire their most abundant elements in leaves (C and O) by consuming H_2O and excessive atmospheric CO_2, while replenishing atmospheric O_2 during photosynthesis (Edwards and Walker, 1983). All these organisms convert CO_2 to organic material by reducing this gas to carbohydrates in a rather complex set of reactions. Electrons for this reduction reaction ultimately come from water, which is then converted to oxygen and protons. Energy for this process is provided by light, which is absorbed by pigments (primarily chlorophylls and carotenoids). Chlorophylls absorb blue and red light and carotenoids absorb blue-green light, but green and yellow light are not effectively absorbed by photosynthetic pigments in plants; therefore, light of these colors is either reflected by leaves or passes through the leaves.

Photosynthesis is composed of three stages: the primary photochemical reaction, the electron transport and photophosphorylation, and the CO_2 assimilation (Hoober, 1984). First, plants and cyanobacteria capture the light of the sun and utilize its energy to synthesize organic compounds from inorganic substances, such as CO_2, nitrate and sulfate, to make their cellular material. In photosynthesis photon energy splits water into oxygen and hydrogen, the latter bound as NADPH (Heldt, 1997). This process takes place in the photosynthetic reaction centres embedded in membranes. It involves the transport of electrons which is coupled to the synthesis of ATP. NADPH and ATP are consumed in CO_2 assimilation.

For higher plants, three biochemical pathways - the C_3 pathway (Calvin cycle), the C_4 pathway (Hatch-Slack pathway) and the crassulacean acid metabolism (CAM) - are involved in CO_2 assimilation.

1.1.1 C_3 photosynthetic pathway.

More than 95% of the terrestrial plants, including major crops such as wheat and rice, assimilate CO_2 exclusively by the C_3 pathway and thus are known as "C_3 plants" (Ku *et al*., 1996). Figure 1.1 represents the CO_2 assimilation pathway in C_3 plants which is known as the Calvin cycle. The Calvin cycle can be subdivided into three sections (Heldt, 1997). First, a molecule of CO_2 reacts with a five-carbon compound called ribulose bisphosphate (RuBP) producing an unstable six-carbon intermediate that immediately breaks down into two molecules of the three-carbon compound phosphoglycerate (PGA). The carbon that was a part of inorganic CO_2 is now part of the carbon skeleton of an organic molecule. The enzyme for this reaction is ribulose bisphosphate carboxylase/oxygenase (Rubisco, EC 4.1.1.39). A total of six molecules of CO_2 must be fixed this way in order to produce one molecule of the six-carbon sugar glucose.

Second, the energy from ATP and the reducing power of NADPH (both produced during the light-dependent reactions) is used to convert PGA to glyceraldehyde-3-phosphate (G3P), another three-carbon compound. For every six molecules of CO_2 that enter the Calvin cycle, two molecules of G3P are produced. Most of the G3P produced during the Calvin cycle is used to regenerate RuBP, thus permitting the cycle to continue. Some of the molecules of G3P, however, are used to synthesize glucose and other organic molecules. Two molecules of the three-carbon G3P can be used to synthesize one molecule of the six-carbon sugar glucose. The G3P is also used to synthesize the other organic molecules required by photoautotrophs.

Third, as mentioned in the previous step, most of the G3P produced during the Calvin cycle are used to regenerate the RuBP so that the cycle may continue. Ten molecules of the three-carbon compound G3P eventually form six molecules of the five-carbon compound ribulose phosphate (RP). Each molecule of ribulose phosphate then becomes phosphorylated by the hydrolysis of ATP to produce ribulose bisphosphate (RuBP), the starting compound for the Calvin cycle.

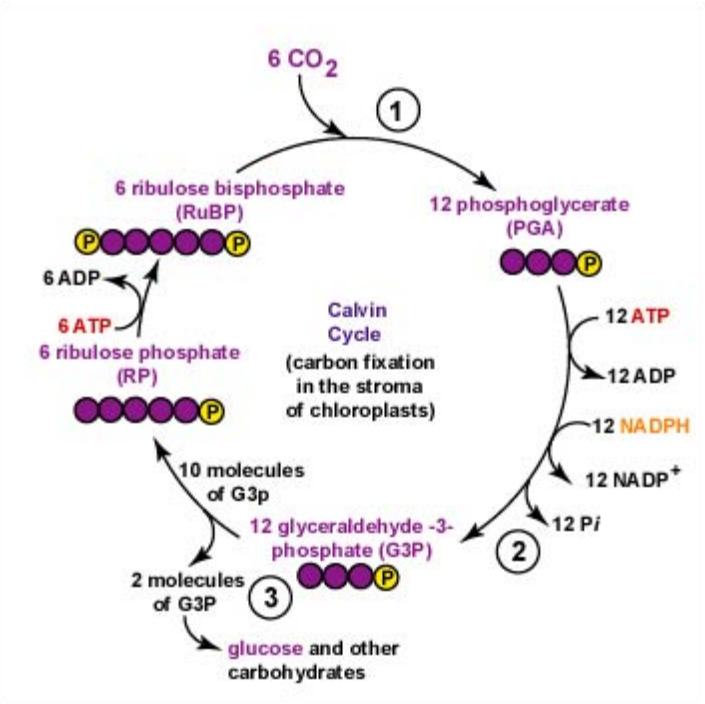

Figure 1.1: Schematic representation of the Calvin cycle.

The carboxylation reaction of Rubisco yields two molecules of 3-phosphoglycerate. This 3-phosphoglycerate is fixed and recycled to RuBP in a series of reactions that is known as the Calvin cycle. Fixation of six molecule of CO_2 requires twelve molecules of NADPH and eighteen molecules of ATP. The Calvin cycle can be subdivided into three sections: (1) In chloroplasts, CO_2 condenses with ribulose-1,5-bisphosphate (RuBP) to form two molecules of the C_3 compound, 3-phosphoglycerate (3-PGA); (2) 3-PGA is then reduced to triose phosphate by consuming ATP and NADPH that have been produced during the light reaction; (3) The triose phosphate is then either utilized to regenerate ribulose-1,5-bisphosphate and to synthesize starch within chloroplasts or is transported into the cytosol for sucrose biosynthesis. (This figure has been taken from the Web site: http://www.cat.cc.md.us/courses/bio141/lecguide/unit1/eustruct/phofig5.html).

1.1.2 C_4 photosynthetic pathway.

The C_4 plants developed a complementary pathway to concentrate CO_2 at the site of Rubisco activity. In warm temperate to tropical grasslands, C_4 plants often account for over 80% of the primary productivity. Relative to C_3 species, C_4 plants have an advantage in many aspects that promote ecological success in warm, low latitude habitats (Sage, 2001). They have higher maximum efficiency in terms of radiation, water and nitrogen use and they generally have higher photosynthetic capacity. The enhancement of photosynthetic performance comes from the ability of C_4 plants to saturate Rubisco for CO_2 in the bundle sheath compartment of the leaf (Sage, 2001). The CO_2 concentrating steps are spatially separated and the co-ordination of two photosynthetic cell types, namely mesophyll cells (MC) and bundle sheath cells (BSC), is required. These two cell types are arranged in layers concentrically around the

vascular tissue, the bundle sheath cells constituting the inner layer and the mesophyll cells forming the outer layer. The MC and BSC are connected by many plasmodesmata and the BSC possess thick cell walls. This arrangement of cells is known as Kranz anatomy (Hatch, 1992) and is schematically represented in Figure 1.2. The initial CO_2 (as HCO_3^-) fixation in the C_4 pathway takes place by phosphoenolpyruvate carboxylase (PEPC) forming the C_4 dicarboxylate, oxaloacetate (OAA), which is subsequently converted to malate (for NADP-ME type as shown in Figure 1.2) or aspartate (for NAD-ME and PCK types), and directly or indirectly decarboxylated in the vicinity of Rubisco for CO_2 re-fixation via the Calvin cycle. Both the fixation and re-fixation of inorganic carbon are separated spatially between the mesophyll cells and bundle sheath cells (Edwards and Walker, 1983; Ku *et al.*, 1996). The compartmentation of individual enzymes in the C_4 pathway results from differential gene expression (Nelson and Langdale, 1992), which is regulated mainly at the transcriptional level (Ku *et al.*, 1996; Sheen, 1999).

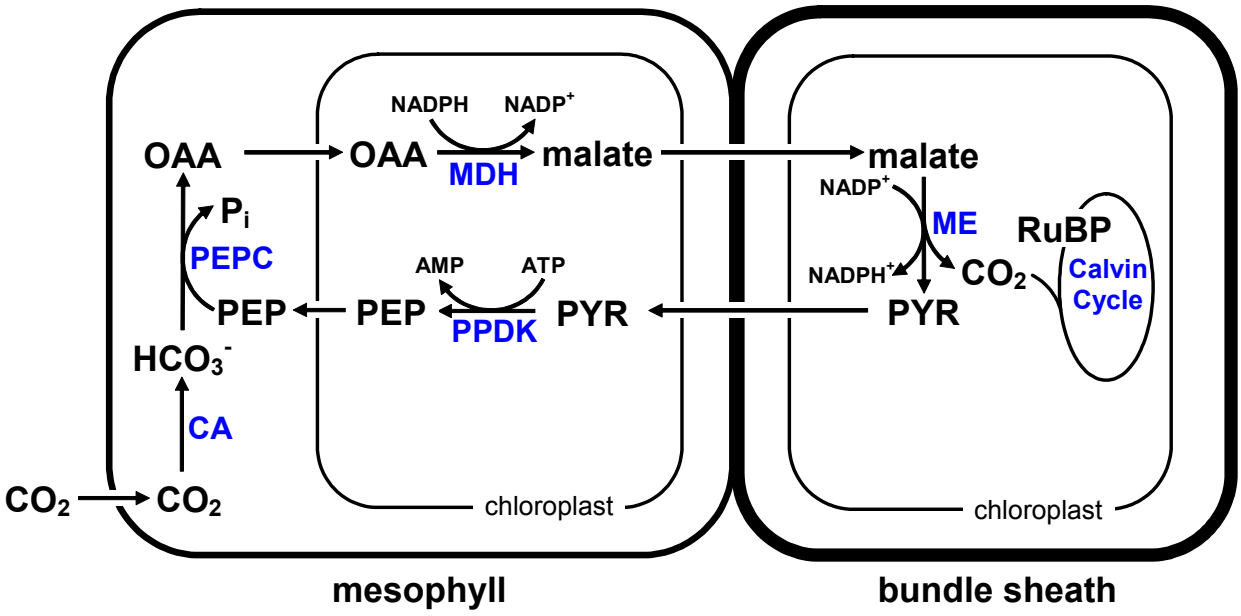

Figure 1.2: Schematic representation of the NADP-ME type C_4 cycle.

A general aspect of the C_4 photosynthetic pathway is shown. CO_2 enters the mesophyll cell and is converted to HCO_3^- and reacts with PEPC to form OAA acid in the cytosol. This OAA enters the chloroplast and converts to malate and then is diffusing to a neighboring bundle sheath cell where it is decarboxylated, and the CO_2 released is fixed by Rubisco and converted to carbohydrate by the Calvin cycle. On the other hand, the PYR produced in the decarboxylation reactions is transported back to the mesophyll cell to regenerate PEP. CA = carbonic anhydrase; OAA = oxaloacetic acid; PEPC = phosphoenolpyruvate carboxylase; ME = malic enzyme; RuBP = ribulose 1,5 bis-phosphate; PYR = pyruvate; PPDK = pyruvate-orthophosphate dikinase.

C_4 plants have been classified into three subgroups (mentioned above) according to their respective predominant decarboxylating enzyme (Hatch *et al*., 1975). However, in some of the NADP-ME type plants (such as maize), in which the decarboxylation of malate via NADP-malic enzyme (ME) is the main decarboxylating event, phosphoenolpyruvate carboxykinase (PCK) is also employed for decarboxylating OAA (Furumoto *et al*., 1999; Walker *et al*., 1997). Likewise, in the PCK-type plants not only PCK but also NAD-malic enzyme (NAD-ME) is utilized as a decarboxylase (Burnell and Hatch, 1988). For the incorporation of one CO_2, C_4 plants require more energy (two ATP in C_3 plants and 3.5 ATP in C_4 plants) when compared with C_3 plants. However, this is negligible when the much greater energy demands for regenerating ribulose-1,5-bisphosphate, which is lost by a process called "photorespiration", in C_3 plants (Edwards and Walker, 1983) is taken into account (details of photorespiration are discussed in chapter 1.2).

1.1.3 Crassulacean Acid Metabolism (CAM) pathway.

Some plants known as CAM plants developed a different pathway other than C_4 plants to concentrate CO_2 at the site of Rubisco activity. The facultative CAM plant *Mesembryanthemum crystallinum* assimilates CO_2 via the C_3 pathway when water supply is sufficient, but reverts to CAM pathway under water stress, whereby the enzyme activities for the C_4-acid metabolism are increased (Cushman and Bohnert, 1997). The CO_2 concentrating mechanism possessed by CAM plants operates by sequentially reducing CO_2 into carbohydrates at two different times of the day. During the day, the deserts are very hot and dry and at the night, the temperature is much lower and humid. CAM plants close their stomata during the day to reduce water loss and open them at night for CO_2 uptake. In this way, desert plants are able to withstand conditions that would desiccate a C_3 or C_4 plant. Figure 1.3 represents the photosynthetic pathway in CAM plants. The initial fixation of CO_2 into oxaloacetate is done by the enzyme phosphoenolpyruvate carboxylase (PEPC) at night, when CAM plant stomata are open to allow CO_2 to enter into the cell. The oxaloacetate is reduced to a four-carbon sugar, malate, via NAD-malate dehydrogenase and pumped into the vacuoles. During the day, when the stomata are closed, the four-carbon sugar is decarboxylated, increasing the plant's intercellular CO_2 concentration and the resulting CO_2 is subsequently fixed by Rubisco in the same way as for C_3 and C_4 plants.

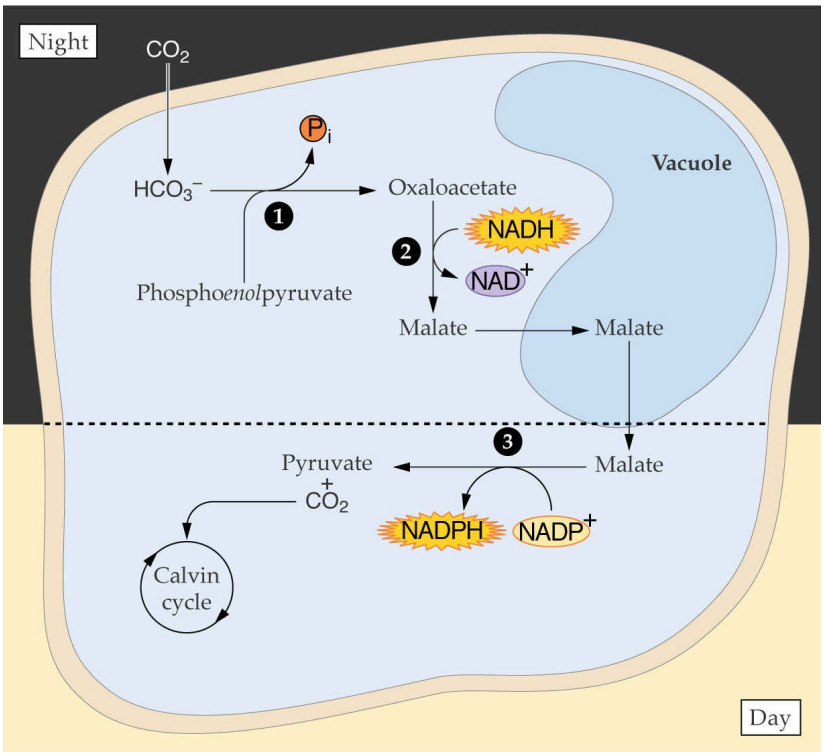

Figure 1.3: Schematic representation of crassulacean acid metabolism pathway.

Crassulean acid metabolism (CAM) is an evolutionary adaptation to photosynthesis in an arid environment. At night CAM plants open their stomata, allowing CO_2 to enter. PEP carboxylase (1) incorporates this CO_2 (as HCO_3^-) into the C_4 organic acid oxaloacetate, which is reduced to malate by malate dehydrogenase; (2) the malate is stored in the vacuole overnight. In the light, CAM plants close their stomata, preventing water loss. The stored malate is decarboxylated by NADP+-malic enzyme; and (3) the resulting CO_2 is converted to carbohydrate via the Calvin cycle (Buchanan *et al*., 2000).

1.2 Photorespiration.

Rubisco, the key enzyme of photosynthesis, catalyses both the carboxylation and the oxygenation of ribulose-1,5-bisphosphate (Bowes *et al*., 1971). CO_2 and O_2 compete for the same active site of the enzyme. Photosynthesis occurs when ribulose-1,5-bisphosphate is carboxylated by Rubisco carboxylase activity and the products, two phosphoglycerate molecules (3-PGA), are processed into carbohydrates and also used to regenerate ribulose-1,5-bisphosphate in a reaction sequence requiring ATP and NADPH. Photorespiration begins with the oxygenation of ribulose-1,5-bisphosphate by Rubisco oxygenase to form one phosphoglycolate (PG) molecule and one phosphoglycerate (PGA) molecule. Phosphoglycerate directly enters into the Calvin cycle, whereas phosphoglycolate enters into the photorespiratory pathway. So photorespiration is a metabolic pathway of

phosphoglycolate produced by the oxygenase activity of Rubisco (Leegood *et al*., 1995). Through photorespiration, plants recover part of the carbon, in which phosphoglycolate is metabolized via the glycolate pathway to glycerate, which can re-enter the C_3 cycle (Andrews and Lorimer, 1987; Keys, 1986; Leegood *et al*., 1995). Despite some evidence that phorespiration is important for energy dissipation to prevent photoinhibition (Kozaki and Takeba, 1996; Osmond *et al*., 1997), it is mainly a wasteful process since for every O_2 reacting with RuBP the equivalent of 2 NADPH are utilized (to re-assimilate the PGA and ammonia formed), the same as when one CO_2 reacts with RuBP (Maroco *et al*., 2000). Furthermore, one-quarter of the carbon metabolized through the glycolate pathway is lost as CO_2 to the atmosphere (Andrews and Lorimer, 1987; Keys, 1986; Leegood *et al.*, 1995). Indeed, in plants possessing the C_3 type of photosynthesis, reducing the O_2 levels from 21% to 2% or increasing CO_2 to 0.1% can increase the net CO_2 assimilation by up to 50% (Gerbaud and Andre, 1987) because of reduced oxygenase activity and photorespiration (Maroco *et al.*, 2000).

The principal factors influencing the rate of photorespiration are the ratio of CO_2 to O_2 and temperature (Leegood *et al.*, 1995). The ratio of the rate of photorespiration to photosynthesis in air (350 ppm CO_2, 21% O_2) is around 0.1 at 10°C, rising to about 0.3 at 40°C, but low intercellular concentration of CO_2, as may occur, for example, under water stress, can result in even higher ratios at high temperatures (Ehleringer *et al*., 1991; Leegood *et al.*, 1995).

C_4 plants as well as CAM plants, overcome the problem by concentrating CO_2 at the vicinity of Rubisco (as described above). C_4 plants are able to concentrate CO_2 in the Rubisco containing bundle sheath cell (Edwards and Walker, 1983) at levels up to 3 to 20 times higher than atmospheric CO_2 (Dai *et al*., 1993; He and Edwards, 1996; Jenkins *et al*., 1989; von Caemmerer and Furbank, 1999). Because of their CO_2 concentrating mechanism, C_4 plants greatly reduce the oxygenase reaction of Rubisco (Edwards and Walker, 1983; Hatch, 1987).

The photorespiration pathway proceeds in the chloroplast, peroxisome and mitochondria. Figure 1.4 represents the photorespiratory pathway of C_3 plants. In this pathway, two molecules of phosphoglycolate are processed to form one molecule each of phosphoglycerate and CO_2, which are used for the regeneration of RuBP through the Calvin cycle (C_3 cycle).

Recycling of phosphoglycolate begins with the hydrolytic release of phosphate by phosphoglycolate phosphatase present in the chloroplast stroma (Heldt, 1997). The glycolate formed is transported from the chloroplast to peroxisomes by a specific translocator present in the inner envelop membrane (Heldt, 1997). In the peroxisomes, glycolate is oxidized to glyoxylate by glycolate oxidase (GOX) in an irreversible reaction. In this reaction H_2O_2 is formed which is readily hydrolyzed to H_2O and O_2 by the enzyme catalase present in the peroxisomes. The glyoxylate formed is then converted to the amino acid glycine by two different reactions proceeding in the peroxisome simultaneously at a 1:1 ratio (Heldt, 1997). In one hand, the enzyme glutamate:glyoxylate aminotransferase (GGAT) catalyses the transfer of an amino group from the glutamate to glyoxylate, on the other hand, the enzyme serine:glyoxylate aminotransferase (SGAT) catalyses the transamination of glyoxylate by serine. The glycine leaves the peroxisomes via pores and is probably transported into the mitochondria.

Two molecules of glycine are oxidized yielding one molecule of serine with the release of CO_2 and NH_3 and a transfer of reducing equivalents to NAD^+ in the mitochondria. The oxidation of glycine is catalysed by the serine synthase complex (SS). Nitrogen is a very important nutrient for the plants and often it is a limiting factor for plant growth. So, the ammonia liberated in the matrix of mitochondria during the course of glycine metabolism, diffuses rapidly to the chloroplast where it is used, with a very high affinity, by glutamine synthetase (GS) catalysing the ATP-dependent conversion of glutamate to glutamine (Ireland and Lea, 1998; Migge *et al*., 1997). Most of the CO_2 released in the mitochondria during photorespiration is lost.

The serine formed in the mitochondria is exported to the peroxisomes. In peroxisomes, serine takes part in the transamination of glyoxylate. This reaction is catalyzed by the enzyme serine:glyoxylate aminotransferase (SGAT) which leads to the production of glycine and hydroxypyruvate. Glycine leaves the peroxisomes and enters into the mitochondria (as described before), whereas hydroxypyruvate is reduced to glycerate by the enzyme hydroxypyruvate reductase (HPR) at the expense of one NADH, which is then released from the peroxisomes and imported into the chloroplast. In the chloroplast, glycerate is phosphorylated by glycerate kinase (GK) to form 3-phosphoglycerate that enters into the Calvin cycle to be used in the biosynthesis of carbohydrates and in the regeneration of RuBP. These reactions complete the recycling of 2-phosphoglycolate.

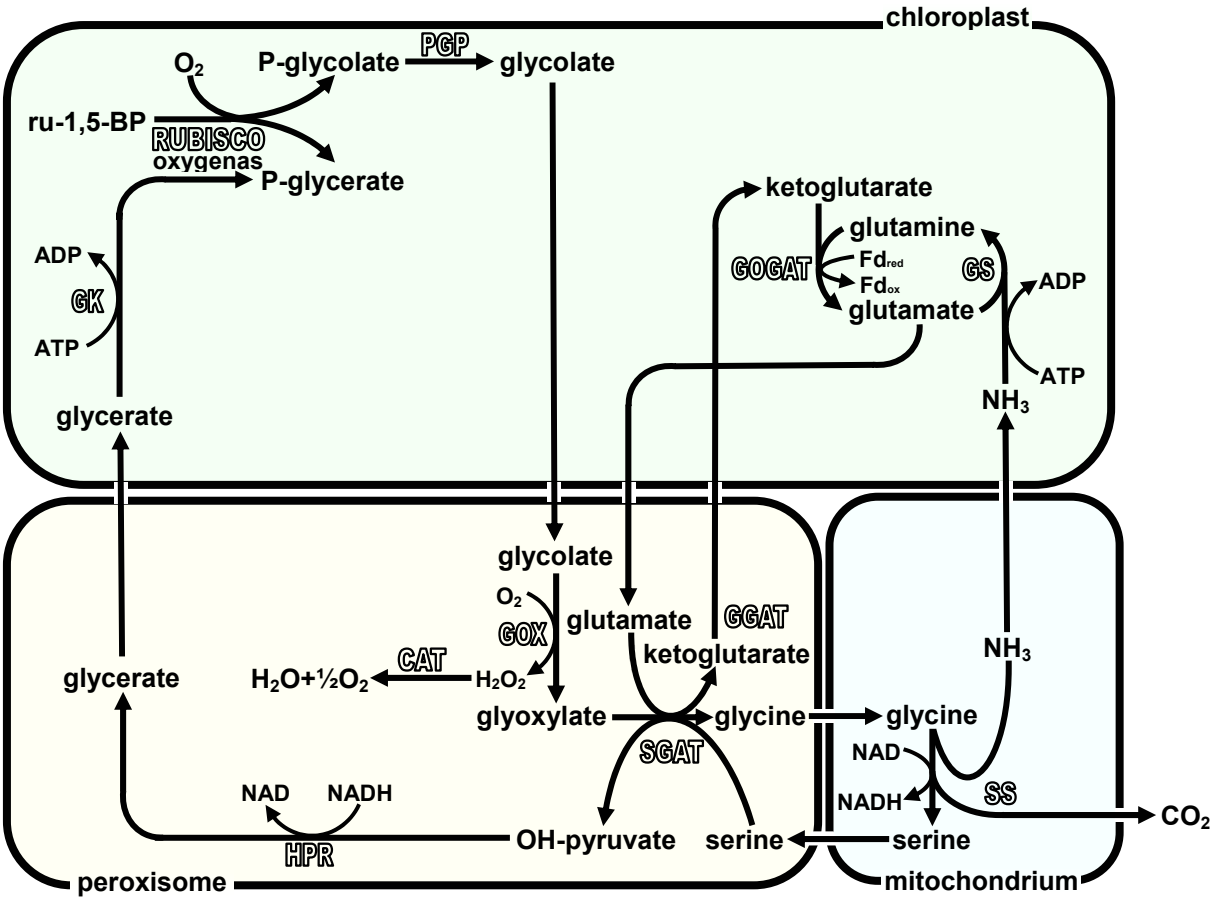

Figure 1.4: Schematic representation of the photorespiratory pathway.

Rubisco, the key enzyme of CO_2 fixation in plants possesses two activities: oxygenation and carboxylation. The oxygenation reactions of Rubisco produce one molecule of phosphoglycerate and one molecule of phosphogycolate. Phosphoglycerate enters into the Calvin cycle whereas phosphoglycolate needs to be converted into phosphoglycerate. Two molecules of phosphoglycolate convert into one molecule of phosphoglycerate in a series of reactions that occurs in three separate subcellular organelles: chloroplasts, peroxisomes and mitochondria. During this conversion, CO_2 and NH_3 are released in the mitochondria. Released NH_3 is refixed by the plastidal glutamine-glutamate cycle whereas CO_2 is lost to the atmosphere. RUBISCO = ribulose-1,5-bisphosphate carboxylase/oxygenase; PGP = phosphogycolate phosphatase; GOX = oxygen-dependent glycolate oxidase; CAT = catalase; GGAT = glyoxylate:glutamate aminotransferase; GOGAT = glutamate:glyoxylate aminotransferase; GS = glutamine synthetase; SS = serine synthase; SGAT = serine:glutamate aminotransferase; HPR = hydroxypyruvate reductase; GK = glycerate kinase.

1.3 Approaches to introduce CO_2 concentrating mechanism into C_3 plants.

Many plants, in nature, developed strategies during the course of evolution to supply elevated concentrations of CO_2 at the site of Rubisco. As a result, the photorespiration is suppressed and the photosynthetic efficiency is increased in those plants. For example, the group of C_4 plants and CAM plants developed a way to concentrate CO_2 at the vicinity of Rubisco (as described above). In high CO_2 and/or low O_2, the oxygenase activity of Rubisco is virtually absent, the flux through the photorespiratory carbon cycle negligible and the CO_2 compensation point close to zero (Häusler *et al*., 2002). The benefit that comes from the CO_2 concentrating mechanism in C_4 and CAM pathways to the plants has prompted researchers to build C_4 like pathways in C_3 plants.

Although there was some interest in engineering Rubisco in favor of carboxylase over oxygenase, current evidence suggests it is unlikely that Rubisco can be engineered for increased carboxylation efficiency under current environmental conditions (Zhu *et al*., 2004). Several attempts to increase the CO_2/O_2 specificity of Rubisco by altering its active site with the techniques of site-directed mutagenesis, by inducing low oxygenase activity mutants (Somerville and Ogren, 1982), or by inserting more efficient Rubisco genes into higher plants have not been successful so far (Normile, 1999; Zelitch, 1989).

There are several reports on the improvement of growth and crop yield of C_3 plants in an atmosphere containing elevated CO_2 (Arp *et al*., 1998; Besford, 1990; Chen *et al*., 1997; Teramura *et al*., 1990). This is mainly based on a faster biomass production due to an increase in CO_2 assimilation rates and a suppression of photorespiration (Häusler *et al.*, 2002). The most extensively employed strategy to increase the supply of CO_2 for Rubisco is introducing C_4 traits into C_3 plants (Häusler *et al.*, 2002). Hybridization between C_3 and C_4 plants by conventional breeding was successful only for a few plant genera, none of them are crop species (Brown and Bouton, 1993). In addition, most of the hybrids exhibited infertility due to irregular chromosome pairing and/or other genetic barriers (Ku *et al*., 1999). Thus, employing traditional breeding methods to incorporate C_4 traits into C_3 crops seems difficult. With the development of plant genetic engineering, transfer of foreign genes into crops has increasingly become routine, providing a new approach to altering plant traits (Ku *et al.*, 1999). Moreover, Kranz anatomy is not essential for terrestrial C_4 plant photosynthesis (Voznesenskaya *et al*., 2001). Many submersed aquatic plants (e.g. *Hydrilla verticillata, Egeria densa*) developed C_4 –like photosynthetic pathway in a single cell (Casati *et al*., 2000). This aquatic plant shows C_3 type photosynthesis in the cooler seasons, but a switch to C_4-type

biochemistry is induced if the soluble CO_2 concentration decreases in summer. Typical C_4 enzymes are strongly activated and in parallel, the CO_2 compensation point declines. Importantly, this mechanism does not depend on the interaction of different cell types but takes place in a single cell (Leegood, 2002).

So introduction of C_4 traits into C_3 plants to improve their photosynthetic characteristics has been an active research area in plant biology (Brown and Bouton, 1993; Furbank and Taylor, 1995). C_3 plants such as rice have been demonstrated to possess the regulatory machinery necessary for the expression of C_4-specific genes at high levels, in a light-dependent, cell-specific manner (Ku *et al.*, 1999; Ku *et al.*, 1996). Introduction of one of the key enzymes in C_4 photosynthesis, PEPC, into rice, shows high levels of expression of the transgene, which did not interfere with growth and fertility of most of the transgenic plants (Ku *et al.*, 1999). More importantly, transgenic rice plants with high levels of expression of the maize C_4 enzyme exhibited reduced sensitivity of photosynthesis to O_2 inhibition (Ku *et al.*, 1999). On the contrary, transgenic potato lines overexpressing functional PEPC shows growth retardation (Rademacher *et al*., 2002). However it is possible that the growth retardation observed in later case is an indirect consequence of an imbalance of growth factors by the constitutive overexpression of functional PEPC in all tissues and cell type (Rademacher *et al.*, 2002).

Many laboratories in different countries attempts to introduce C_4-like features into terrestrial C_3 plants by a transgenic approach (Matsuoka *et al*., 2001). However, to my knowledge, no one has obtained any C_3 plant overexpressing all the enzymes necessary for a C_4 pathway.

1.4 The glycerate pathway in *E.coli*.

Many micro-organisms (e.g. *Pseudomonas* spp., *E.coli*) can grow on glycolate as a sole carbon source. The biosynthesis of cell material of these organisms growing on glycolate has been shown to be effected by a series of reactions in which, initially, glycolate is converted into glycerate (Gotto and Kornberg, 1961). At first, glycolate is oxidized to glyoxylate (Hansen and Hayashi, 1962; Kornberg and Sadler, 1961) in a reaction catalyzed by the enzyme glycolate oxidase (Lord, 1972). Glyoxylate is a branching point in the metabolic pathway since it is metabolized by two divergent condensation reactions (Pellicer *et al*., 1996). One reaction condenses glyoxylate with acetyl coenzyme A and is catalyzed by malate

synthase G, while the other reaction condenses two molecules of glyoxylate in a process catalysed by glyoxylate carboligase, which simultaneously decarboxylates the condensation product to tartronic semialdehyde (Chang *et al*., 1993). This latter compound is reduced to glycerate and subsequently phosphorylated to glycerate-3-phosphate. The last two reactions are catalyzed by tartronic semialdehyde reductase and glycerate kinasae. The pathway in which glycerate is produced from glycolate is known as the glycerate pathway (Pellicer *et al.*, 1996).

The first enzyme of this pathway, glycolate oxidase (GO), is a multiprotein complex that is capable of oxidizing glycolate in an oxygen independent manner to produce glyoxylate. So this enzyme is also known as glycolate dehydrogenase (GDH) (Lord, 1972). The active form of this multiprotein complex is constituted from three different protein subunits that are encoded by three different genes known as *glc*D, *glc*E and *glc*F (Pellicer *et al.*, 1996), which are located in the *glc* operon of *E. coli*.

Enzymes that catalyse the oxidation of glycolate to glyoxylate have been isolated from a variety of plants and animal tissues. It is also found in several unicellular algae. The known glycolate oxidases of plants and animals differ in many ways from bacterial and algal glycolate dehydrogenases. On the one hand, the plant and animal glycolate oxidases use O_2 as an electron acceptor, produce H_2O_2, oxidize L(+)-lactate as an alternative substrate and is cyanide insensitive. On the other hand, the algal and bacterial dehydrogenase uses an organic compound as an electron acceptor, oxidizes D(-)-lactate and is cyanide sensitive. Moreover, the algal and bacterial dehydrogenases do not produce H_2O_2. In the second step of the glycerate pathway, two molecules of glyoxylate condense in a process in which simultaneously decarboxylates the condensation product to tartronic semialdehyde. This reaction is catalysed by glyoxylate carboligase (GCL) and CO_2 is released in this reaction because of the decarboxylation reaction. Tartronic semialdehyde is then converted to glycerate by tartronic semialdehyde reductase (TSR), and then glycerate is integrated into the bacterial basal carbon metabolism.

A similar pathway was also discovered as a photorespiratory cycle in some green algae and cyanobacteria (Nelson and Tolbert, 1970). In this pathway, glycolate oxidation is catalysed by glycolate dehydrogenase that is located inside the mitochondria. This enzyme is not oxygen dependent and uses organic electron-acceptors as NAD^+ instead of O_2. The glyoxylate is converted to glycine in the mitochondrion by glyoxylate aminotransferase and afterwards by different pathways to glycerate, serine or related compounds (Igamberdiev and Lea, 2002; Winkler and Stabenau, 1992).

1.5 The aim of the present study.

In the present study, a biochemical pathway should be established in the chloroplast of the C_3 plant *Nicotiana tabacum* in order to suppress photorespiration resulting in an improvement of its photosynthetic efficiency. As described before, Rubisco oxygenase activity leads to the oxidation of RuBP to form phosphoglycerate and phosphoglycolate. The phosphoglycerate enters into the Calvin cycle to form carbohydrates. On the other hand, phosphoglycolate is converted to glycolate inside the chloroplast and then transported to the peroxisome.

The aim of the proposed biochemical pathway (details of the pathway are described in the results section) is to convert the glycolate produced in the photorespiratory pathway into glycerate inside the chloroplast. During this conversion, CO_2 will be released inside the chloroplast. The proposed pathway is aiming to suppress photorespiration in the transgenic plants in two ways. On the one hand, CO_2 concentration will be increased in the vicinity of Rubisco resulting in a decrease of oxygenase activity. On the other hand, glycolate will not enter into the photorespiratory pathway.

In the present study, all enzymes required to establish the biochemical pathway should be cloned. Transgenic tobacco plants should be generated encoding those enzymes using both nuclear and chloroplast transformation. It was expected to prove that the enzymes involved in the establishment of the pathway are active *in planta*. Additionally, alternatives to the bacterial multisubunit glycolate oxidase should be analysed.

2 MATERIALS AND METHODS.

2.1 Materials.

2.1.1 Chemicals and consumables.

The chemicals used throughout the work were purchased from the following companies: Amersham Pharmacia Biotech (Freiburg), BioRad Laboratories GmbH (München), Calbiochem (Bad Soden), Carl Roth GmbH (Karlsruhe), Eurogentec (Cologne), Hartmann Analytic (Braunschweig), Invitek (Berlin, Germany), Invitrogen (Leck, Netherlands), KMF Laborchemie Handels GmbH (St. Augustin), Kodak (Stuttgart), Macherey-Nagel (Düren), MBI Fermentas (St. Leon-Rot), Metabion (Planegg-Martinsried), Molecular Probes (Leiden, Netherlands), New England BioLabs (Frankfurt), Novagen (Darmstadt), Pharmacia (Freiburg), Promega (Madison, USA), QIAGEN (Hilden), Roche Applied Science (Mannheim), Röhm (Darmstadt), Sigma (Taufkirchen), Serva (Heidelberg) Sigma ARK (Taufkirchen).

The consumables were obtained from: Applied Biosystems (Darmstadt), Biometra (Göttingen), BioRad Laboratories GmbH (München), Eppendorf (Hamburg), Fuji (Düsseldorf), Gibco BRL (Eggenstein), Greiner (Solingen), Hanna Instruments (Kehl), Heraeus (Osterode), Herolab (Wiesloch) Kodak (Stuttgart), Kontron Instruments (München), Labomedic (Bonn), Leica (Heidelberg), Millipore (Eschborn), MWG Biotech (München), Pharmacia (Freiburg), Raytest (Berlin), Serva (Heidelberg), Schott Glaswerke (Mainz), Sorvall (Bad Homburg), Wissenschaftliche Technische Werkstätten (Weilheim), Whatman (Maidstone, UK).

2.1.2 Enzymes and Antibodies.

I) Enzymes

Table 2.1 Restriction enzymes that are used throughout the work.

*Afl*III	MBI Fermentas, St. Leon-Rot
*Asc*I	New England Biolabs, Frankfurt
*Bam*HI	New England Biolabs, Frankfurt
*Bpu*1102I	MBI Fermentas, St. Leon-Rot
DNaseI	Roche Applied Science, Mannheim
*Ecl*136 II	MBI Fermentas, St. Leon-Rot

*Eco*RI	New England Biolabs, Frankfurt
*Eco*RV	MBI Fermentas, St. Leon-Rot
*Hind*III	MBI Fermentas, St. Leon-Rot
Klenow-DNA polymerase	MBI Fermentas, St. Leon-Rot
*Mlu*I	MBI Fermentas, St. Leon-Rot
M-MLV Reverse transcriptase	Promega, Mannheim
*Nco*I	MBI Fermentas, St. Leon-Rot
*Pme*I	New England Biolabs, Frankfurt
*Pvu*I	MBI Fermentas, St. Leon-Rot
*Sgr*AI	New England Biolabs, Frankfurt
T4-DNA-Ligase	New England Biolabs, Frankfurt
Taq-Halle-DNA polymerase	T. Lahaye, Universität Halle, Halle
*Xba*I	MBI Fermentas, St. Leon-Rot
*Xho*I	MBI Fermentas, St. Leon-Rot
*Sma*I	MBI Fermentas, St. Leon-Rot
*Sal*I	MBI Fermentas, St. Leon-Rot

II) Antibodies

Anti-His HRP Conjugate (Horse Radish Peroxidase) (Qiagen, Hilden).

Mouse anti-His antibody (Qiagen, Hilden).

Goat anti-mouse HRP Conjugate (Qiagen, Hilden).

2.1.3 **Instruments.**

- ABI-7000 (Appliedbiosystems, Darmstadt).
- Agarose gel electrophoresis accessories: electrophoresis chambers, gel carriers and combs (BIO-RAD, München), power sources (the mechanical workshop of the Institute of BiologyI, RWTH Aachen).
- Automatic Sequencer: “4200L-2” (LI-COR, Lincoln, USA).
- Centrifuges: “RC-5B” with GS-3 and SS-34 rotors (SORVALL, Bad Homburg), “Varifuge RF” with 5315 rotor (HERAEUS, Osterode) for Falcon tubes, “Biofuge A” and “Hermle” (HERAEUS, Osterode) for Eppendorf tubes.
- Cuvettes: quartz glass cuvettes (Hellma), disposable cuvette (Sarstedt).

- Confocal microscope: Leica TCS-SP spectral confocal microscope (Leica, Heidelberg).
- Disposable reaction tubes: 1.5 and 2 ml (Eppendorf, Hamburg); 15 and 50 ml (FALCON, Eppendorf, Hamburg).
- Electroblotting apparatus: “mini-transblot” (BIO-RAD, München).
- Electropestle: motor-driving stainless steel pestle for 1.5 ml Eppendorf tubes (driven by a RZ O type motor, Heidolph).
- Electrophoresis chamber: horizontal electrophoresis unit “Multiphor II” (Pharmacia, Freiburg); vertical mini gel apparatus “Mini Protean II Dual Slab Cell” (BIO-RAD, München).
- Fuji Fluoreszenzscanner LAS-1000 CCC camera (Raytest, Berlin).
- Leica TCS-SP spectral confocal microscope (Leica, Heidelberg).
- Nitrocellulose membrane: “Hybond C” and “Hybond ECL” (Amersham, Freiburg).
- pH-Meter: WTW (Wiss Techn.Werkstatten, Weilheim).
- Photographic apparatus: camera “429K”; software “E.A.S.Y. store Win 32” (Herolab, Wiesloch).
- Photometer: “Uvikon 930” (KONTRON) with 12 temperature-controlled cuvette holders; Gene Quant RNA/DNA calculator (Pharmachia, Freiburg).
- Shaker: Innova^{TM} 4340 incubator shaker (New Brunswick Scientific, Nürtingen)
- Sonicator Bandelin Sonopuls GM 70 (Berlin).
- Sterile filter: with the pore size of 0.22 µm (Millipore, Schwalbach).
- Thermocycler: Biometra T personal (Biometra, Göttingen), Thermocycler Primus (MWG Biotech, München), LightCycler (Roche Applied Science, Mannheim).
- UV-chamber (Bio-Rad, München).
- UV transilluminator: wavelength 302 nm and UVT-20M (Herolab, Wiesloch).

2.1.4 Solutions, buffers and media.

Most of the buffers, media and solutions were prepared as described by Sambrook and Russel (2002) unless supplied with the kits. The pH was adjusted with 1M, 5M and 10M NaOH, 1M and 5M KOH or 37 % (v/v) HCl. Sterilization of all solutions, buffers and media was achieved by autoclaving (20 min; 120°C, 1 bar) or, for thermolabile solutions, by filtration through 0.2 µm filters. Heat-sensitive components, such as antibiotics, were prepared as stock solutions, and added to the medium/buffer after cooling to 50°C.
Buffer and media used during the present work are given in table 2.2.

Table 2.2 Buffer and media.

Name	Component	Concentration
Acrylamide/Bisacrylamide	Acrylamide N',N'–Methylenbisacrylamide	30 % (w/v) 0.8 % (w/v)
Ammonium per sulphate (APS)		10 % (w/v)
Anti-His HRP Conjugate blocking buffer	From QIAGEN, Germany.	
Bradford–Solution	Coomassie Brilliant Blue G 250 Ethanol 96 % (v/v) Phosphoric acid 85 % (v/v)	100 mg/L 50 ml/L 100 ml/L
Coomassie-fixation solution	Methanol Acetic acid	30 % (v/v) 10 % (v/v)
DNA–Extractions–Buffer	Tris–HCl, pH 8,5 NaCl EDTA, pH 8,0 SDS	100 mM 100 mM 10 mM 0.2 % (w/v)
dNTP–Mix	dATP dCTP dGTP dTTP	2.0 mM 2.0 mM 2.0 mM 2.0 mM
Gelelectrophoresis–loading Buffer	Kresolred Sucrose	1mM 60 % (w/v) in TAE buffer
Grinding buffer (GB)	HEPES-KOH pH 8.0 EDTA Sorbitol BSA ascorbate	50 mM 10 mM 0.33 M 0.5 g/l 5 mM
HEPES buffer I	HEPES –KOH pH 7.5	1 mM

HEPES buffer II	HEPES–KOH pH 7.5 Glycerol	1 mM 10 % (v/v)
Induction medium	YEB medium MES pH 5.6 Acetosyringone (Aldrich)	 10 mM 20 µM
Lammili-Loading Buffer	Tris–HCl, pH 6.8 SDS Saccharose Bromphenolblue	100 mM 4 % (w/v) 10 % (w/v) 0.04 % (w/v)
LB–Ampicillin	LB–Medium Ampicillin	 100 µg/ml
LB–Amp–Plate	Bactotrypton Yeastextract NaCl Agar Ampicillin	10 g/L 5 g/L 10 g/L 15 g/L 100 µg/ml
LB–Medium	Bactotrypton Yeast extract NaCl	10 g/L 5 g/L 10 g/L
Ligase–Buffer	Tris–HCl, pH 7.8 $MgCl_2$ DTT ATP PEG 8000	40 mM 10 mM 10 mM 0.5 mM 5 % (w/v)
MMA medium	MS-salts (Duchefa) Sucrose MES pH : 5.6 Acetosyringone (Aldrich)	4.3 g/L 20 g/L 10 mM 200 µM
MS Medium	Murashige and Skoog Basal medium (Duchefa)	
MS + Kanamycin Plates (for *Arabidopsis*)	MS salt Agar Kanamycin	2.2 g/L 0.7 % (w/v) 20 mg /ml
MS medium (for tobacco)	MS-salts (Duchefa) Sucrose NaOH pH 5.8 Agar (for solid medium) Vitamin Solution	4.3 g/L 20 g/L 1M 8 g/L 500 µL/L

MS II medium	MS-medium 6-Benzylaminopurine (BAP, Sigma) Naphtaline Acetic Acid (NAA, Sigma) Kanamycin (Applichem) Claforan (Duchefa)	1 mg/L 0.1 mg/L 100 mg/L 200-250 mg/L
MS III medium	MS-medium Kanamycin Claforan	 100 mg/L 200-250 mg/L
PCR–Buffer (10 x)	Tris–HCl pH 8.5 KCl Tween 20	100 mM 500 mM 0.5 % (v/v)
Percoll-buffer	Percoll Hepes-KOH pH 8.0 sorbitol	35 % 50 mM 0.33 M
Ponceau S–Red–solution	Ponceau S–Red Acetic acid	0,25 % (w/v) 1 % (v/v)
Protein elution buffer	Tris HCl pH 7.5 NaCl Imidazol	20 mM 300 mM 300 mM
Protein extraction buffer	Protein resuspension buffer Ascorbate DTT Polyclar	 0.5 % (w/v) 5 mM 2 % (w/v)
Protein lysis buffer	Tris HCl pH 7.5 NaCl Glycerol DTT Lysozyme	20 mM 300 mM 10 % 5 mM 5 µg/µl
Protein resuspension buffer	HEPES–KOH pH 7.5 $MgCl_2$ EDTA	50 mM 5 mM 1 mM
Protein wash buffer I	Tris HCl pH 7.5 NaCl Imidazol NP-40	20 mM 300 mM 5 mM 0.5 % (v/v)
Protein wash buffer II	Tris HCl pH 7.5 NaCl Imidazol NP-40	20 mM 300 mM 30 mM 0.5 % (v/v)
1xSH	Hepes-KOH pH 8.0 Sorbitol	50 mM 0.33 M

TAE (1 x)	Tris–Acetat, pH 8,0 EDTA, pH 8,0	40 mM 1 mM
TBE (10 x)	Tris Boric acid EDTA	0.9 M 0.9 M 0.02 M
TBS buffer	Tris-CL, pH 7.5 NaCl	10 mM 150 mM
TBS-Tween buffer	Tris-Cl, pH 7.5 NaCl Tween 20 Triton X-100	20 mM 500 mM 0.05 % (v/v) 0.2 % (v/v)
TE (1 x)	Tris–HCl, pH 8.0 EDTA, pH 8.0	10 mM 1 mM
TfB I	K–Acetate $MnCl_2$ RbCl $CaCl_2$ Glycerin	30 mM 50 mM 100 mM 10 mM 15 % (v/v)
TfB II	RbCl $CaCl_2$ MOPS Glycerin	10 mM 75 mM 10 mM 15 % (v/v)
Transfer buffer (1x)	Tris-HCl pH 8.3 Glycine SDS Methanol	48 mM 39 mM 0.037 % (w/v) 20 % (v/v)
Tris-Glycine-buffer (1x)	Glycine Tris SDS	192 mM 25 mM 0.1 % (w/v)
TRIZOL	Guanidinthiocyanate Ammoniumthiocyanate NaAc, pH 5.0 Glycerol Phenol solution (H_2O)	0.8 M 0.4 M 0.1 M 5 % (w/v) 38 % (v/v)
YEB medium	Nutrient Broth or Beef Extract Yeast Extract Peptone Sucrose $MgSO_4$ pH	5 g/L 1 g/L 5 g/L 5 g/L 2 mM 7.4

2.1.4 Matrix and membranes.

- Hybond^{TM}-ECL^{TM}-nitrocellulose membrane (0.45 μm) from Amersham Pharmacia biotech (Braunschweig), and Whatman no.1 paper from Whatman were used in Western blotting.

2.1.5 *Escherichia coli* strains.

- DH5α. F^{-}, Lambda^{-}, *rec*A1, *end*A1, *hsd*R17 (r_K^-, m_K^+), (*lac*ZYA-*arg*F), *sup*E44, U169, Φ80d*lac*ZΔM15, *thi*-1, *gyr*A96, *rel*A1 (Hanahan, 1983). This bacterial strain possesses a modified recombination system (*rec*A1), which results in reduced recombination probability, and lacks endonuclease (*end*A1). It was therefore used in the cloning experiments.
- ER2566 New England BioLabs (Frankfurt)
- JA 155 (Pellicer *et al.*, 1996)
- JA 156 (Pellicer *et al.*, 1996)
- JA 157 (Pellicer *et al.*, 1996)

2.1.6 *Agrobacterium* strain.

- GV3101 (pMP90RK): Gm^r, Km^r, Rif ^{r} (Koncz and Schell, 1986). This *Agrobacterium* strain contains a non-oncogenic Ti plasmid pMP90RK that represents one component of the binary vector system described by above authors. This plasmid contains the *vir*-region as well as the genes for gentamycin and kanamycin resistances. After introduction of derivatives of the plasmid pS, this bacterial strain was used for the transformation of tobacco and *Arabidopsis* plants on the basis of kanamycin resistance.

2.1.7 Plant materials.

- *Nicotiana tabacum* L. cv. Petit Havana SR1 (Maliga *et al*., 1973). This tobacco line was used for the transformation with *TSR* and *GCL* gene.
- *Nicotiana tabacum* L. cv. Petit Havana. This tobacco line was used for the plastidal transformation as well as nuclear transformation of the genes required for the proposed pathway.
- *Arabidopsis thaliana* ecotype Columbia plants were used for the stable expression of AtGDH fused to RFP.

2.1.8 Synthetic oligonucleotides.

The following primers (from Sigma and Metabion) used for cloning and sequencing of the genes required for the novel pathway.

Table 2.3 List of the primers used throughout the work.

NAME OF THE PRIMER	SEQUENCE
Actin2 Fw	GGT AAC ATT GTG CTC AGT GGT GG
Actin2 Rev	GGT GCA ACG ACC TTA ATC TTC AT
AtglcD(Nco1) F	TCG ACC ATG GCT TTC GCT TCA AAA TTC GCT
AtglcD(Bam) R	TCG GAT CCT CAG TGG TGG TGG TGG TGG TG
AtglcD-1353 F1	CCT TGC AGA ACT CAT ATC AAG ATC
AtglcD-1671 R1	CAT GAG GAG GAA TTA ACT TTC C
AtglcD-1293 F2	CTA TGC TAT GGC GCC AGG TCA
AtglcD-1666 R2	TCA TGA TAT CGT TTG GGT CCA ACG
GCL1	ACG TCC ATG GGG ATG GCA AAA ATG AGA GCC GTT G
GCL2	ACG CTC GAG TTC ATA GTG CAT GAA GCA GGT TTC
GCL3	TAG TCG ACG AAT TCA TAG TGC ATG AAG CAG GTT TC
GCL 1470	CTG CGT GCA ACT CGC TTT CGA
GCL-cDNA –F1	GCG CGC AGT TCA ACA TTC C
GCL-cDNA- R1	CGC TGC CCA TCG AAA TAT TGG
GCL-SD-F-HindIII	TGA AGC TTA GGA GGG AAC ATG GCA AAA ATG AGA GCC G
GCL-inter-new	AGT TTG CTG AAC TGA CCA GCG
GCL-inter-new2	ACA GTT CGT GAA GCG GCG CTG G
GCL-Mlu	TCG AAC GCG TTA GGT GCA TGG GGA TGG CAA AAA T
GCL-Mun	TTA GCA ATT GCT TCA ATA TC
GlcD-F (Bam)	TCG AGG ATC CCA TGG CTT TCG CTT CAA AAT
GlcD-R (Sal)	TCG AGT CGA CGA AAC ATA CAT GAG GAG G
inter pri glcD seq-F	TGG AGA TGT TGT GAA GAC AGC
inter pri glcD seq-R	CCA CAG CGC CTC TTT TC
GO in E-coli-Forward	TCG ACC ATG GGC ATC TTG TAC GAA GAG C
GO in E-coli-Reverse	TCG ACT CGA GTT ATT CCT TTT CAA GGG C
GO in E-coli pri-2	GGC GTG CGT AAC CTG GCG ATC
GO in E-coli pri-3	CGG CGG GCT GGA GAT GAT G

GO in E-coli pri-4	CAT GCA CCC GTT AAT CCT TTT CG
GO in E-coli pri-5	GTG ATT CAG GGC AGC AAT AGC
GO in E.coli pri-6	TGG CGT GCT CAC TGA AAT CTC
GO in E-coli pri-7	GTG ATT CAG GGC AGC AAT AGC
GO in E-coli pri-8	CTG CCT CAC TTG CCG TAA TTG TG
GO in E-coli pri-9	CAG GCT GTT GTG GCG CGG TGG
GO in E-coli pri-10	CGA CAG CCA TCT GTG CTG CG
Oligo dT 18	TTT TTT TTT TTT TTT TTT TTT TTT T
pS5`	GAC CCT TCC TCT ATA TAA GG
pS3`	CAC ACA TTA TTC TGG AGA AA
TSR1	ACG TCC ATG GGG ATG AAA CTG GGA TTT ATT GGC TT
TSR2	ACG CTC GAG GGC CAG TTT ATG GTT AGC CAT T
TSR3	ACG CTC GAG TCA GGC CAG TTT ATG GTT AGC CAT
TSR 561	GCT ATT TGC TTC AAA AGC CGG
TSR-cDNA –F1	GGA CGT TGT CGA TTA TGG TTG
TSR-cDNA-R1	TGC CAG GTT GAG ATC TTT CTG
TSR –MLU NEW	TCG AAC GCG TTA GGT GCA TGA AAC TGG GAT TTA TTG
TSR-pTRAK-122R	AGT GAC AGT AAT TCA TCA GCA ACC
TSR-Sac	ATG GAG CTC ATA TCA ACA AT
TSR-SD-F-XhoI	GAC TCG AGA GGA GGG AAC ATG AAA CTG GGA TTT ATT GG
TSR-SD-R-Xho-Hind	GAC TCG AGA AGC TTC AGG CCA GTT TAT GGT TAG CC
T7-Reverse	GCT AGT TAT TGC TCA GCG G
T7-universe	AAT TAA TAC GAC TCA TCA CTA TAG GG

2.1.9 Plasmids.

I)

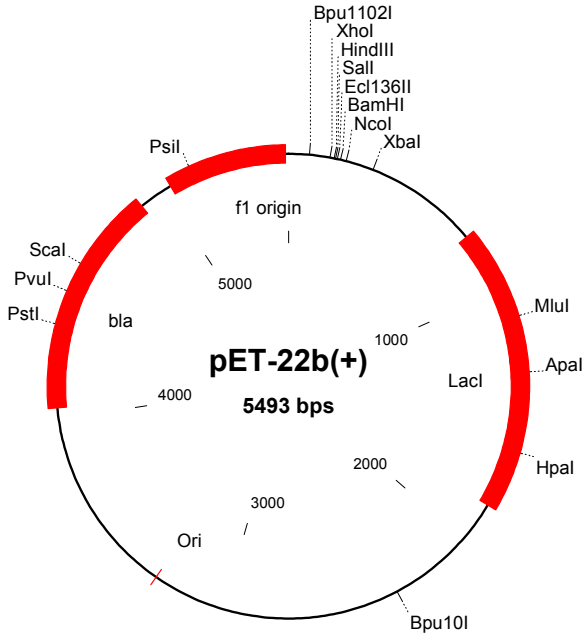

Figure 2.1: Bacterial expression vector pET 22b(+) (commercial vector, Novagen, Darmstadt).

i) pET-GCL (7221 bps)

Vector	pET22b (+) was restricted with *Nco*I, *Xho*I followed by purification with PCR purification kit (Qiagen).
Insert	*GCL* gene was amplified from *E.coli* genomic DNA using primer pair GCL1 and GCL2, restricted with *Nco*I, *Sal*I followed by purification with PCR purification kit (QIAGEN).
Diagnostic restriction	*Xba*I, *Xho*I, expected size 5445 + 1776 bps.

ii) pET-TSR (6315 bps)

Vector	pET22b (+) was restricted with *Nco*I, *Xho*I followed by purification with PCR purification kit (Qiagen).
Insert	*TSR* gene was amplified from *E.coli* genomic DNA using primer pair TSR1and TSR2, restricted with *Nco*I, *Xho*I followed by purification with PCR purification kit (Qiagen).
Diagnostic restriction	*Xba*I, *Xho*I, expected size 5325 + 990 bps.

iii) pET-HGR (6423 bps)

Vector	pET22b (+) was restricted with *Nco*I, *Xho*I followed by purification with PCR purification kit (Qiagen).
Insert	*HGR* gene was amplified from cDNA prepared from human liver mRNA using primer pair HGRl 1and HGR 2, restricted with *Nco*I, *Xho*I followed by purification with PCR purification kit (QIAGEN).
Diagnostic restriction	*Xba*I, *Xho*I 5325 + 1098 bps

iv) pET-AtGDH (7161 bps)

Vector	pET22b(+) was restricted with *Bam*HI, *Xho*I followed by purification with PCR purification kit (Qiagen).
Insert	*AtGDH* coding sequence was amplified from cDNA prepared from young *Arabidopsis* plants using primer pair AtglcD F and AtglcD R, restricted with *Bam*HI, *Sal*I followed by purification with PCR purification kit (Qiagen).
Diagnostic restriction:	*Nco*I, expected size 1139+394+27+5601 bps.

v) pET-EcGO (9219 bps)

Vector	pET22b (+) was restricted with *Nco*I, *Xho*I followed by purification with PCR purification kit (Qiagen).
Insert	*GO* gene was amplified from *E.coli* genomic DNA using primer pair GO in E-coli-Forward and GO in E-coli-Reverse, restricted with *Nco*I, *Xho*I followed by purification with PCR purification kit (QIAGEN).
Diagnostic restriction	*Nco*I, *Xho*I expected size 3788 + 5431 bps.

vi) pET-GOTG (11920 bps)

Vector + Insert	In order to clone *GO*, *TSR* & *GCL* in pRB96, first the three genes were cloned into pET with SD (Shine dalgarno) sequence followed by recloning it into pRB96. As the first step of this cloning, the pET-EcGO construct was used as a vector and was restricted with *Xho*I. *TSR* gene was amplified with the primer pair TSR-SD –F-XhoI and TSR-SD-R-Xho-Hind, restricted with *Xho*I and ligated into pET-EcGO (pET-GO-TSR). pET-GO-TSR was used as a vector to clone *GCL* gene into it. pET-GO-TSR was restricted with *Hind*III and *Bpu*1102I, and purified with PCR purification kit (QIAGEN). *GCL* gene was amplified from pET-GCL using primer pair Gcl-SD-F-HindIII and T7 reverse followed by restriction with *Hind*III and *Bpu*1102I. The restricted insert was purified and ligated in pET-GO-TSR and the construct was named pET-GOTG
diagnostic restriction	First pET-GO-TSR construct was checked with *Xho*I, expected size 889 + 8,000bps. pET-GOTG construct was checked with *Hind*III and *Bpu*1102I expected size 1880 + 10,040 bps.

II)

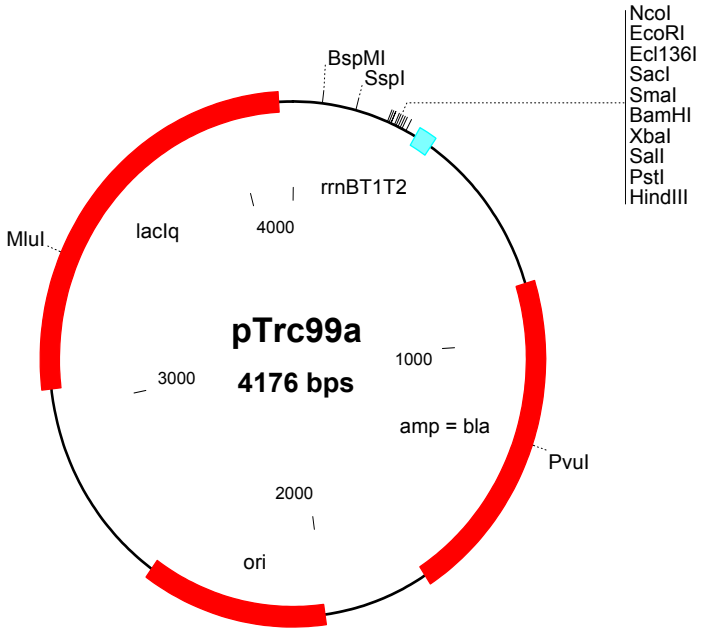

Figure 2.2: Bacterial expression vector pTrc99a (commercial vector, Pharmacia Freiburg).

vii) pTrc99a-AtGDH

Vector	pTrc99a was restricted with *Sal*I, fill in with klenow polymerase followed by restriction with *Bam*HI, followed by purification with PCR purification kit (Qiagen).
Insert	pET-AtGDH construct was restricted with *Bpu*1102I, fill-in with klenow polymerase followed by restriction with *Bam*HI. The restricted sample was separated by agarose gel electrophoresis and 1760 bps was purified from gel (see above).
Diagnostic restriction	*Pvu*I 3751+2203 bps, *Sma*I 4275+1679 bps

viii) pTrc99a-GO (7926 bps)

Vector	pTrc99a was restricted with *Nco*I and *Sal*I, followed by purification with PCR purification kit (Qiagen).
Insert	pET-GO construct was restricted with *Nco*I *and Xho*I, followed by agarose gel electrophoresis and the GO fragment was purified from gel (see methods).
Diagnostic restriction	*Pvu*I, 7034+2185 bps and *Sal*I, 7119+807 bps

III)

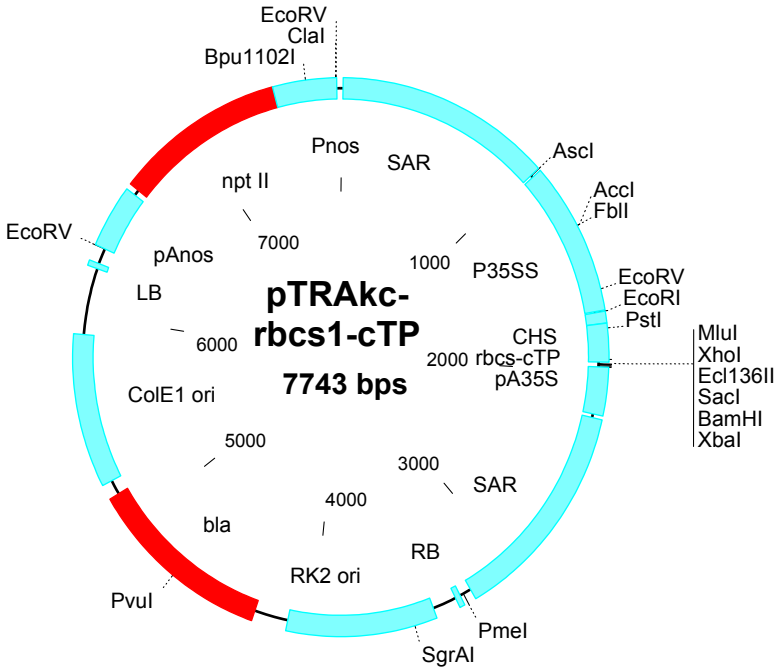

Figure 2.3: Plant expression vector pTRA-K-rbcS1-cTP (7743 bps) (Kindly provided by Thomas Rademacher, BioVII, RWTH-Aachen, Germany).

ix) pTRA-K-rbcS1-cTP-GCL (9601 bps)

Vector	pTRA-K-rbcS1-cTP was restricted with *Ecl*136II, fill-in with klenow polymerase followed by restriction with *Mlu*I. The sample was purified by PCR purification kit (Qiagen).
Insert	*GCL* coding sequence was amplified from pET-GCL constructs using primer pair GCL-Mlu and T7 reverse, restricted with *Bpu*1102I, fill-in with klenow polymerase followed by retriction with *Mlu*I. The restricted sample was purified with PCR purification kit (Qiagen).
Diagnostic restriction	*Bpu*1102I, *Bam*HI, 5606 + 3995 bps.

x) pTRA-K-rbcS1-cTP-TSR (8689 bps)

Vector	pTRA-K-rbcS1-cTP was restricted with *Ecl*136II, fill-in with klenow polymerase followed by restriction with *Mlu*I. The sample was purified by PCR purification kit (Qiagen).
Insert	*TSR* coding sequencewas amplified from pET-TSR construct using primer pair TSR-MLU-NEW and T7 reverse, restricted with *Bpu*1102I, fill-in with klenow polymerase followed by retriction with *Mlu*I. The restricted sample was purified with PCR purification kit (QIAGEN).
Diagnostic restriction	*Bpu*1102I + *Bam*HI 5606 + 3083 bps

xi) pTRA-K-rbcS1-cTP-GCL-TSR (12786 bps)

Vector	pTRA-K-rbcS1-cTP-GCL construct was restricted with *pme*I and *Bpu*1102I. The fragment contains GCL was extracted from gel and was used as vector.
Insert	pTRA-K-rbcS1-cTP-TSR.His was restricted with *Asc*I, fill-in with klenow polymerase followed by retriction with *Bpu*1102I The restricted sample was purified with PCR purification kit (Qiagen) and ligated with vector.
Diagnostic restriction	*Mlu*I and *Xho*I, 7800+2400+1681+889bp bps.

IV)

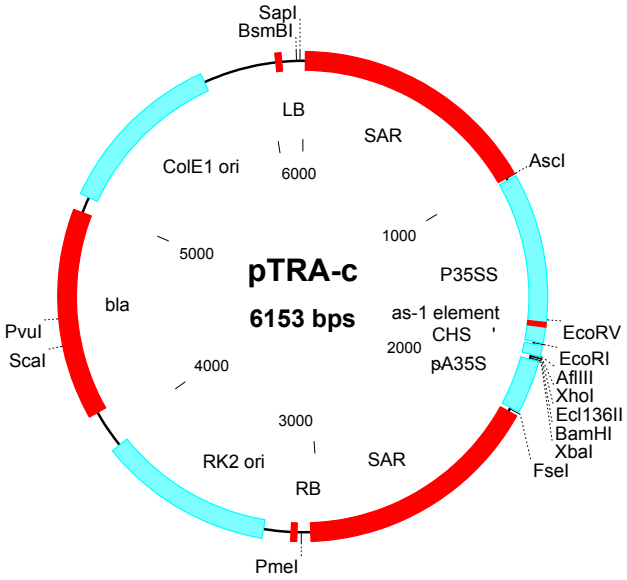

Figure 2.4: Plant expression vector without chloroplast targeting sequence (pTRA-K-c) (kindly provided by Thomas Rademacher, BioVII, RWTH-Aachen, Germany).

xii) pTRA-K-c-gfp-AtGDH (77) (8586 bps)

Vector	pTRA-K-c-gfp .(provided by Thomas Rademacher, BioVII, RWTH-Aachen, Germany) restricted with *Nco*I.
Insert	The coding sequence of first 77 amino acids of N-terminal domain of AtGDH was amplified with primer pair AtglcD -gfp-F and AtglcD-gfp-R using pET-AtGDH constructs as template. The PCR product was restricted with *Nco*I enzyme. The vector and insert was ligated.
Diagnostic restriction	*Asc*I, *Pme*I 3083+ 5503 bps.

xiii) pTRA-K-rfp-AtGDH (77) (8548 bps)

Vector	pTRA-K-rfp (provided by Thomas Rademacher, BioVII, RWTH-Aachen, Germany) restricted with *Nco*I enzyme.
Insert	The coding sequence of first 77 amino acids of N-terminal domain of AtGDH was amplified with primer pair AtglcD-gfp-F, AtglcD-gfp-R using pET-AtGDH constructs as template. The PCR product was restricted with *Nco*I enzyme. The vector and insert was ligated.
Diagnostic restriction	*Asc*I and *Pme*I 3083+ 5503 bps.

2.2 Methods.

2.2.1 Molecular methods.

2.2.1.1 Isolation of plasmid DNA.

Plasmid DNA midi and mini kits (Qiagen and Invitek) were used to isolate plasmid DNA from transformed DH5α bacteria (competent *E.coli* strain) that was transformed with the different constructs according to the instructions provided with these kits. For verification of quality and quantity, 2-5 µl of the total DNA eluate were visualised on a 1 % (w/v) agarose gel containing ethidium bromide.

2.2.1.2 Isolation of plant genomic DNA.

50-100 mg of leaf materials were harvested, frozen into liquid nitrogen and were homogenized with pestle. 500 µl of DNA extraction buffer was added to the homogenized leaf materials. 1 volume of phenol/$CHCl_3$ was added and mixed gently for 10 minutes in a shaker followed by centrifugation at 4700 x g for 10 minutes. The upper phase was transferred to a new tubes and 0.1 volumes of 3 M NaAc (pH 5.2) and 2 volume of ethanol (96 %) was added and mixed well. Genomic DNA was precipitated by incubation for 30 minutes at -20°C followed by centrifugation (15000 x g/4°C/20 min). The resulting pellet was washed with 300 µl of 70 % ethanol, dried and resuspended in 100-200 µl of sterile H_2O.

2.2.1.3 Agarose gel electrophoresis.

All the gel electrophoresis was performed according to Sambrook and Russel (2002).

2.2.1.4 Isolation of DNA fragments from agarose gel.

To isolate DNA fragments (70 bp - 10 kb) from agarose gels, the QIAquick Gel Extraction Kit (Qiagen) was employed according to the manufacturer's instruction.

2.2.1.5 Polymerase chain reaction (PCR).

Polymerase chain reaction (PCR) is a method for enzymatic amplification and modification of a target DNA sequence flanked by two known sequences (Saiki *et al*., 1988). Two synthetic oligonucleotides complementary to the (+)- and (−)-strands, respectively, of this sequence were used as primers. After heat denaturation of the target double-stranded DNA, these primers hybridize to its opposite strands. New (−)- and (+)-strands fragments are then synthesized across the region between these primers by the catalysis of a thermostable *Taq* DNA polymerase. The newly created DNA strands are themselves templates for the PCR primers. Repeated cycles of denaturation, primer annealing, and extension result in an exponential accumulation of the target DNA fragment. The reaction conditions (e.g. template concentration, annealing temperature and extension duration) were optimized for individual experiments (see results) on the basis of standard conditions.

2.2.1.6 Restriction enzyme digestion.

Restriction and Ligation reactions was performed as described in Sambrook and Russel (2002).

2.2.1.7 DNA sequencing.

Sequencing reactions were kindly performed by Jost Muth and colleagues at the institute of Molecular Biotechnology, RWTH Aachen. 20 pmol of the used primers were added to 1.2-1.5 µg of vector and sequencing reactions were performed using the di-desoxy chain termination method with labeled nucleotides and a cycle sequencing protocol (Sanger *et al*., 1977).

2.2.1.8 Isolation of total RNA from plant leaves.

For the extraction of total RNA from transgenic *Arabidopsis* leaves, frozen leaves were ground in liquid nitrogen to a fine powder with a mortar and pestle. Total RNA was extracted using 1 ml of Trizol (Table 2.2) per 150 mg leaf material, mixed for 5 min, and incubated 5 min at room temperature. 0.2 volumes of chloroform was added to induce the separation of organic and aqueous phases, the suspension was then mixed for 5 min and incubated at room temperature for another 5 min. The sample was centrifuged for 10 min (20000 x g/ 4°C). The upper water phase was carefully transferred to a new reaction tube, and then 1 volume

chloroform was added. The sample was mixed for 10 min then was centrifuged 5 min (20000 x g/4°C/10 min). The upper water phase was taken and 2 volumes of 96 % (v/v) ethanol was added to it, mixed for 2 min and incubated 20 min at -20°C. After that, the sample was centrifuged 10 min (20000 x g/4°C/10 min). The RNA pellet was washed with 70 % (v/v) ethanol foloowed by spin down (20000 x g/4°C/10 min). The sample was left some time at room temperature to dry then was resuspended in 30 µl bidest H_2O and visualised on 1 % agarose gel with ethidium bromide.

2.2.1.9 First strand cDNA synthesis from RNA.

The isolated total RNAs samples from transformed *Arabidopsis* plants were digested with DNAse enzyme to remove the genomic DNA. 1 unit of the DNase enzyme was added to 5 µl of the isolated RNA and then the reaction mixture was incubated at 37°C for 10-15 min. The DNase activity in the reaction mixture was stopped by incubation of the sample at 65°C for 15 min then 1µl from the sample was visualised in 1 % (w/v) agarose gel containing ethidium bromide to check whether the genomic DNA was digested or not and to be sure that the RNA was not affected. After that the cDNA was synthesized as follows: 2 µl from the isolated RNA sample were mixed to 10 µl bidest H_2O and 1 µl Oligo-dT 18 primer (10 pmol/µl) then the reaction was incubated 5 min at 65°C, cooled and 2µl dNTPs, 4µl MLvRT buffer (5x reverse transcriptase buffer) and 1.5 units of reverse transcriptase enzyme were added. Then the reaction mixture was incubated for 40 min at 37°C. After that the enzyme activity was stopped by incubation at 65°C for 15 min. For negative samples, the enzyme reverse transcriptase was not added i.e. in the negative samples, no cDNA should be synthesized but conditions are otherwise identical. The synthesized cDNA was used as a template for Real Time PCR amplification.

2.2.1.10 Real Time PCR.

The quantitative or Real Time PCR is used not only for the amplification of specific fragments of DNA but also for the quantitative analysis of the resulting products in each cycle throughout the amplification reaction. In this type of PCR, SYBR Green I is used to give the fluorescence signals that indicate the formation of double stranded DNA and as a result the amount of double stranded PCR product can be measured each cycle by this fluorescence. If fluorescence is plotted against cycle number, the accumulation of PCR products can be visualised on a sigmoidal curve. The melting temperature curves, which are formed as a result

of plotting the first deviation of the fluorescence against temperature help in the identification of the products in addition to other functions (Meuer *et al*., 2001).

The ABI-7000 (Applied Biosystems) was used for the amplification of about 300 bps from the first strand cDNA that was synthesised from the isolated RNA from the transgenic plants in order to check the expression of the genes at the RNA level. The instructions in the qPCR™ Core Kit for SYBR® Green I (Eurogentec) were followed using reading frame specific forward and reverse primers. The resulting products from the Real Time PCR were visualised in 2 % (w/v) agarose gel containing ethidium bromide.

2.2.1.11 Analysis of transcript abundance.

RNA was isolated and first strand cDNA synthesis was performed as described above for the cloning of AtGDH. Quantitative PCR reactions were performed on an ABI PRISM® 7700 Sequence Detection System (Applied Biosystems, Weiterstadt, Germany) following the manufacturer's instructions. Amplifications were performed in the presence of SYBR Green as the fluorescent dye using 2 % of a reverse transcription reaction as a template. Reaction kits were derived from Eurogentec (Cologne, Germany) and oligonucleotides were purchased from Metabion. For the detection of AtGDH transcripts, forward and reverse primers were AtglcD-1353 F1 and AtglcD-1671 R1 respectively, with a final primer concentration of 300 nM in the reaction mixture. For the detection of Actin2 transcripts, primers were Actin2 Fw and Actin2 Rev with a final primer concentration of 900 nM in the reaction mixture. The $MgCl_2$ concentration was always 2 mM and the dNTP concentration 200 µM. Amplification conditions were 10 min of initial denaturation at 95°C, followed by 40 cycles of each 15 s denaturation at 95°C and 1 min combined annealing and extension at 60°C.

2.2.1.12 Subcellular localization of AtGDH.

Plant Expression vectors containing the first 77 amino acids of AtGDH in translational fusion to dsRED (see above) were transferred into *A. tumefaciens* GV3101 by electroporation. The recombinant *A. tumefaciens* were selected in YEB medium containing appropriate antibiotics (rifampicin 100 µg/ml, kanamycin 25 µg/ml, and carbenicillin 50 µg/ml). The construct was transferred to *Arabidopsis* by floral dip transformation (Clough and Bent, 1998) and regeneration of kanamycin-resistant transgenic plants was carried out according to standard protocols. For dsRED localization and mitochondrial staining, leaves were collected from

4 weeks old plants and cut in small pieces. Protoplasts were isolated by incubating the leaf pieces in protoplast isolation buffer (0.5 M D-mannitol, 5 mM MES pH 5.8, 10 mM $CaCl_2$, 3 % (v/v) Rohalase 7069 (Röhm), Rohament PL 2 % (v/v) (Röhm) and 0.12 % (w/v) Mazeroenzyme R-10 (Serva)) at 30°C for 2h. Supernatant containing protoplasts was collected carefully followed by staining with MitoTracker Green (Molecular Probes) as described by the supplier. Images of the protoplasts were taken with a Leica TCS-SP spectral confocal microscope (Leica). Images were acquired with a 1.2 N.A. 63x oil immersion PLAN-APO objective. The entire sample was excited with the 488 nm and 568 nm laser line. The confocal sections were collected using a 515-535 nm emission setting for MitoTracker Green, 570-610 nm emission setting for dsRED and 660-720 nm emission setting for chlorophyll fluorescence.

2.2.2 Microbiological methods.

2.2.2.1 Culture of bacteria.

I) *Escherichia coli*.

E. coli was cultured in LB medium on a roller or shaker at 37°C.

II) *Agrobacterium tumefaciens*.

A. tumefaciens was cultured in YEB medium at 28°C.

2.2.2.2 Transformation of bacteria.

I) Preparation of competent *E. coli* (DH5α) cells for heat shock transformation.

A single colony from a LB plate containing competent bacterial colonies was inoculated into 5 ml LB medium and incubated overnight at 37°C with continuous shaking (200 x g/min). 200 ml LB medium were inoculated with 1 ml of the overnight culture; the cells were left to grow at the same conditions until the OD_{580} reached 0.5 - 0.6. Cells were spun down for 10 min (4791 x g/ 4°C), then washed with 15 ml ice-cold TFBI (Table 2.2), incubated on ice for 10 min and spun down by centrifugation for 10 min (4791 x g/ 4°C). The pellet was resuspended afterwards in 4 ml TFBII (Table 2.2) and 200 µl-aliquots of the suspension were dispensed into prechilled Eppendorf tubes, frozen immediately in liquid nitrogen and stored at -80°C.

II) Transformation of competent *E. coli* (DH5α) by heat-shock

As soon as the competent cells were thawn, plasmid DNA (up to 100 ng) or 1-3 µl from the ligation products were mixed gently with the competent cells and then incubated on ice for 30 min. The cells were incubated at 42°C for 90 seconds and placed on ice for 2 min. 1ml of LB medium was added immediately to the tubes containing the heat shocked bacteria and transformed cells were incubated at 37°C for 45 min with continuous shaking (200 x g). 200 µl of the transformed cells were plated onto LB-agar plates supplemented with ampicillin and incubated at 37°C overnight.

III) Preparation of competent *Agrobacterium* cells for electroporation.

A single colony of *Agrobacterium tumefaciens* grown on YEB-agar plates containing 100 µg/ml rifampicin (rif) and 25 µg/ml kanamycin (Kan) (YEB-rif-kan) was inoculated in 5 ml of YEB-rif-kan medium in a 100 ml Erlenmeyer flask and incubated at 28°C for two days with shaking (200 x g). 1 ml of the culture was transferred into 400 ml of YEB-rif-kan

medium and the culture was incubated at 28°C for 15-20 h with shaking (200 x g) until the $OD_{660\ nm}$ reached 1-1.5. The cells were chilled on ice for 15 min and spun down by centrifugation (4791 x g/4°C/5 min). The culture medium was decanted and the cells were washed three times with 100 ml, 50 ml and 25 ml HEPES buffer I (Table 2.2), respectively, and one time with 10 ml HEPES buffer II (Table 2.2). The cells were centrifuged (4791 x g/4°C/5 min) and resuspended in 500 µl of sterile HEPES buffer II (Table 2.2). 45 µl aliquots of the suspension were dispensed into prechilled Eppendorf tubes, frozen immediately in liquid nitrogen and stored at -80°C.

IV) Transformation of *Agrobacterium* by electroporation.

0.2-1.0 µg of plasmid DNA in dest. H_2O was added to a thawn aliquot of *Agrobacterium* electrocompetent cells and incubated on ice for 3 min. The cell/DNA mixture was transferred into a prechilled electroporation cuvette (0.2 cm) and assembled into a safety chamber. After application of the pulse (25 µF, 2.5 kV, 200 Ω), the cells were diluted in 1 ml of YEB medium in a 2.0-ml tube and incubated at 28°C with shaking (200 x g) for 2 h. Finally, 1-10 µl of the cells were plated on YEB-agar containing 50 µg/ml rifampicin (rif), 25 µg/ml kanamycin (kan) and 50 µg/ml carbenicillin (carb) (YEB-rif-kan-carb plates) and incubated at 28°C for 2-3 days.

2.2.2.3 Complementation analysis.

Complementation analyses were done with mutants of *E. coli* deficient in any of the three subunits forming the active endogenous glycolate oxidase (Pellicer *et al.*, 1996). All of the transformed bacteria were grown for 2 days in minimal medium (Miller, 1972) using glycolate as a sole carbon source supplemented with the appropriate antibiotics (25 µg ml^{-1} chloramphenicol, 100 µg/ml ampicillin). The cells were diluted in fresh medium and allowed to grow until the OD reached 0.7. The cells were spun down at 2.000 x g and resuspended in 100 µl of minimal medium and were serially diluted from 10^{-1} to 10^{-5}. 10 µl of the cells from each dilution were spotted on plates containing minimal medium, antibiotics, and 1mM IPTG for the induction of recombinant protein expression. The plates were then incubated at 37°C for 3 days.

2.2.3 Biochemical methods.

2.2.3.1 Recombinant protein expression in bacteria.

The constructs were transformed into the bacterial strain ER2566 (see above). For protein expression, a 2 L culture of LB-medium was grown up to an OD_{600} of 0.4. The expression of the proteins was induced by adding 1 mM IPTG and culture growth was continued for 2 h at 37°C. The cells were washed once in 10 mM potassium phosphate (pH 8.0) and were resuspended in the same buffer to give a 15-20 % (v/v) cell suspension. After the cells were lysed by sonication on ice (40 % duty cycle, 2 x 1 min, Sonicator Bandelin Sonopuls GM 70, Berlin), the extract was centrifuged for 30 min at 30,000 x g. The presence of specific protein in the supernatant was tested by Western Blot using an Anti-His-HRP conjugate (Qiagen) following the protocol provided by the supplier.

2.2.3.2 Extraction of proteins from bacterial cells.

Proteins were extracted from bacterial cells either by ultrasonication or by lysozyme method.

I) Ultrasonication method.

Single colonies of bacterial cells were inoculated in 5 ml LB medium with appropriate antibiotics and were grown overnight at 37°C. The overnight grown bacterial cultures were diluted 100x and were grown until it reaches in logarithmic phase. 50 ml of bacterial culture from the logarithmic growth phase was centrifuged (4791 x g/4°C/10 min) to collect cells. The resulting pellet was washed twice with 20 ml of extraction buffer, resuspended in 1 ml of extraction buffer, and transferred to 2 ml Eppendorf tubes for ultrasonication. Ultrasonic cell disintegration was performed on ice by 40 % duty cycle, 2 x 1 min (Sonicator Bandelin Sonopuls GM 70, Berlin) with a 30 sec interval between two of them. The cell debris was pelleted by centrifugation (15000 x g/4°C/20 min), and the supernatant was transferred to fresh tubes on ice and used for determinations of protein concentrations and enzyme activities.

II) Lysozyme method.

The bacterial cultures were grown in the same way as described for protein extraction by ultrasonication until OD reaches at logarithmic phase. The cells were collected by centrifugation (4791 x g/4°C/10 min). The resulting pellet was washed twice with resuspension buffer (see buffer sections) and resuspend in resuspension buffer containing 5 mg/ml lysozyme, 5 mM DTT and an appropriate amount of DNAse. The cells were then

incubated either at room temperature or in ice depending on further experiments. The cells debris was pelleted by centrifugation (30000 x g/4°C/20 min) and the supernatant was transferred to fresh tubes on ice and used for the determination of protein concentrations.

2.2.3.3 Extraction of proteins from plant leaves.

For the extraction of proteins from plant leaves, the frozen leaves were ground in liquid nitrogen to a fine powder with a mortar. 700 µl of protein extraction buffer (Table 2.2) was added to the grounded leaf followed by centrifugation (30000 x g/15 min/4°C). The supernatant was taken in a 1.5 ml eppendorf tube, again centrifugation (30000 x g/15 min/4°C). The pellet was discarded and the supernatant was transferred into a new 1.5 ml eppendorff tube. The concentration of protein in the supernant was measured using Bradford solution and the protein was stored at an appropriate temperature.

2.2.3.4 Determination of protein concentrations in leaf extracts.

Proteins were determined according to the method described by Bradford (1976). 2 µl of leaf extract was mixed with 1 ml of Bradford reagent (buffer section). After 15 min incubation at RT, the extinction at 595 nm was measured against a reagent blank prepared from 2 µl of the corresponding extraction buffer and 1 ml of Bradford reagent. Bovine serum albumin (pH 7.0, Serva) was used as a standard in a range between 1 and 10 µg.

2.2.3.5 Purification of proteins by Ni-NTA column.

A single colony of *E.coli* strain ER2566 harboring recombinant plasmid DNA was inoculated in 5 ml of LB medium containing 100µg/ml ampicillin and cultivated over night at 37°C. 1 ml of the o/n culture was transferred into 1000 ml LB + Amp medium and cultured at 37°C to OD_{600nm} of 0.4-0.6. The culture was induced for 1-3 hrs at the same temperature by addition of IPTG to a final concentration of 1 mM. Cells were harvested by centrifugation (4791 x g/4°C/10 min) and resuspended in 5 ml of cold protein lysis buffer. The cells were then disrupted by ultrasonication or lysozyme (2.2.3.2). The His-tagged protein of interest was affinity purified by IMAC. A 0.5 cm (diameter) x 20 cm (lenth column (Bio-Rad) was packed with 150 µl of prosep chelating matrix. The cleared supernatant was then applied to the column. Non-specifically bound proteins were removed by washing with 10 column volume of protein-wash-buffer I and protein-wash-buffer II. Ni-NTA bound His-tagged proteins were eluted using 3x 100 µl of protein elution buffer.

2.2.3.6 Isolation of chloroplast from *Arabidopsis* plants leaves.

2 g of leaves from 4 weeks old *Arabidopsis* plants were ground in 80 ml of icecold GB in a ultrathorax (1x 10 sec; 75% power) followed by filtration through two layers of miracloth (biochem.). The chloroplasts were pelleted by centrifugation at 10000 x g for 1 min in a SS34 rotor (Sorvall). The resulting pellet was resuspended in 1 ml 1x SH buffer. 0.5 ml of resuspended solution was overlayed with 1 ml of 35% percoll-buffer (in 2 ml eppendorf tube) followed by centrifugation for 3 minutes at 500 x g in 4°C. The supernatant was carefully taken off and the pellet was washed with 1x SH and centrifuged at 4500 x g for 1 min at 4°C. The washing step was repeated once more and the pellet was resuspendedin 200 µl 1x SH buffer.

2.2.3.7 SDS-Polyacrylamide Gel electrophoresis.

Discontinuous SDS-polyacrylamide gels (for the stacking gel: 5 % (w/v) acrylamide/bisacrylamide 29:1, 0.125 M Tris/HCl, pH 6.8; for the separating gel: 10 % (w/v) acrylamide/bisacrylamide 29:1, 0.375 M Tris/HCl, pH 8.8) were used for the separation of protein samples under denaturing conditions according to Laemmli (1970). The BIO-RAD MINI PROTEIN II apparatus was used for all gel electrophoresis. After preparation, each protein sample was mixed with 5 x SDS-PAGE-samples buffer (Table 2.2), boiled at 95°C for 5 min, chilled on ice and spun down for 5 seconds. Then the boiled sample was loaded into submersed wells. 1 x SDS-PAGE electrophoresis buffer (Table 2.2) was used for the electrophoresis that was performed for 120 min at 120 V/cm. Separated proteins were visualised by gel staining with Coomassie brilliant blue (2.2.3.8) or transferred onto a nitrocellulose membrane for Western blot analysis (2.2.3.9) (Ausubel *et al*., 1994).

2.2.3.8 Coomassie brillant blue staining.

Protein precipitation and non-specific protein staining with coomassie blue (Wilson, 1993) was used to visualize protein bands. The separating gel was placed carefully in coomassie dye solution (2.1.4) and stained for 30 min at room temperature while shaking gently. Non-specific background staining was removed using coomassie-destaining solution overnight at room temperature.

2.2.3.9 Western blot.

Electrophoretically separated proteins were transferred from a SDS-PAGE gel to a Hybond™-ECL™-nitrocellulose membrane (0.45 µm). A nitrocellulose membrane piece was cut according to the gel dimensions and soaked in transfer buffer (Table 2.2) for few minutes. The opened gel holder was positioned in a way that the gray panel (cathode) lays flat on the bottom. Then a pre-soaked fiber pad was put on the gray panel of the cassette. Two pieces of transfer buffer saturated Whatman filter were placed on top of the fiber pad and overlaid with 5ml transfer buffer. The equilibrated gel was carefully transferred on top of the filter papers. The gel surface was covered with transfer buffer and the pre-wetted nitrocellulose membrane was put on the top of the gel. A glass pipette was rolled over the top of the membrane to remove all air bubbles from the area between the gel and the membrane. The surface of the membrane was submersed with buffer, the sandwich completed by placing two pieces of saturated Whatman filter papers on the top of the membrane and a saturated fiber pad was put on the top of the filter papers. The cassette setup was closed and the gel holder was transferred to the buffer tank so that the gray panel of the holder faced the black cathode electrode panel. The tank was filled with transfer buffer and placed in an icebox. Protein transfer was performed at 250 mA for 1h. Upon completion of the protein transfer, the remaining free binding sites on the membrane were washed two times 10 min each with TBS buffer (Table 2.2) at room temperature then incubated 1h or over night in blocking buffer (Table 2.2) at 4°C. The blocked membrane was washed 4 times 10 min each at room temperature with TBS-Tween/Triton buffer (Table 2.2) and two times for 10 min each with TBS buffer then incubated in Anti-His HRP conjugate solution (Qiagen) containing 1/2000-1/1000 dilution of antibody in blocking buffer (Qiagen) at room temperature for 1h.
Then the membrane was washed 4 times for 10 min, each time with TBS-Tween/Triton buffer (Table 2.2) at room temperature and 2 times 10 min each with TBS buffer (Table 2.2) at room temperature. Lumi-Light Western blotting substrate (lumi-light stable peroxide solution : lumi-light luminol/enhancer solution = 1:1 from Roche Diagnostics GmbH, Mannheim, Germany) was added and incubated in dark for 5 min then luminescence was recorded on a LAS3000 CCD camera (Raytest) according to the manufacturer's recommendations.

2.2.3.10 Enzymatic assays.

I) Tartronic semialdehyde reductase (TSR) assay.

Tartronic semialdehyde reductase activity was assayed according to Kohn and Jakoby (1968). Preparation of tartronic semialdehyde: A 50 mM solution of lithium hydroxypyruvate was adjusted to pH 10.5 and incubated at 0°C until aliquots of the solution revealed no further increase in absorbance at 272 nm; a period of 2 hours was sufficient. After adjustment to pH 6.5 with HCl, the resulting solution provided tartronic semialdehyde in 50 to 75 % yield, with hydroxypyruvate representing the chief contaminant.

Measurment of tartronic semialdehyde reductase activity was conducted at 25°C and followed spectrophotometrically by measuring the decrease in absorbance at 340 nm resulting from the utilization of reduced pyridine nucleotide. In a total volume of 1.0 ml were included the following: potassium phosphate at pH 6.3, 200 mM; NADH, 0,2 mM; crude extract from induced and non-induced bacterial culture, 30 µg; and an amount of tartronoic semialdehyde equivalent to 5 mM lithium hydroxypyruvate used for its preparation as described above.

II) Glyoxylate carboligase (GCL) assay.

Glyoxylate carboligase was assayed according to Gotto and Kornberg (1961).

The activity of glyoxylate carboligase was assayed spectrophotometrically by measurement of the rate of oxidation of NADH when this enzyme was incubated with glyoxylate, in the presence of its required cofactor Mg^{2+} ions and thiamine pyrophosphate, and an excess of tartronic semialdehyde reductase. The complete system contained in 1 ml: 100 mM potassium phosphate, pH 7.5; 5 mM $MgCl_2$; 0.5 mM thiamine pyrophosphate; 0.2 mM NADH; 30 µg of crude extracts from induced bacterial culture containing tartronic semialdehyde reductase and 30 µg of crude extract from bacterial culture containing GCL enzyme or soluble protein from plants. OD_{340nm} was recorded for 1-2 min after which the reaction was started by addition of 6 mM sodium glyoxylate.

III) Glycolate dehydrogenase (GDH) assay.

Glycolate dehydrogenase activity was assayed according to Lord (1972). Bacterial cell extract containing 100 µg of protein was added to 100 µmoles of potassium phosphate (pH 8.0), 0.2 µmole of DCIP, 0.1 ml of 1% (w/v) PMS, and 10 µmoles of potassium glycolate. At fixed time intervals, individual assays were terminated by the addition of 0.1 ml of 12 M HCl. After standing for 10 min, 0.5 ml of 0.1 M phenylhydrazine·HCl was added. The mixture was

allowed to stand for a further 10 min, and then the extinction due to the formation of glyoxylate phenylhydrazone was measured at λ_{324nm}.

IV) Lactate dehydrogenase assay.

Lactate dehydrogenase activity was assayed according to Gutheil (1998). Cell extract containing 50 µg of protein was added to a 1 cm cuvette containing 4.8 mM NAD^+ and 1.0 mM D-lactate or L-lactate, respectively, in 0.1 mM Tris·HCl, pH 8.5, in a final volume of 1 ml and the activity was determined from the progress curve at λ_{340nm}. As an inhibitor, 1 mM KCN was added to the reaction mixture before addition of the protein extract.

2.2.4 Plant culture, Generation and characterization of transgenic plants.

2.2.4.1 Transformation of *Arabidopsis* plants through *Agrobacterium*-mediated floral dip transformation.

I) Preparation of *Agrobacterium*

A single colony of *Agrobacterium tumefaciens* carrying the recombinant plasmid was inoculated into 5 ml YEB medium (with 100 µg/ml rifampicin, 25 µg/ml kanamycin, 100 µg/ml carbenicillin) (Table 2.2) to prepare the pre-culture. The culture was incubated at 28°C for 2 days with shaking at 150 x g. The previous pre-culture was inoculated to 200 ml YEB medium (100 µg/ml rifampicin, 25 µg/ml kanamycin, 100 µg/ml carbenicillin) and incubated 2 days at 28°C with strong shaking at 200 x g. Cells were spun down at 4791 x g at 4°C for 20 min. The pellet was resuspended in 5 % sucrose till OD_{600} 0.8. Then 0.04 % silwet L-77 (400 µl/1000 ml) was added to the resuspended cells and the cells were used directly for floral dip transformation of *Arabidopsis thaliana*.

II) Transformation of *Arabidopsis* plants (floral dip transformation).

Transformation was performed as described by Clough and Bent (1998) as follows:

The *Arabidopsis* wild type seeds were allowed to grow for three weeks under short day conditions (8h light, 16h dark at 20°C). The growing plants were transferred to a long day conditions (16h light and 8h dark at 23-25°C) to enhance the flower production. The first bolts were clipped to encourage the proliferation of many secondary inflorescences. The *Agrobacterium tumefaciens* containing the desired constructs were prepared as described before. The above ground parts of the *Arabidopsis* plants were dipped in the *Agrobacterium* solution for 3 to 10 mins.

The dipped plants were placed under a dome or cover for 16 to 24 hours in order to maintain high humidity. The plants were then transferred to normal growth conditions (16h light and 8h dark at 23-25°C). The loosed bolts were tied with wax paper and after seed maturation, watering the plants was stopped and the dry seeds were harvested and were then selected on MS medium containing the respective antibiotics.

III) Selection of the transgenic plants.

The harvested seeds were sterilized by submerging in 75 % (v/v) ethanol for 15 min then washed three times with 98 % (v/v) ethanol, and then the seeds were left to dry on a sterile whatman paper. The seeds were selected by using antibiotic or herbicide selectable markers. Per Plate 40 mg = 2000 seed (resuspended in 4 ml 0.1 % (w/v) agarose) on 0.5 x MS/0.8 % tissue culture agar plates with 50 ug/ml kanamycin, cold treat for 2 days, and grown in short day conditions (light intensity, 50-100 microEinsteins) for 10-15 days. Then the plants, which survived, were transferred to soil and allowed to grow for 10 days in the same conditions and were then transferred to the long day conditions to enhance flowering and seed production.

2.2.4.2 Stable transformation of tobacco through *Agrobacterium*-mediated transformation.

I) Preparation of *Agrobacterium*.

The constructs were transformed into Agrobacteria by electroporation and selected in appropriate antibiotics. A single positive colony (checked by PCR) was inoculated in 5 ml YEB medium containing appropriate antibiotics. The culture was grown for 2 days at 28°C and used as a preculture. The preculture was diluted 100 x and inoculated in 100 ml YEB medium with appropriate antibiotics and was grown overnight at 28°C. The cells were spun down in falcon tube by centrifugation (4792 x g/20 min/4°C) from the overnight grown culture and resuspended in 100 ml induction medium followed by overnight incubation at 28°C. The cells were pelleted in the morning by centrifugation (4791 x g/20 min/4°C). and resuspended in MMA medium to OD_{600} 0.8. The culture was further incubated 1h at room temperature without shaking.

II) Infiltration.

Wildtype tobacco plants were grown on MS medium in weck glasses. The youngest leaves (length up to 6 cm) from 6 weeks old plants were used for transformation. Each leaf was cut into 6-8 pieces (avoiding the midrib) and transferred into weck glasses (sterile) containing 50-100 mL of agrobacteria suspension in MMA medium (see above) followed by incubation at

room temperature for 30 minutes. The leaf pieces were transferred onto sterile water-wetted Whatman filters in plastic dishes, closed with saran wrap and incubated at 26-28°C in the dark for two days. The leaf pieces were washed with distilled water containing 100 µg/mL kanamycin, 200 mg/ml claforan and transferred onto MS-II plates. The plates were closed with saran wrap and incubated at 25°C (16h light) for 3-4 weeks.

III) Selection of transgenic plants.

After 3-4 weeks in the MS-II medium shoots were appearing from the infiltrated leaf pieces. The shoots were cut out and transferred onto MS-III plates containing appropriate antibiotics followed by incubation at the same conditions as described for MS-II medium. After 10-14 days, while roots appeared from the shoot, the regenerants were transferred into weck glasses containing MS-III medium and were incubated (same conditions) until they could be transferred to soil (1-2 weeks).

3 RESULTS.

3.1 A novel pathway aiming to increase the CO_2 fixation in C_3 plants.

The aim of this PhD thesis is to build up a biochemical pathway inside the chloroplast of tobacco plants in order to increase the CO_2 concentration in the vicinity of Rubisco that will subsequently suppress the photorespiration resulting in an improvement of CO_2 fixation. C_3 plants will benefit from this pathway in two ways: CO_2 production inside the chloroplast and shortcircuiting of photorespiration avoiding the loss of CO_2 and NH_3 inside the mitochondrium.

Figure 3.1 shows the proposed pathway in the background of the photorespiratory pathway According to this pathway, phosphoglycolate produced from the oxygenase reaction of Rubisco is phosphorylated to glycolate by phosphoglycolate phosphatase which is present in the chloroplast. The glycolate is then converted to glyoxylate by an oxygen independent glycolate dehydrogenase (GDH). Two molecules of glyoxylate are condensed in a process catalyzed by glyoxylate carboligase (GCL), which simultaneously decarboxylates the condensation product to tartronic semialdehyde. In this reaction, CO_2 is released because of the decarboxylation reaction. Tartronic semialdehyde is reduced to glycerate by the enzyme tartronic semialdehyde reductase (TSR). Glycerate is subsequently phosphorylated to glycerate-3-phosphate by a reaction catalyzed by glycerate kinase which is present in the chloroplast of C_3 plants. In the final step, Glycerate-3-phosphate enters into the Calvin cycle and is used in the biosynthesis of carbohydrates and in the regeneration of RuBP. The photorespiratory pathway has been described in chapter 1.2.

Three genes namely *GO*, *TSR* and *GCL* that are required to establish the pathway inside the chloroplast of C_3 plants are highlighted in Figure 3.1.1 in red. In order to complete the above pathway inside the chloroplast of the C_3 plant, *Nicotiana tabacum*, all the three genes have been cloned in both prokaryotic and plant expression vectors. The cloning, level of expression in both prokaryotes and plants, and the enzymatic assays will be discussed in the next chapters of this thesis.

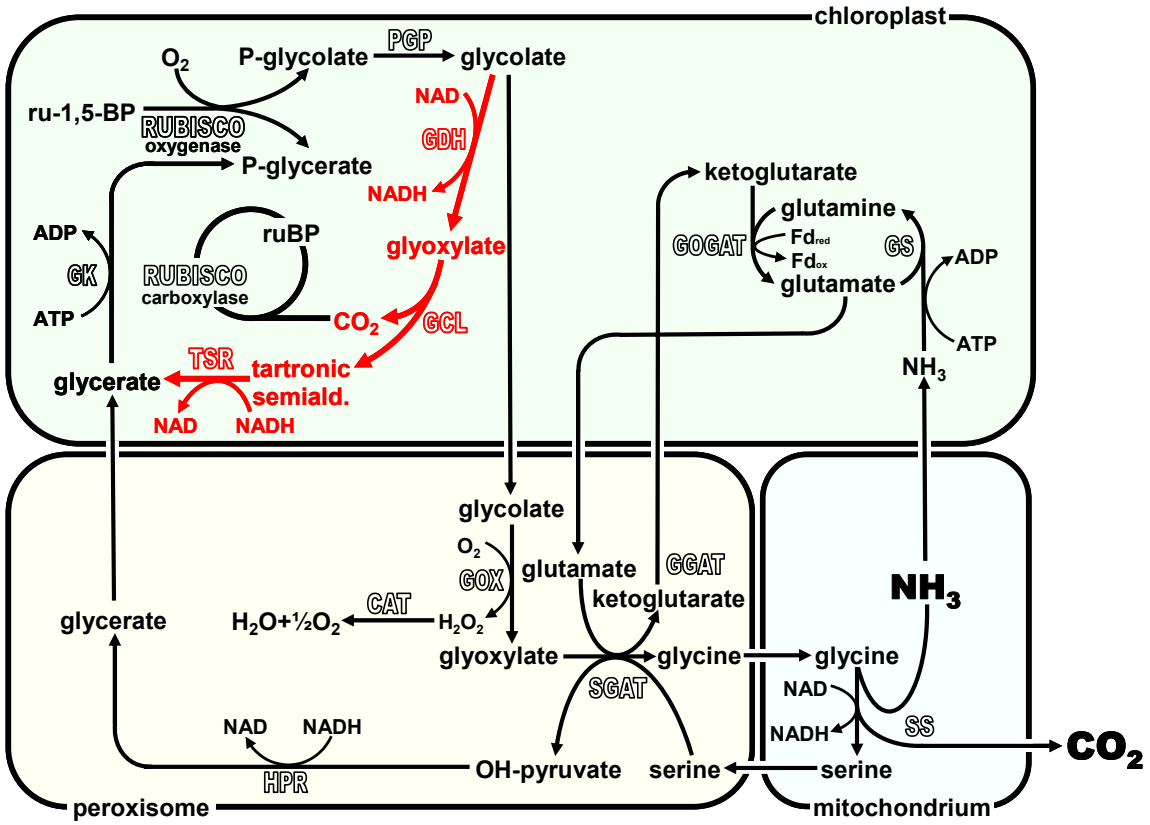

Figure 3.1: The proposed pathway for the conversion of glycolate to glycerate in the background of the photorespiratory cycle.
The oxygenase reaction of RUBISCO results in the formation of P-glycerate and P-glycolate. P-glycolate is dephosphorylated by PGP forming glycolate that is oxidized by GOX to form Glyoxylate. Two molecules of glyoxylate are condensed by GCL forming tartronic semialdehyde and CO_2 is released in the chloroplast. Tartronic semialdehyde is then reduced by TSR forming glycerate. Glycerate is phosphorylated by GK to form P-glycerate that is used directly for carbohydrate biosynthesis through the Benson Calvin cycle. PGP = phosphoglycolate phosphatase; GDH = glycolate dehydrogenase; GCL = glyoxylate carboxyligase; TSR = tartronic semialdehyde reductase; GK = glycerate kinase, the photorespiratory enzymes are described in chapter 1.2.

3.1.1 Construction of a prokaryotic expression vector carrying the *TSR* gene from *E. coli*.

The *TSR* coding sequence from *E. coli* was cloned into a bacterial expression vector as a N-terminal translational fusion to a His-tag (2.1.9). The construct was used for over expression in bacteria and the crude extracts from induced bacterial culture were used in order to characterize the enzymatic properties of the over expressed fusion protein before plant transformation.

The full length coding sequence of *TSR* gene was amplified by PCR from the genomic DNA of *E. coli*. The PCR product was cloned into a bacterial expression vector (pET 22b+) (2.1.9) as a N-terminal translational fusion to a His-tag. Plasmid DNA isolated from ampicillin-resistant clones was analyzed by restriction using the restriction endonucleases *Nco*I and *Xho*I (data not shown). The clones that showed the right restriction patterns were further checked by sequencing and the one that showed no mutation compared to the wild type sequence were chosen for further application.

3.1.2 Expression analysis of *TSR* gene in bacteria.

The expression levels of the recombinant proteins in the transformed bacteria were tested by Western blot analysis (2.2.3.9). The construct was transformed into the bacterial strain ER2566 (2.1.5) and was induced for over expression of *TSR* using 1mM IPTG.

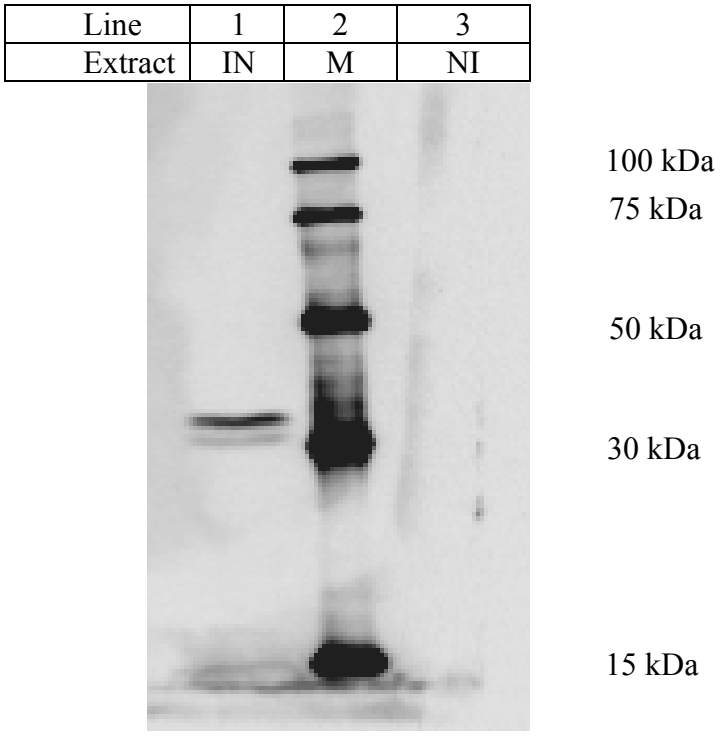

Figure 3.1.1: Expression of the *TSR* gene in bacteria.
The figure shows the Lumi Light mediated light emission of His tagged proteins in a Western Blot analysis. 15 µg of *E. coli* protein extract were separated on a 10 % SDS-PAGE gel and transferred to a nitrocellulose membrane. His-tagged proteins were detected using an anti-His_5 antibody covalently linked to horseradish peroxidase**.** Luminescence was recorded on a LAS3000 CCD camera. Lane1 = total soluble proteins from induced bacterial culture; Lane2 = 6x his tagged protein marker; Lane3 = total soluble proteins from non-induced bacterial culture.

The soluble proteins were extracted (2.2.3.3) from the bacterial cell and were subjected to western blot analysis for the detection of the His-tagged TSR protein. Figure 3.1.1 shows the result of the western blot analysis. A single band (lane 1) of the expected size was detected in the extract from induced bacteria, whereas no band was detected (lane 3) in the protein extract of non-induced bacteria that was also transformed with the construct containing the *TSR* gene. In lane 2, 6x His tagged protein marker was used to determine the size of the protein band. The result shows that a protein band of the expected size was easily detectable in the induced protein extract whereas it was not detected in non-induced bacterial protein extract.

3.1.3 Enzymatic activity assay of TSR protein in vitro.

The enzymatic activity of tartronic semialdehyde reductase (TSR) was assayed spectrophotometrically by measuring the rate of oxidation of NADH. Tartronic semialdehyde was used as a substrate that was prepared from lithium hydroxypyvurate (2.2.3.10). The reaction is catalyzed by TSR as follows:

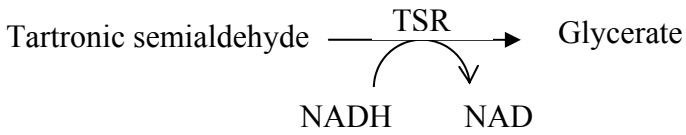

When the crude extract from the over expressing bacteria was added to the cuvettes containing tartronic semialdehyde and NADH, OD_{340nm} of the solution decreased rapidly (Figure 3.1.2). The reduction rate was much lower when a similar quantity of crude extract from the non-induced bacterial culture was used. It was expected that the non-induced crude extract should show some reduction since there are other reductases and their substrates present in the bacterial crude extract which also can reduce NADH. The reaction in which the substrate was omitted also showed some activity proving the presence of the substrate for those bacterial reductases (Figure 3.1.2, W/O subs). Initially, a high background activity was observed in the enzymatic assays (data not shown). Therefore, an ultracentrifugation step was included into the protocol resulting in a reduction of the background activity. In order to be free from the background activity, TSR enzyme was purified by Ni-NTA column chromatography. Unfortunately, for some unknown reason, the purified enzymes loose most of its activity during the purification procedure (data not shown).

The *TSR* gene was also cloned into pET vector without fused to His-tag. The enzymatic activity has been measured from the crude extract from induced bacteria in the same way as described for the His-tagged TSR protein. In both cases, TSR fused to His-tag and without His-tag, shows similar activity. This proves that the histidine residues fused to TSR do not interfere with its activity. It is concluded from the result of the enzymatic assays that the enzyme is active *in vitro*. So the enzyme is suitable for transformation into the plant.

	1	2	3
Extract	IN	NI	IN
Substrate	+	+	-

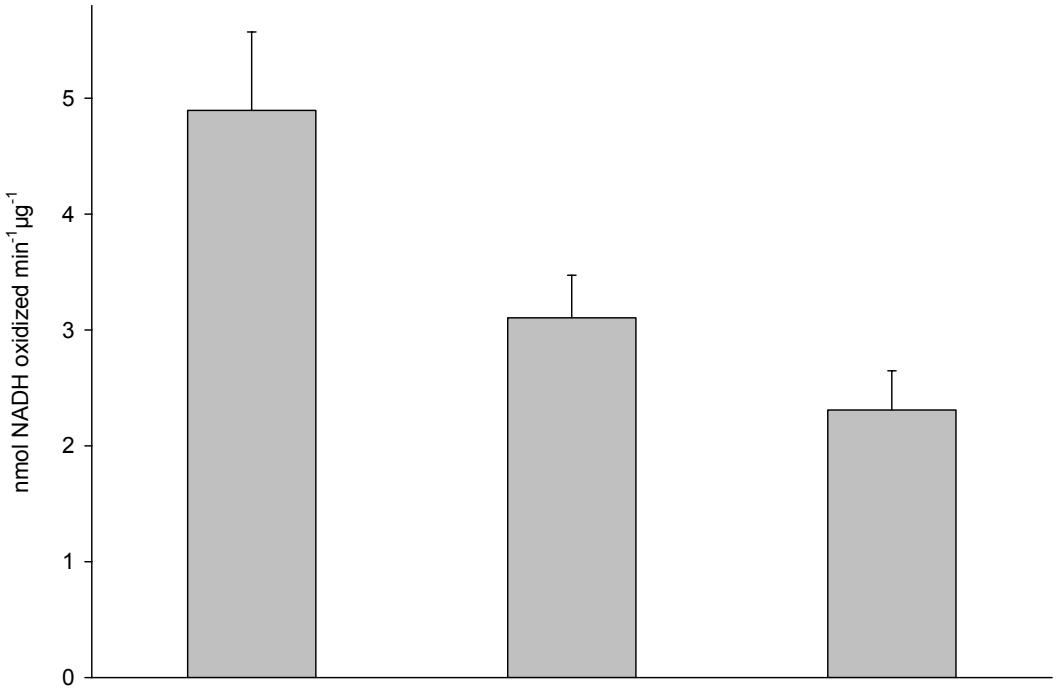

Figure 3.1.2: Measurement of tartronic semialdehyde reductase activity *in vitro*.
Shown is the tartronic semialdehyde dependent oxidation of NADH in crude extracts from bacteria. Each data point shows the amount of NADH reduced per minute and is based on at least three independent experiments. Vertical bars show standard deviations. IN = extract from induced bacterial culture; NI = extract from non-induced bacterial culture.

3.1.4 Construction of a prokaryotic expression vector carrying the *GCL* gene from *E. coli*.

The coding sequence of *GCL* from *E. coli* was cloned into a bacterial expression vector as a N-terminal translational fusion to a His-tag in the same way as described for *TSR*. Like the *TSR* construct, the *GCL* construct was also over expressed in bacteria and the crude extract from over expressed bacterial culture has been used in order to characterize the enzymatic properties of the fusion protein before plant transformation.

The full length coding sequence of the *GCL* gene was amplified by PCR from the genomic DNA of *E. coli*. The PCR product was cloned into a bacterial expression vector (pET 22b+) (2.1.9) as a N-terminal translational fusion to a His-tag (as described for *TSR*). Plasmid DNA isolated from ampicillin-resistant clones was analyzed by both restriction and sequencing.

3.1.5 Expression analysis of the *GCL* gene in bacteria.

The *GCL* gene was expressed in the bacterial strain ER2566 in the same way as described for *TSR*. The soluble proteins from bacterial cells were subjected to Western blot analysis to detect the His-tagged GCL protein. At the beginning, a very faint band was detected meaning that the expression level of the *GCL* gene in bacteria is very low. The His-tagged GCL protein was purified using Ni-NTA column chromatography and again subjected to western analysis. Figure 3.1.3 shows the result of the western blot.

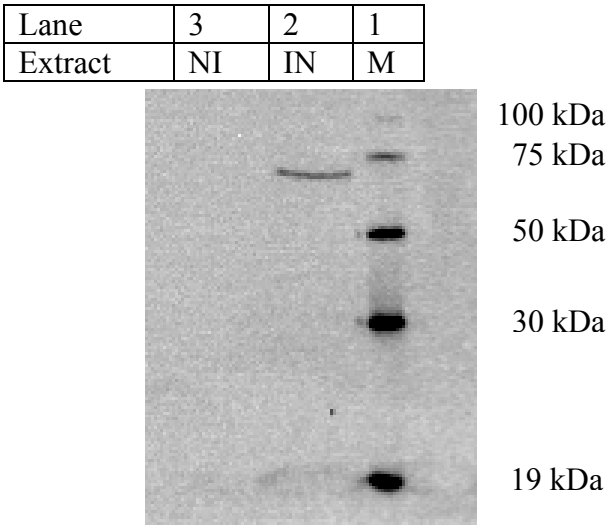

Figure 3.1.3: Expression of the *GCL* gene was analyzed in bacteria by western blot analysis.
The figure shows the Lumi Light mediated light emission of His tagged proteins in a Western Blot analysis. Proteins were purified by Ni-NTA column chromatography, separated on a 10 % SDS-PAGE gel and transferred to a nitrocellulose membrane. His-tagged proteins were detected using an anti-His_5 antibody covalently linked to horseradish peroxidase**.** Luminescence was recorded on a LAS3000 CCD camera. Lane1 (from right) = His-tagged marker; Lane2 (from right side) = total soluble proteins from induced bacterial culture; Lane3 (from right) = total soluble proteins from non-induced bacterial culture.

When the purified GCL protein was subjected to Western blot analysis, a single band was visible at the expected position (lane 2) which corresponds to the GCL protein fused to the His-tag protein. In lane 1, 6x his protein marker was used in order to determine the size of the

protein and in lane 3, an extract from non-induced bacterial culture was used as negative control and no band was detected as expected. So the *GCL* gene was expressed in bacteria at very low level, but it is detectable after enrichment.

3.1.6 Enzymatic activity assay of GCL protein *in vitro*.

The enzymatic activity of glyoxylate carboligase was assayed spectrophotometrically by measuring the rate of NADH oxidation (2.2.3.10). The reaction catalysed by glyoxylate carboligase in which tartronic semialdehyde is produced from glyoxylate was problematic to assay spectrophotometrically because this reaction does not produce or utilize NADH or NADPH. The problem was overcome by coupling this assay to the tartronic semialdehyde reductase assay. So the condensation and decarboxylation reaction catalyzed by glyoxylate carboligase in which TS (tartronic semialdehyde) is produced was coupled to the reduction of tartronic semialdehyde, catalyzed by tartronic semialdehyde reductase. The reaction of the enzymes is as follows:

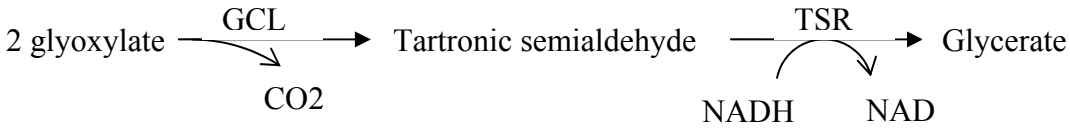

The enzymatic assay was started by adding the crude extracts from bacteria (in which the genes, *TSR* and *GCL,* were over expressed) into the cuvettes containing glyoxylate and NADH. At E_{340nm}, the absorbance of the solution decreased rapidly (Figure 3.1.4, IN TSR + IN GCL). The reduction rate was lower when a similar quantity of crude extract from induced bacterial culture containing either tartronic semialdehyde reductase (IN TSR) or glyoxylate caboligase (IN GCL) was used. The crude extract from the non-induced bacterial culture also shows some activity (NI TSR + NI GCL) as described in the enzymatic assays of TSR protein. Even if the substrate is omitted from the reaction, the crude extracts also showed some oxidation of NADH that proves the presence of substrate for other bacterial NADH-dependent reductases (W/O subs) in the crude extract. Initially, a high background activity similar with that in the enzymatic assays of TSR was observed when the crude extracts from bacterial cultures were used for the enzymatic assays (data not shown). The background activity was reduced by an ultracentrifugation step. In the above assays, the induced crude extract showed much higher activity than non-induced and without substrate reaction. GCL enzyme was purified by Ni-NTA column and subjected to the enzymatic assay. But

unfortunately, like TSR, the purified GCL enzyme also lost its activity during the purification (data not shown). However, it is concluded from this assay that the enzyme in translational fusion to histidine residues is active *in vitro* and is suitable for the plant transformation.

lane	1	2	3	4	5	6
IN TSR	+	-	-	+	+	-
NI TSR	-	-	+	-	-	-
IN GCL	-	+	-	+	+	-
NI GCL	-	-	+	-	-	-
subs	+	+	+	+	-	-

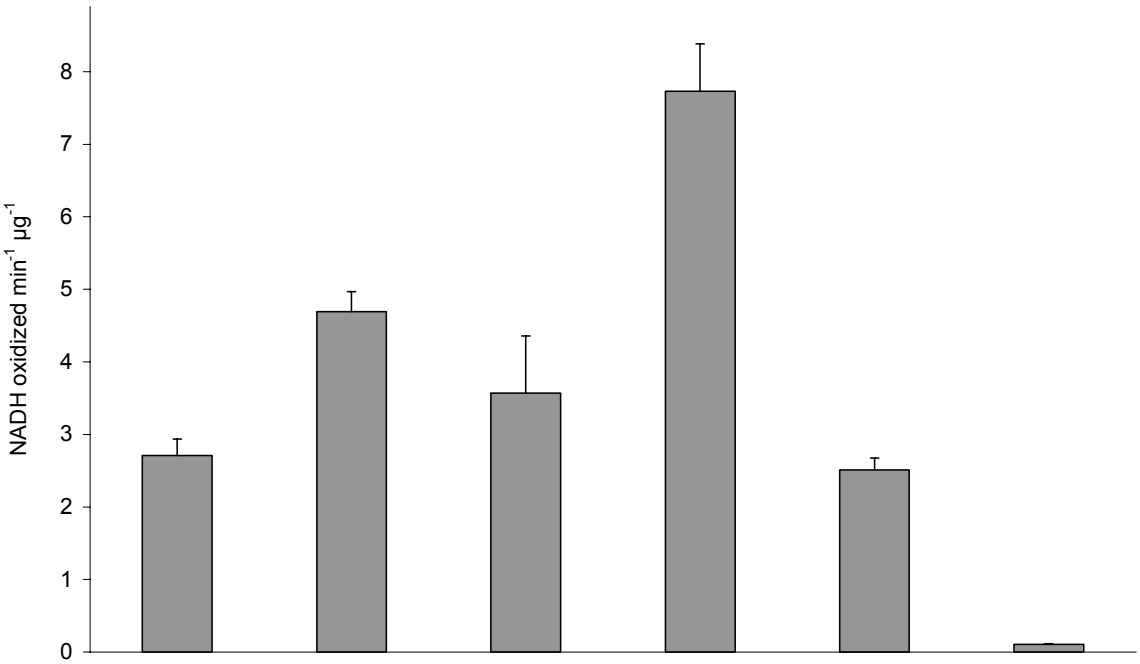

Figure 3.1.4: Measurement of glyoxylate carboligase activity *in vitro.*
Crude extract from both induced and non-induced bacterial culture that were transformed with the construct containing the *GCL* gene were tested for glyoxylate carboligase activity. Each data point shows the amount of NADH oxidized per minute and is based on at least three independent experiments. Vertical bars show standard deviations. IN TSR = crude extract from induced bacterial cultures that were transformed with the construct containing the *TSR* gene; IN GCL = crude extracts from induced bacterial cultures that were transformed with the construct containing the *GCL* gene; NI TSR+NI GCL = crude extracts from non-induced bacterial cultures that were transformed with the constructs containing either the *GCL* or the *TSR* gene; Subs = Substrate (glyoxylate).

3.1.7 Cloning of *TSR* and *GCL* genes into a plant expression vector.

The *TSR* and *GCL* gene in translational fusion to a His tag (*TSR-His*, *GCL-His*) were cloned into the plant expression vector pTRA-K-rbcS1-cTP (2.1.9). Each coding sequence of *TSR-His* and *GCL-His* was cloned into a single plant expression vector. It is a time-consuming process to transfer each individual construct into the nuclear genome of a tobacco plant, generate homozygous lines and combine both activities in a single plant by retransformation or crossing. Therefore, it was decided that in addition to the single construct, both coding sequences should also be cloned together into one plant expression vector (pTRA-K-rbcS1-cTP) resulting in double construct (2.1.9). This strategy has been successfully applied by others before (Padidam and Cao, 2001). The cloning of the double construct was done by Rashad Kebeish and details of the cloning strategy can be found in the diploma thesis of Rashad Kebeish, Institute for Biology1, RWTH Aachen, Germany.

Stable transformation of *Nicotiana tabacum* with *TSR* and *GCL*.

The objective of this study was to clone and characterise genes necessary for the establishment of the novel biochemical pathway inside the chloroplast of the C_3 plant, *Nicotiana tabacum*. It was decided that *TSR* and *GCL* genes should be transfered first followed by the transformation of a gene encoding a glycolate dehydrogenase activity, because the latter step seemed to be the most problematic as described in detail in chapter 3.2. Stable transformation of tobacco, *Nicotiana tabacum* L. cv. Petit Havana SR1, with the construct carrying both genes was worked out by *Agrobacterium* mediated transformation. The traditional leaf disc transformation method (Horsch *et al*., 1985) was optimized (2.2.4.2) and utilized for the stable transformations.

Expression of *TSR* and *GCL* in plants.

The transgenic plants were selected using kanamycin since the vector contains the *npt*II gene which confers resistance to kanamycin. The expression of the foreign genes in this vector (pTRAK-rbs1-cTP) is under the control of a derivative of the constitutive CaMV 35S promoter. The expression of the TSR and GCL proteins was analysed by Western analysis from crude leaf protein extracts with an antibody specific for the His-tag. Figure 3.1.5A shows the results of the Western blot analysis for the proteins isolated from 8 transgenic tobacco plants. TSR and GCL proteins were purified from bacteria and used here as a positive control (lane1 in both Figure 3.1.5A and 3.1.5B). A single band was visible in some samples

as in lane 6 and in lane 7 whereas some of the samples showed two bands as in lane 8. The single band corresponds in size to the GCL protein fused to the His-tag protein (in the positive control). In lane 8, the signal is split into two bands of slightly different sizes for some unknown reason. The samples from some plants also show no expression (for example, lane 2 and lane 3 in Figure 3.1.5A).

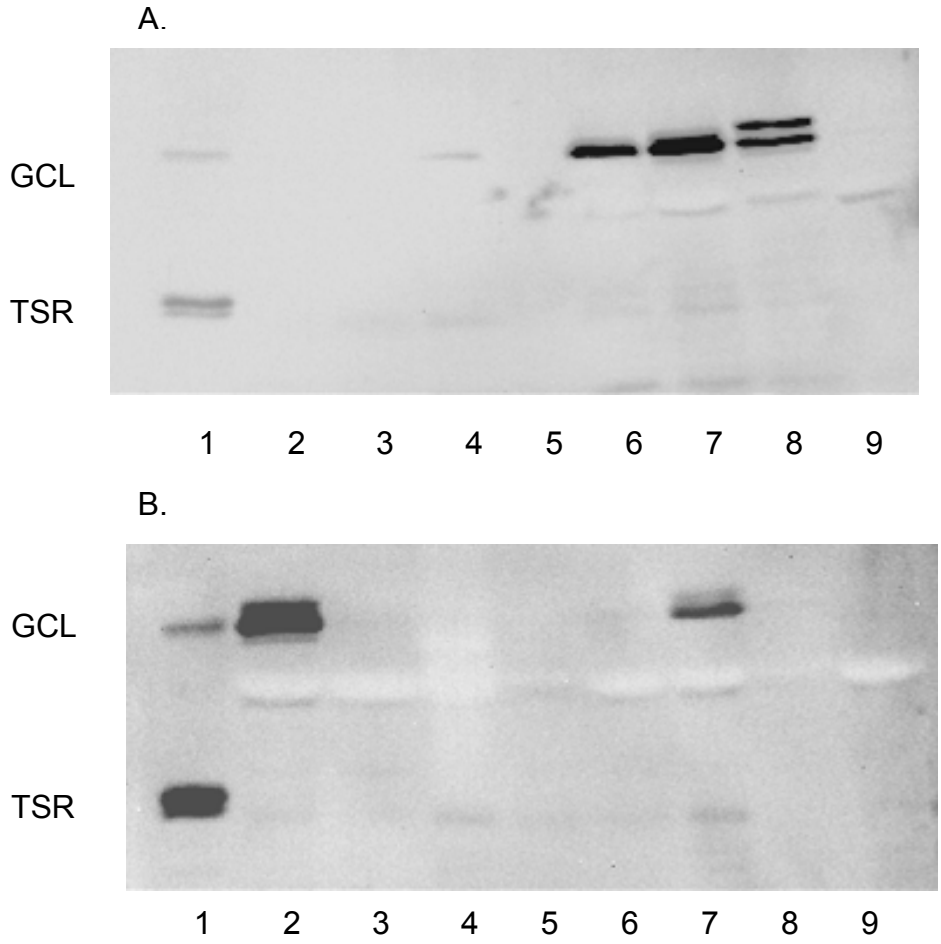

Figure 3.1.5: Expression of the *GCL* and *TSR* genes in plants.
The figure shows the Lumi Light mediated light emission of His-tagged proteins in a Western Blot analysis. 15 µg of leaf protein extracts were separated on a 10 % SDS-PAGE gel and transferred to a nitrocellulose membrane. His-tagged proteins were detected using an anti-His_5 antibody covalently linked to horseradish peroxidase**.** Luminescence was recorded on a LAS3000 CCD camera. In Figure 3.1.5A, Lane1 = TSR and GCL protein that were purified from bacteria; Lane2-lane9 = transgenic plants no. 4, 5, 6, 7, 8, 9, 10 and 11 respectively. In Figure 3.1.5B, lane1 = TSR and GCL protein that were purified from bacteria; Lane2-lane9 = Proteins extracted from transgenic plants no. 12, 13, 14, 16, 17, 18, 19 and 20 respectively.

However, none of the plants showed any expression of the *TSR* gene. Altogether 50 transgenic plants were analyzed by western blot (Figure 3.1.8). Many of them have shown different levels of expression of the *GCL* gene whereas none of them expressed *TSR*. It was suggested that the TSR protein may be pelleted with the cell debris during the centrifugation

steps of the extraction. So, it was decided to extract the total instead of the soluble protein from the leaf of the transgenic plants followed by the western blot analysis. Figure 3.1.6 shows the result of the Western blot analysis for the total proteins isolated from the leaf of the transgenic tobacco plants that were transformed with the double construct (construct carrying both *TSR* and *GCL*). In lane 1, His-tagged Marker was used to determine the molecular weight of the proteins. Two bands that correspond in size to the GCL and TSR protein fused to the His-tagged are detected in lane 2 & lane3.

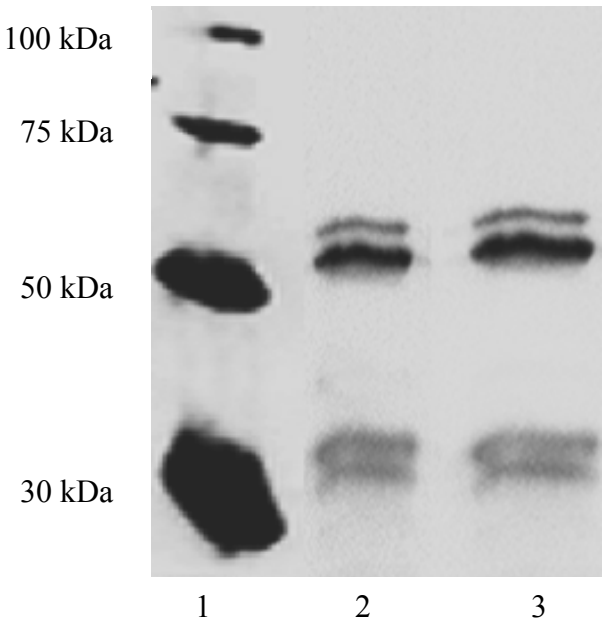

Figure 3.1.6: Expression of both *TSR* and *GCL* was detected in transgenic plants.
The figure shows the Lumi Light mediated light emission of His tagged proteins in a Western Blot analysis. 15 µg of leaf protein extracts were separated on a 10 % SDS-PAGE gel and transferred to a nitrocellulose membrane. His-tagged proteins were detected using an anti-His_5 antibody covalently linked to horseradish peroxidase**.** Luminescence was recorded on a LAS3000 phospho CCD camera. Lane1 = 6x his protein marker; Lane2 and lane3 = total protein extracted from transgenic plants.

Finally, 38% of 50 plants investigated showed immunosignal(s) for proteins encoded by *GCL* and *TSR* genes. The expression levels for both genes were similar in a single plant (Figure 3.1.6), whereas strong variation among the individual lines was observed (Figure 3.1.8). The expression levels of the genes correlate with the phenotypic effect of the plants which is discussed in the next chapter of this thesis. However, the results indicate that both *TSR* and *GCL* were successfully expressed in the analyzed plants making these lines a suitable starting point for the completion of the proposed pathway.

3.1.8 Phenotypic effect of the transgenic plants.

Many of the regenerants exhibited chlorotic effects in the leaf. The severity of the chlorosis varied comparing individual lines. Figure 3.1.7 shows an example of the different phenotypic effects of the transgenic plants. Approximately 3-4 weeks after germination, first chlorotic spots were visible on the leaves of most of the plants. However, few of the plants exhibited chlorosis even when they start to give shoot. The latter plants usually showed severe chlorotic effects later on and died before flowering (Figure 3.1.7C).

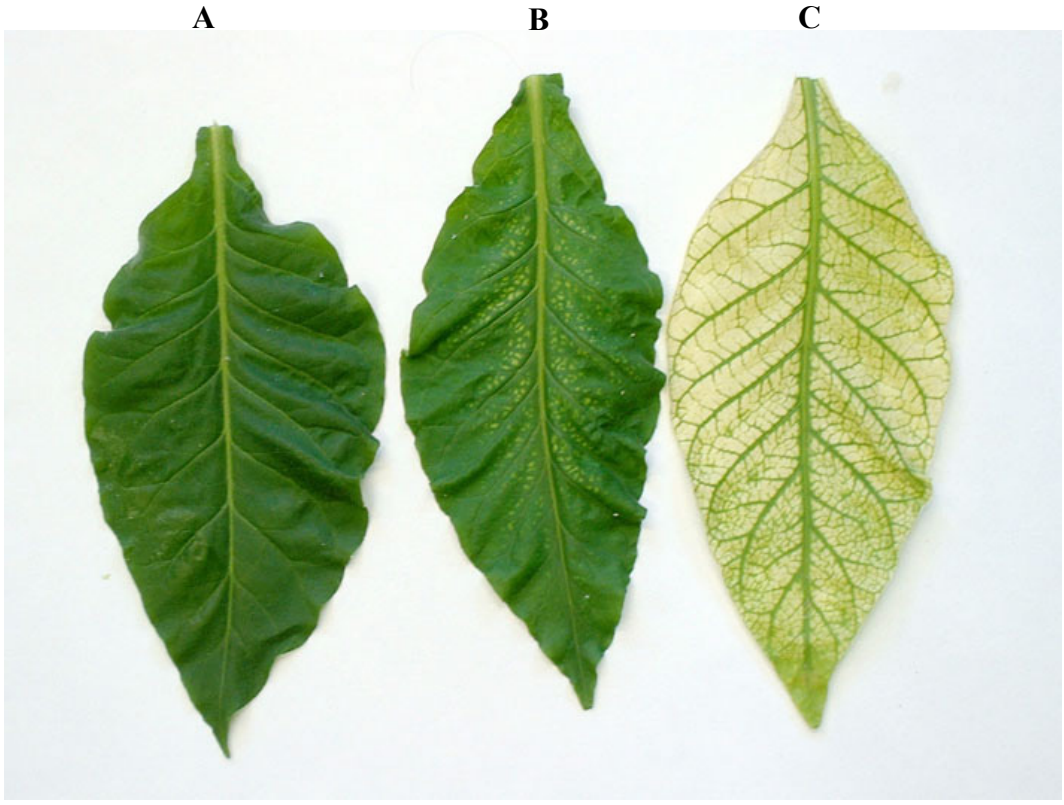

Figure 3.1.7: Phenotypic effects of the transgenic plants.

Photographic image of leaves from plants transformed with the double construct carrying both *TSR* and *GCL*. A typical leaf was harvested from individual lines that were grown at 300 µmol m^{-2} s^{-1} and in ambient air. A = Leaf from a transgenic plant showing no chlorosis; B = Leaf from transgenic plant showing less chlorotic effect; C = Leaf from transgenic plant showing high chlorotic effect.

The plants that exhibited phenotypic effects only after 4 weeks are normally less severely affected and survive (Figure 3.1.7B). The next generation of these plants also shows the chlorotic phenotype. This chlorosis eventually spreads over the whole leaf but the veins are

usually green (Figure 3.1.7B and C). Some of the regenerants also revealed no chlorosis in their leaves (Figure 3.1.7A).

Correlation between transgene expression and the phenotypic effect.

In order to determine whether there is any correlation between the expression of the foreign genes and the phenotypic effects observed in the transgenic plants, 50 lines were tested for the expression of the *TSR* and *GCL* genes.

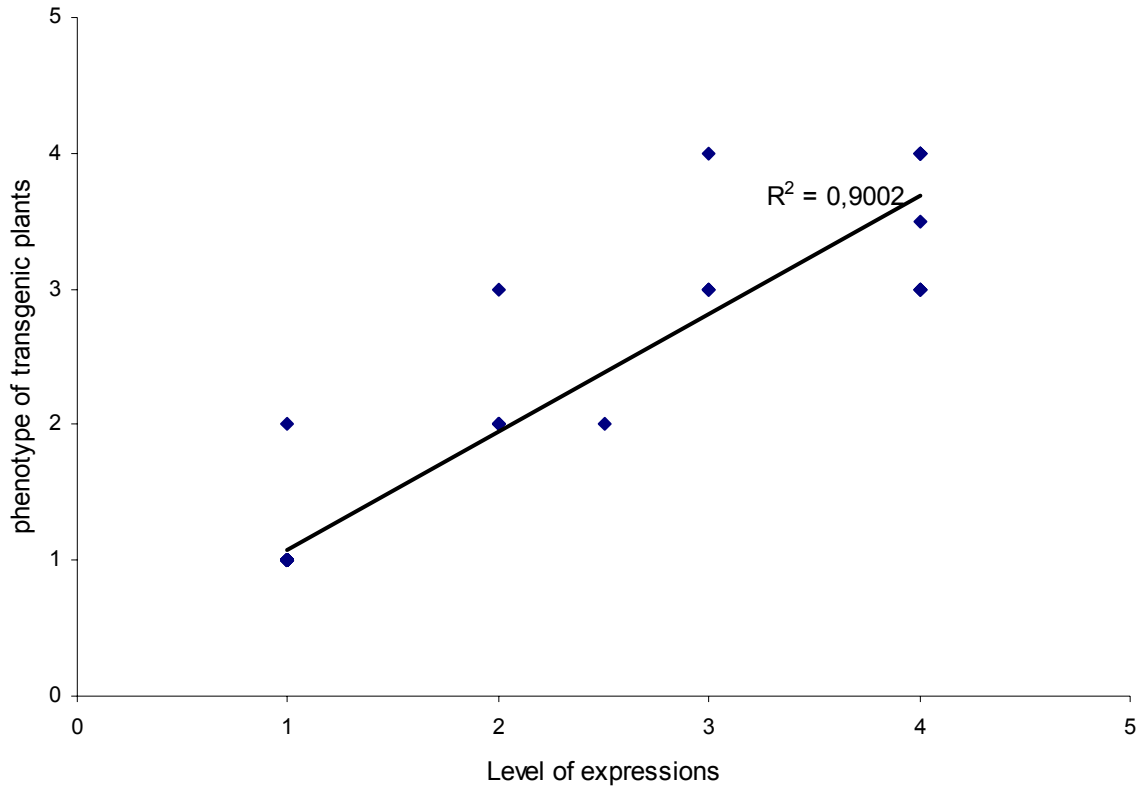

Figure 3.1.8: Correlation between the expression of the *GCL* gene and the phenotypic effects observed in the transgenic plants.
Shown is the correlation between the phenotype of the transgenic plants and the level of expression of foreign genes. Total 50 individual transgenic line were analyzed for the expression of the recombinant proteins (as described in 3.1.7) and for the severity of chlorotic symptoms (3.1.8). Data were taken 8 weeks after germination from plants grown at 300 µmol m^{-2} s^{-1} light and in ambient air. Similar amount of soluble proteins from each plants were used for the westernblot analysis. Both values were scored on a scale from 1 (weak) to 4 (very strong). R^2 indicates the correlation coefficient for a linear correlation of the two data sets.

The correlation between the phenotypic effects and the expression levels is shown in Figure 3.1.8. Out of 50 transgenic plants that were analyzed for the expression of the foreign proteins, 19 plants exhibited the expression of *GCL* and *TSR* genes. 10 of them showed higher expression level of the foreign genes leading to the higher chlorosis whereas 9 of those

transgenic plants revealed medium or lower expression levels leading to comparatively lower chlorotic phenotype. The 30 plants that did not have any chlorotic effect also showed no expression of the foreign genes. In Figure 3.1.8, phenotypic changes and expression levels were both scored on a scale from 1 (weak) to 4 (very strong). Here, it should be noted that the levels of expression are determined from the intensity of the bands that were detected on a western blot. So these results indicate that the level of expression of the foreign genes in the transgenic plants correlates with their phenotypic effect.

3.1.9 Discrimination of effects obtained by *TSR* and *GCL* overexpression.

In order to understand better the reasons for the phenotypic effect observed in the transgenic plants, a single construct (containing either *GCL* or *TSR*) was transformed into tobacco plants. It was expected that it will become clear from this experiment whether GCL or TSR or both proteins are responsible for the observed chlorotic phenotype.

A. B.

Figure 3.1.9: Phenotypic effects of the transgenic plants expressing *TSR* or *GCL* gene. Shown are the transgenic plants that are expressing either *GCL* or *TSR* gene. A. Transgenic plants expressing *TSR* gene. B. Transgenic plant expressing *GCL* gene.

Stable transformation of tobacco, *Nicotiana tabacum* L. cv. Petit Havana, with the constructs carrying single genes has been done by *Agrobacterium* mediated transformation as described in Materials and Methods (2.2.4.2). The plants were selected on MS medium containing

kanamycin (Table 2.2). When the regenerates started to form roots, they were transferred to soil and were grown in ambient air (in the same way as described for the double construct). The transgenic plants are shown in Figure 3.1.9. In Figure 3.1.9A, regenerates transformed with the construct containing the *TSR* gene showed no phenotypic changes compared to wild type (data not shown) plants. Figure 3.1.9B exhibits a regenerant that was transformed with the construct containing *GCL* gene showing chlorosis in the leaf of the plant.

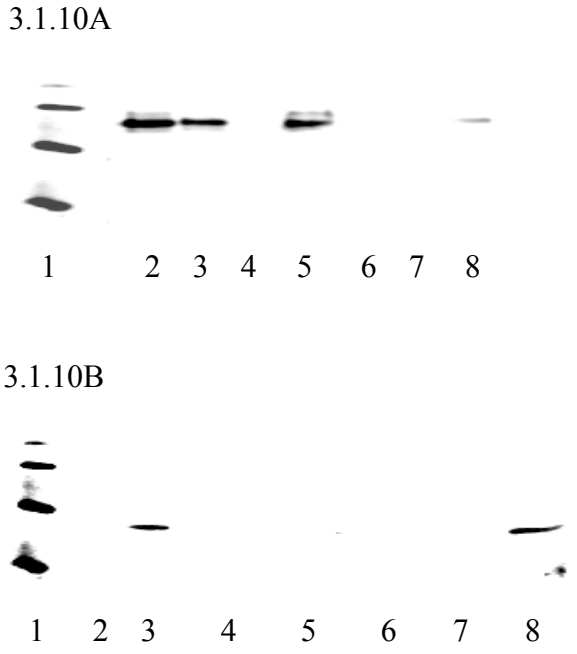

Figure 3.1.10: Expression of single *TSR* or *GCL* constructs in tobacco.
The Figures show the Lumi Light mediated light emission of His tagged proteins in a western blot analysis. 15 µg of leaf protein extracts were separated on a 10 % SDS-PAGE gel and transferred to a nitrocellulose membrane. His-tagged proteins were detected using an anti-His_5 antibody covalently linked to horseradish peroxidase**.** Luminescence was recorded on a LAS3000 CCD camera. lane1 = 6x his protein marker; Lane2- lane8 = transgenic plants that were transformed with the construct containing the *GCL* coding sequence. Figure 3.1.11B, lane1 = 6x his protein marker; Lane2-lane8 = transgenic plants that were transformed with the construct containing the *TSR* coding sequence.

In order to make sure which protein is responsible for the chlorotic effect, the expression of each gene in the transgenic plants was analyzed by western blot. Figure 3.1.10A and B show the western blot results from the transgenic plants containing either the *GCL* or the *TSR* gene. In Figure 3.1.10A, 4 plants (lane2, lane3, lane5 and lane8 in Figure 3.1.10A) out of 7 transgenic plants that were analyzed by western blot showed the expression of *GCL* gene. All these 4 plants also exhibited the chlorotic effect in their leaves (data not shown). In Figure 3.1.10B, only 2 plants (lane2 and lane8 in Figure 3.1.10B) out of 8 plants that were

transformed with the construct containing *TSR* gene expressed the transgene. However, none of the transgenic plants expressing the *TSR* gene revealed any phenotypic change. The results from the western blot indicate that the plants expressing the *GCL* gene have caused the chlorotic phenotype whereas those plants expressing the *TSR* gene shows no chlorotic effect. From the above results it is obvious that the GCL protein is responsible for the chlorosis in the transgenic plants.

3.1.10 Enzymatic assay of GCL protein *in vivo*.

Because of the severity of symptoms caused by overexpression of *GCL*, we wanted to assay whether the enzyme is active inside the plant. In the previous experiment (3.1.6), it has been shown that the enzyme, glyoxylate carboligase, is active *in vitro*, while the enzymatic assay was performed with crude extract from bacteria over expressing the *GCL* gene. In order to understand more about the reasons for the chlorotic phenotype observed in *GCL* overexpressing lines, the enzymatic assay has been performed with the total soluble protein extracted from the leaf of the transgenic plants.

The enzymatic activity of glyoxylate carboligase was assayed spectrophotometrically as described for the GCL activity assay (2.2.3.10) *in vitro*. The assay was performed in a coupled reaction where glyoxylate carboligase condenses two molecule of glyoxylate into one molecule of tartronic semialdehyde. Tartronic semialdehyde is further reduced to glycerate by a reaction catalyzed by tartronic semialdehyde reductase. In this coupled assay, crude extract from bacteria expressing *TSR* has been used for the latter reaction. The assay with soluble leaf protein of the transgenic plants shows higher oxidation of NADH compared to the soluble protein extracted from wild type (Figure 3.1.11, GCL+IN TSR and WT+IN TSR). If the crude extract from bacterial culture containing empty vector (pET) is used instead of the crude extract from induced bacteria expressing *TSR*, the reduction of NADH is similar for both soluble proteins from wild type and transgenic plants expressing *GCL* gene (Figure 3.1.11, WT+NI TSR and GCL+NI TSR). This result also indicates that some unspecific oxidation of NADH is observed in both bacterial and plant extracts However, it is clear from the assay that glyoxylate carboligase enzyme is active in the transgenic plants.

Lane	1	2	3	4
WT	+	-	+	-
GCL	-	+	-	+
TSR	-	-	+	+
pET	+	+	-	-

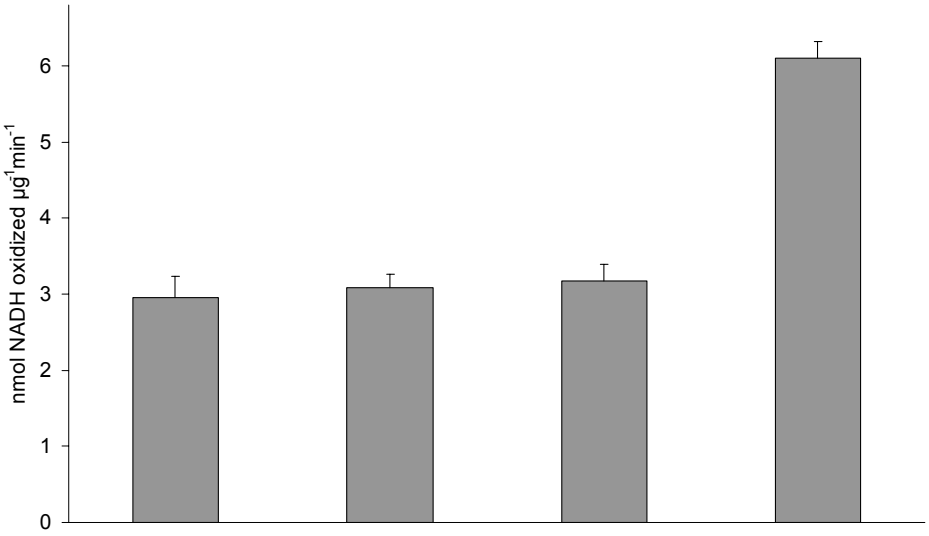

Figure 3.1.11: Measurement of glyoxylate carboligase activity *in planta*
Soluble proteins from both wild type and transgenic plants expressing GCL protein were tested for glyoxylate carboligase activity. Each data point shows the amount of NADH oxidized per minute and is based on at least three independent experiments. Vertical bars show standard deviations. WT = wild type tobacco plant; pET = crude extract from induced bacteria containing empty vector; GCL = soluble protein from the leaf of the transgenic plants containing *GCL* gene; TSR = crude extract from induced bacterial culture containing *TSR* gene.

3.2 Establishment of a glycolate dehydrogenase activity in the chloroplast of transgenic lines.

In the first part of this thesis the successful establishment of tobacco plants overexpressing *TSR* and *GCL* is shown. For the completion of the proposed pathway it is necessary to transform the plants with a gene coding for a glycolate oxidizing enzyme. The most obvious source for such an ezymatic activity is the use of the *E. coli* enzyme as described for the two other necessary activities before. The glycolate dehydrogenase from *E. coli* has been investigated in great detail. *Escherichia coli* can grow on glycolate as the sole carbon source. Glycolate is oxidized to glyoxylate by an enzyme traditionally named glycolate oxidase that is dependent on organic co-factors. The enzyme is encoded by the *glc* operon that consists of

6 open reading frames. Mutational analyses have shown that the subunits *glc*D, *glc*E, and *glc*F are necessary and sufficient to form the active enzyme (Lord, 1972; Pellicer *et al.*, 1996).

The coding sequence of *glc*D, *glc*E and *glc*F were amplified by PCR from the genomic DNA of *E. coli*. The PCR product was cloned into a bacterial expression vector (pET 22b+) (2.1.9). Plasmid DNA isolated from ampicillin-resistant bacterial colonies was analyzed by both restrictions and sequencing. The clones that showed no mutation were chosen for further experiments.
It is problematic to transform the whole *GO* operon into the nucleus of tobacco plants under one chloroplast targeting sequence since this operon consists of three open reading frames. If each of the genes would be transferred individually, it is not sure whether the subunits would form an active complex inside the chloroplast. Moreover, it is time consuming to generate homozygous transgenic plants with each single open reading frame and then cross with transgenic plants containing TSR and GCL protein in order to complete the pathway.

Therefore, all 5 genes {*GO* from *E. coli* (encoded by *glc*D, *glc*E and *glc*F), *TSR* and *GCL*} that are necessary for the establishment of the proposed biochemical pathway were cloned into one chloroplast transformation vector pRB96 (kindly provided by Ralph Bock, Uni Münster). The aim of this cloning was to transform all genes simultaneously into the chloroplast of the plant. This approach is not only time-saving but also allows the expression of the encoded proteins directly in the organelle they are targeted to. Moreover, all genes employed here are from bacterial source and are therefore suitable for expression in an organelle using a similar expression system compared to prokaryotes.

The part of the *glc* operon from *E. coli* encoding the *glc*D, *glc*E, and *glc*F polypeptides was amplified using the PCR method. The coding sequences for tartronic semialdehyde reductase (*TSR*) and glyoxylate carboligase (*GCL*) from *E. coli* were amplified and shine dalgarno sequences were added upstream of the coding sequence using the PCR method. A C-terminal translational fusion of six histidines was added to the *GCL* coding sequence. In each case oligonucleotides homologous to the beginning and the end of the respective coding sequences with extensions for the addition of the mentioned sequence elements were used. The complete construct was restricted with *Nco*I and *Bpu*1102I and transferred into a vector for plastidic transformation that was restricted with *Nco*I and *Xba*I (Bock, 2001). Before ligation, the

protruding ends of the *Xba*I and *Bpu*1102I restriction sites were blunted with Klenow polymerase. A schematic representation of the vector insert is given in Figure 3.2.1.

The construct was coated with gold particles and transformed into the chloroplasts of *Nicotiana tabacum* cv. Petit Havana plants using particle bombardment. Transformed lines were selected using spectinomycin antibiotics (Bock, 2001). The plastidic transformation and the selection procedure were done in the lab of Professor Dr. Ralph Bock, Universität Münster.

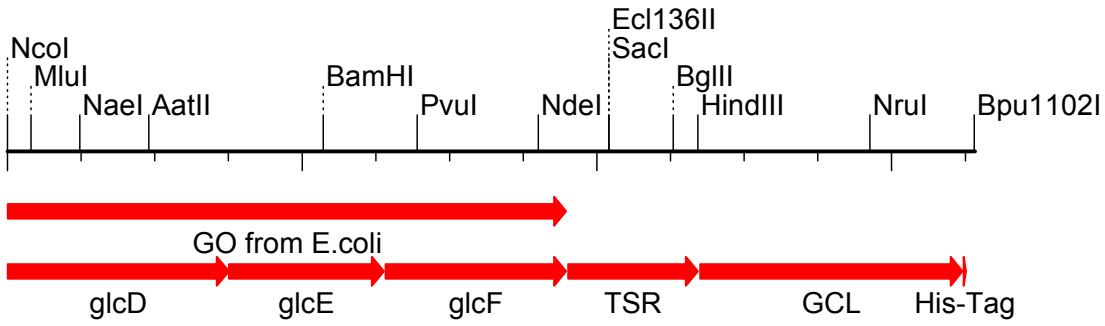

Figure 3.2.1: Schematic representation of the construct used for the plastidic transformation.
All genes required for the proposed pathway were cloned in a single construct. GO = glycolate oxidase; *glc*D, *glc*E and *glc*F = three subunits of the glc operon that are necessary for encoding an active glycolate dehydrogenase enzyme in *E.coli*; TSR = tartronic semialdehyde reductase; GCL = glyoxylate carboligase.

Screening of the transgenic plants.

The regenerants were selected in spectinomycin. The plants were first checked on the DNA level in order to determine the presence of the genes of interest. The southern blots were done by Dr. Stephanie Ruf, Universität Münster.

The construct (pRB96-*GOTG*) was restricted with *Pst*I and *Spe*I. DNA from the transformants was extracted (2.2.1.2) and subjected to Southern analysis with the plasmid insert as a probe. The heteroplasmic transgenic plants containing the right construct should show bands at 13,860 bps and 1480 bps positions and wild type plants should give a band at 1480 bps position whereas the homoplasmic transgenic plants should show only 13,860 bps band. Southern blot results are shown in Figure 3.2.2. The wild type plants in lane 11 shows a single band at the expected position. Among the 19 transforments shown here, the DNA from only

two plants (lane 2 and lane 15) shows a band at above 10000 bps as expected for a transgenic line. All the transformants show an additional very strong band at the position of about 3000 bps (estimated) whereas no band at this position can be detected in control. It is not clear at this moment, how and from where this band appears. It is possible that some part of the transgenes is probably homologous to the tobacco chloroplast genome and trasgenic lines loose that part because of homologous recombination. It is just a speculation at this moment. The plants that show the right pattern in the southern blot (i.e. lane 2 and lane 15) currently give seeds. The next generation of these plants will be investigated at the level of expression of gene expression and possibly by enzymatic assay.

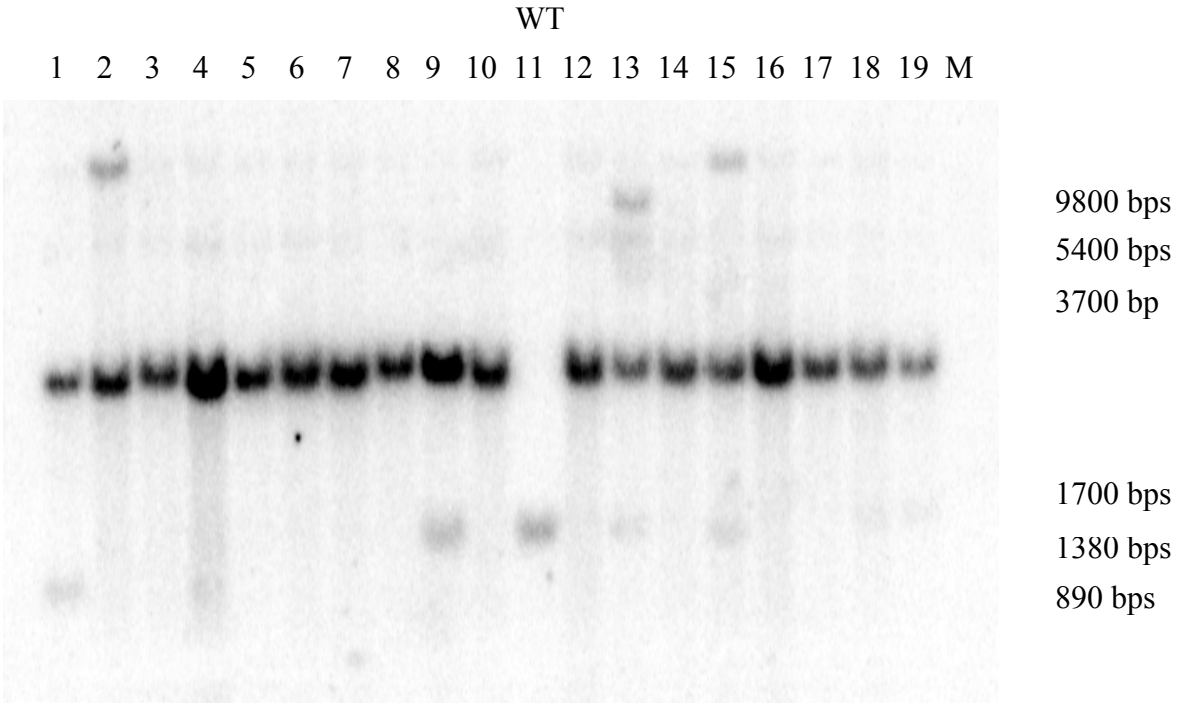

Figure 3.2.2: Southern blot results of the chloroplast transformants.
Shown is an autoradiography of a Southern analysis. Plasmid DNA was restricted with *Pst*I and *Spe*I and hybridized with DNA that was extracted from both transformant and wild type plants. The numbers indicate the lane; WT = wild type; M = marker.

3.3 Characterization of a glycolate dehydrogenase in the mitochondria of *Arabidopsis thaliana*.

The establishment of a GDH activity in plant chloroplasts based on the *E. coli* enzyme has proven to be difficult as described in the last chapter. Therefore, an alternative to the glycolate dehydrogenase enzyme of *E. coli* was desirable to complete the proposed pathway. Sequence analysis of the *Arabidopsis* genome showed an open reading frame (At5g06580) with significant homology to the subunit D of *Escherichia coli* glycolate oxidase. In order to clarify the question whether the enzyme encoded by this open reading frame is really active as a glycolate dehydrogenase, it was partially characterized. The gene was provisionally named *AtGDH* for *Arabidopsis thaliana* glycolate dehydrogenase.

3.3.1 *Arabidopsis* encodes a glycolate dehydrogenase.

Sequence analysis of the *Arabidopsis* genome revealed an open reading frame (At5g06580) with homology to the subunit D of *Escherichia coli* glycolate oxidase and to yeast D-lactate dehydrogenase. As shown in Figure 3.3.1, all three enzymes share significant homology over the complete sequence length apart from the first one hundred amino acids. According to RPS-BLAST (Altschul *et al*., 1997), the *Arabidopsis* open reading frame contains homologous regions to a FAD-binding domain in between amino acids 150 and 300 and a C-terminal FAD-oxidase domain with a ferredoxin-like fold from amino acid 320. Both domains are frequently found in oxygen-dependent oxygenases as well as dehydrogenases dependent on organic co-factors (Dym and Eisenberg, 2001).

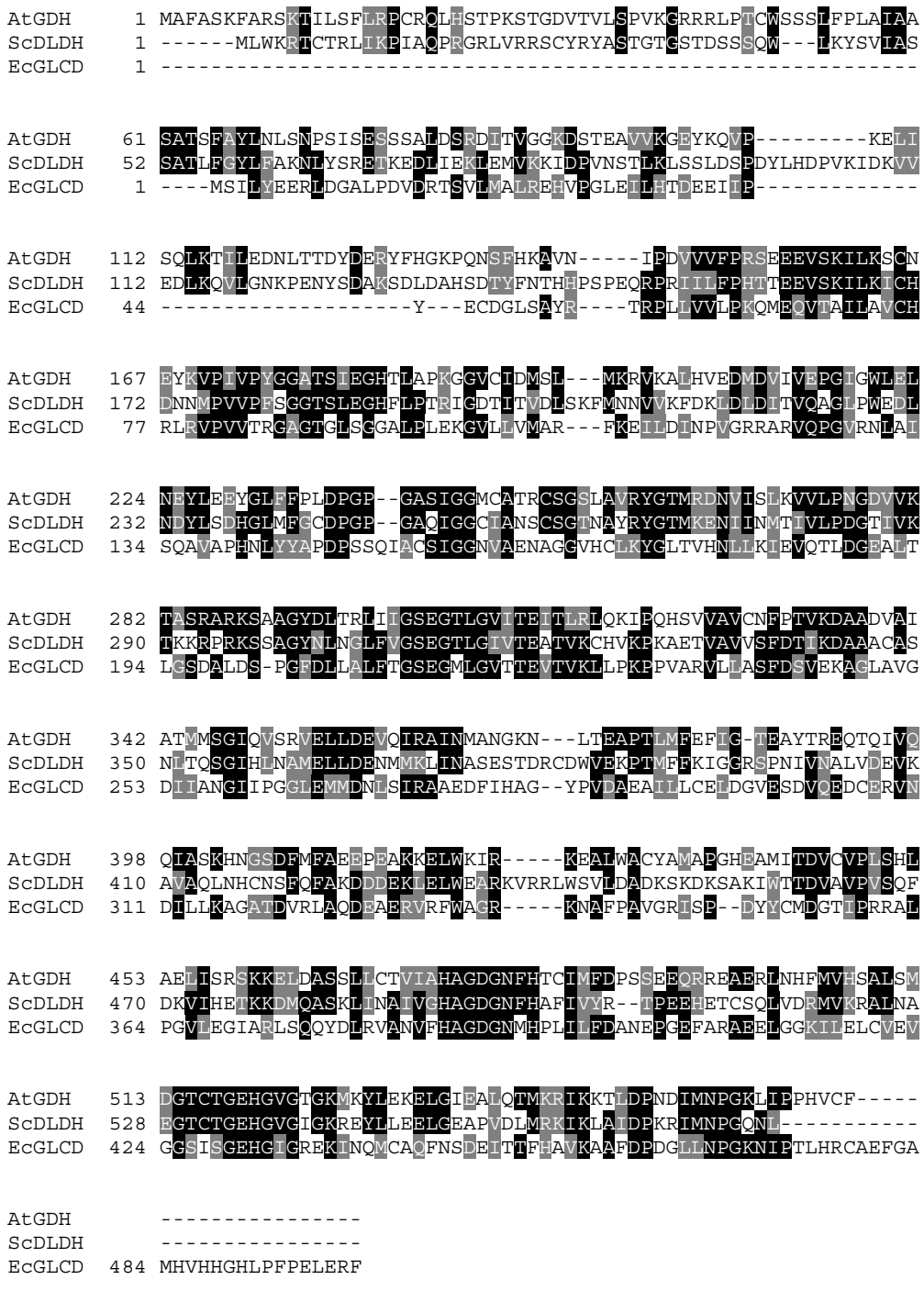

Figure 3.3.1: *AtGDH* shows homology to glycolate dehydrogenases and lactate dehydrogenases.
Shown is an alignment of the novel identified sequence and related sequences. Black shaded boxes indicate identical amino acids and grey shaded boxes indicate similar amino acids. *At*GDH = *Arabidopsis thaliana* glycolate dehydrogenase; *Sc*DLDH = *Saccharomyces cerevesiae* D-lactate dehydrogenase; *Ec*GLCD = Subunit D of *Escherichia coli* glycolate oxidase.

3.3.2 Construction of a prokaryotic expression vector carrying *AtGDH* gene from Arabidopsis.

In order to characterize the enzymatic properties of the *AtGDH* open reading frame, the gene was cloned into the bacterial expression vector pET (2.1.9). Firstly, RNA was isolated (2.2.1.8) from the leaves of both young and old plants. The isolated RNAs were converted to cDNA using reverse transcriptase (2.2.1.9). The above mentioned open reading frame was amplified by PCR from the cDNA library of both young and old *Arabidopsis* plants. Successful amplification was only obtained from the cDNA isolated from younger plants

The PCR product was cloned into pET vector (as described for *TSR*, *GCL* and *GO*) as a N-terminal translational fusion to a His-tag. Plasmid DNA was isolated from ampicillin-resistant clones that were analyzed by restriction using the restriction endonucleases *Nco*I and *Xho*I (data not shown). The clones showing right restriction pattern were further checked by sequencing. The construct was transformed into the bacterial strain ER2566 and was induced for over expression of *AtGDH* using 1mM IPTG. The soluble proteins were extracted from the bacterial cell and were subjected to western blot analysis (as described for the expression of *TSR* and *GCL* in bacteria) for the detection of the His-tag fused AtGDH protein. The result from the western blot shows a band at the size estimated for the AtGDH protein. So the *AtGDH* was expressing in bacteria.

3.3.3 Enzymatic activity of AtGDH protein was assayed *in vitro*.

Enzymatic assays (2.2.3.10) are performed with crude extracts from a bacterial strain over expressing the gene as an N-terminal fusion to six histidine residues. Crude extracts were used because for unknown reasons we did not succeed in purifying the enzyme from the extract without losing most of the activity. Figure 3.3.2 and Table 3.1 show the results of the assays. The extract containing over expressed *AtGDH* shows appreciable formation of glyoxylate from glycolate as specifically determined by the formation of glyoxylate phenylhydrazone in a coupled reaction. These levels are reduced to background if an unrelated protein (with similar accumulation levels after induction of expression) is used. The same reduction is also found when the substrate (glycolate) or the organic electron acceptors (DCIP/PMS) are omitted from the reaction. Thus, *At*GDH catalyzes the formation of glyoxylate from glycolate dependent on organic co-factors.

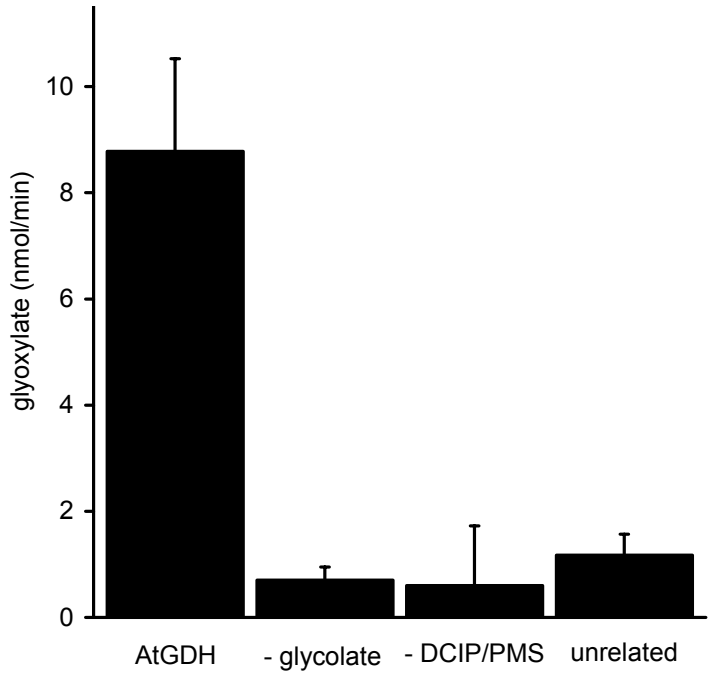

Figure 3.3.2: *At*GDH shows glycolate dehydrogenase activity *in vitro.*
Protein extracts from *E. coli* ER2566 overexpressing the listed constructs were tested for glycolate dehydrogenase activity. Each data point shows the amount of glyoxylate formed per minute and is based on at least three independent experiments. Vertical bars show standard deviations. *At*GDH = overexpression of the *Arabidopsis thaliana* glycolate dehydrogenase; - glycolate = assay in the absence of glycolate; - DCIP/PMS = assay in the absence of organic electron acceptors; unrelated = over expression of the unrelated maize transcription factor *DOF*1.

Further characterization of the enzymatic properties revealed that the enzyme shows an apparent K_M for glycolate of approximately 3,5 x 10^{-2} mM whereas the K_M for glyoxylate is approximately 4 x 10^{-1} mM. The optimum pH for glycolate oxidation is in between pH 8.0 and pH 8.5 (data not shown).

Bacterial and algal glycolate dehydrogenases show a high preference for D-lactate over L-lactate and are sensitive to cyanide ions, whereas the plant oxygen-dependent glycolate oxidases show a preferential affinity for L-lactate and are cyanide-insensitive (Nelson and Tolbert, 1970). As listed in Table 3.1, crude bacterial extracts over expressing *AtGDH* show D-lactate dehydrogenase activity that is reduced to a background activity of approximately one third by addition of cyanide ions. No L-lactate dehydrogenase activity can be detected in this assay compared to controls with the empty vector construct. Taken together, *At*GDH shows all properties of a glycolate dehydrogenase and can be clearly discriminated from the so far described higher plant glycolate-oxidizing enzymes.

Table 3.1: Substrate specificity and potassium cyanide sensitivity of *At*GDH

construct	substrate	KCN	activity (%)
*At*GDH*	D(-)-lactate	-	100 %
*At*GDH	D(-)-lactate	+	37 %
*At*GDH	L(+)-lactate	-	29 %
*At*GDH	L(+)-lactate	+	29 %
empty vector	D(-)-lactate	-	37 %

* 50 µg of crude extract overexpressing AtGDH

3.3.4 *AtGDH* can complement *E. coli* glycolate oxidase mutants.

We wanted to learn whether *AtGDH* is capable of complementing glycolate oxidase mutants of *E. coli*. As specified in the introduction, the *E. coli* enzyme is identical to algal glycolate dehydrogenases in its specificity for organic co-factors and its enzymatic properties and only traditionally named an oxidase. The mutants JA155, JA156, JA157 carry transposon insertions in the *glc*D, *glc*E, and *glc*F subunits of the *glc* operon and are uncapable of growing on glycolate as a sole carbon source (Pellicer *et al.*, 1996). As shown in Figure 3.3.3, over expression of *AtGDH* in any of these mutants restored growth of the bacteria on medium containing glycolate as the sole carbon source. Comparing the dilution series of bacteria transformed with *AtGDH* or the intact *E. coli* glycolate oxidase (*Ec*GO), similar growth rates are observed whereas no colonies are detectable when bacteria were transformed with the empty expression vector under identical conditions. However, replicate platings on rich medium were capable of growing independent of the transformed construct (data not shown). The results indicate that *AtGDH* can complement for all three subunits of the active *Ec*GO enzyme *in vivo* and thus encodes a functional equivalent.

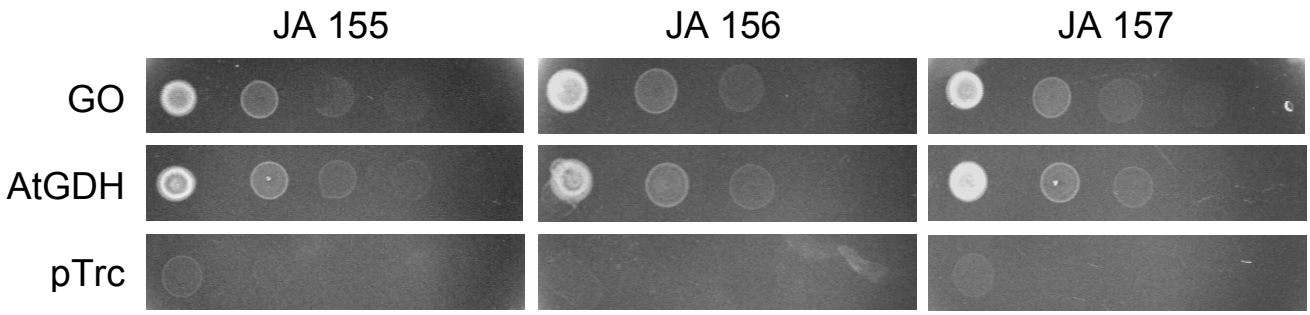

Figure 3.3.3: Complementation of *E. coli* glycolate oxidase mutants with *At*GDH. Bacterial strains deficient in glycolate oxidase subunits were transformed with the listed constructs and a dilution series was spotted on agar plates containing glycolate as the sole carbon source. The figure shows photographs of the plates after 3 days of growth at 37 °C. JA 155 = mutant deleted in *glc*D; JA 156 = mutant deleted in *glc*E; JA 157 = mutant deleted in *glc*F; *GO* = overexpression of *E. coli* glycolate oxidase subunits *glc*D-F, *AtGDH* = overexpression of the *Arabidopsis thaliana* glycolate dehydrogenase; pTrc = transformation with empty vector.

3.3.5 *AtGDH* shows preferential transcript accumulation in illuminated leaf tissues.

In order to determine the gene expression profile of the *AtGDH* gene, we measured the accumulation of the corresponding transcripts in different plant tissues and the diurnal rhythm of transcript accumulation by Real-Time RT-PCR (2.2.1.10). The amount of *AtGDH* signal in the different RNA preparations was standardized for the abundance of the Actin2 transcript (Igarashi *et al*., 2003). As shown in Figure 3.3.4A, the transcript accumulates in leaves as well as stems, flowers and roots when samples were taken in the middle of the light period. The accumulation is approximately 2-fold in illuminated leaves compared to leaves from plants that were kept for two days in the dark or to the other tissues. When the transcript abundance is compared at different time points after the onset of light (Figure 3.3.4B), a constitutive low level of expression and an increase during the light period is observed. This increase becomes only apparent after 5 h of illumination but not after 1 h. Taken together, *AtGDH* is expressed in any of the investigated tissues, but transcripts accumulate preferentially in illuminated leaves.

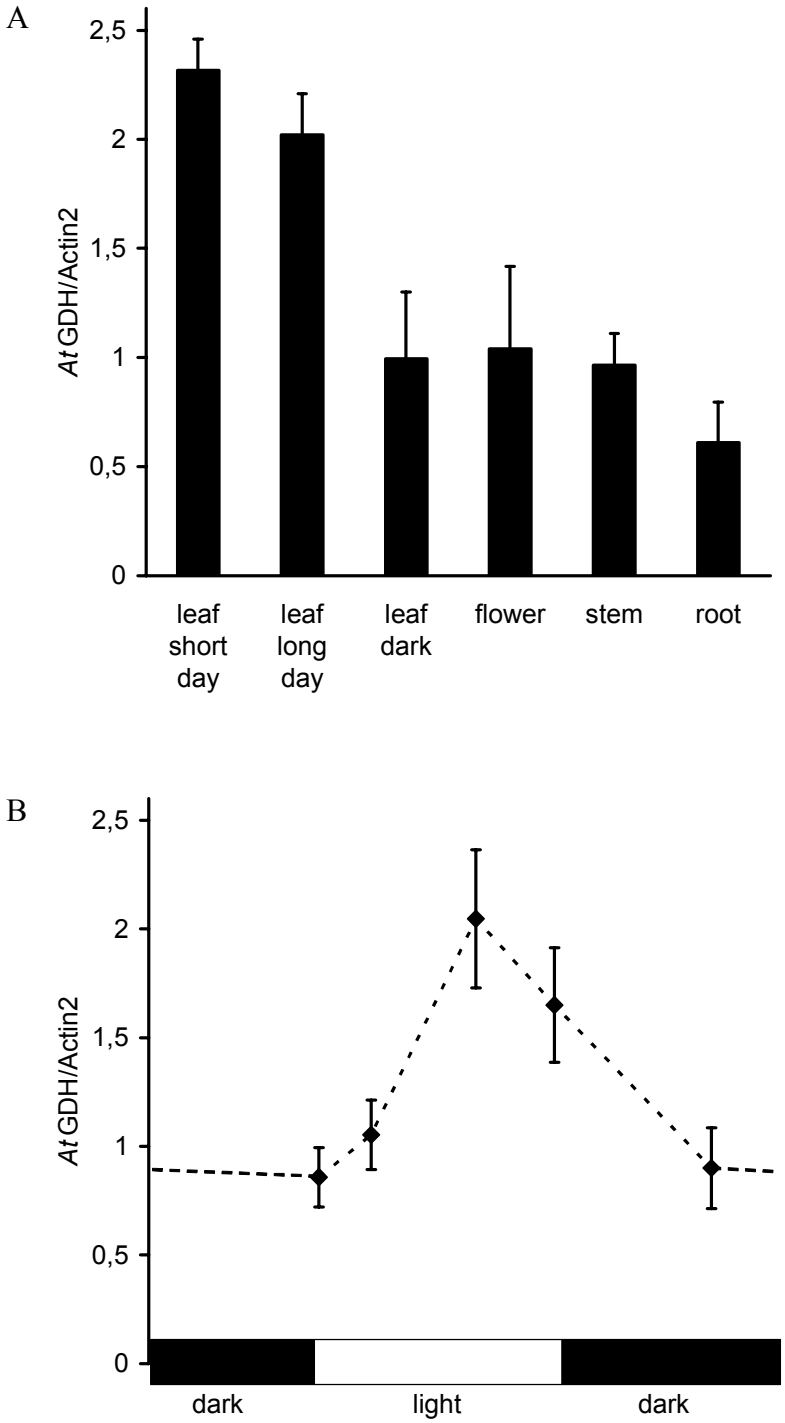

Figure 3.3.4: Tissue specificity and diurnal rhythm of *AtGDH* transcript accumulation.
The amount of *AtGDH* mRNA was measured by Real-Time PCR and calculated in arbitrary units by comparison to a standard dilution series. Each value is the relative accumulation of the respective RNA compared to the Actin2 levels measured in the preparation. Each data point is based on at least three independent RNA preparations and for each preparation the quantification was repeated at least three times. Vertical bars show standard deviations. A = Tissue samples were collected five hours after onset of illumination; B = Leaf samples were collected 0 h, 1 h, 5 h, and 7 h after the onset of light and 6 h after the beginning of the dark period.

3.3.6 The N-terminal domain of AtGDH targets proteins to mitochondria.

Sequence analysis of *AtGDH* using the TargetP algorithm (Emanuelsson *et al*., 2000) identified high scores both for a putative chloroplast transit sequence of 56 amino acids and a putative mitochondrial target sequence of 30 amino acids. In order to test whether this sequence stretch targets proteins to plastids or mitochondria *in vivo*, *Arabidopsis* plants were transformed with a plant expression construct carrying the coding sequence of first 77 amino acids of AtGDH in translational fusion to red fluorescent protein (dsRED) (Jach *et al*., 2001). Microscopic analysis of transgenic lines revealed an accumulation of the red fluorescence in particles of approximately 1 µm in size resembling mitochondria (data not shown). For further analysis, protoplasts were prepared from leaves of the transgenic plants and mitochondria were specifically stained with the MitoTracker Green dye.

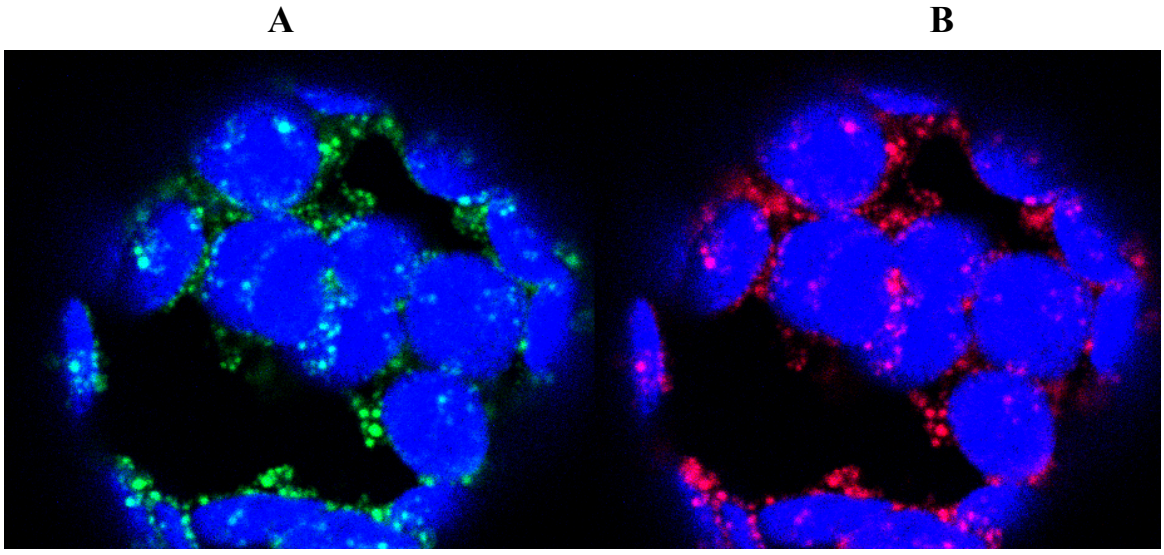

Figure 3.3.5: Subcellular localization of *At*GDH.
The picture shows epifluorescence photographs of protoplasts from *Arabidopsis* plants that were transformed with a construct expressing the N-terminal part of *AtGDH* in translational fusion to red fluorescent protein (dsRED). Excitation wave lenghts were 488 nm and 568 nm and emission filters were 515-535 nm (MitoTracker Green, shown in green), 570-610 nm (dsRED, shown in red) and 660-720 nm (chlorophyll fluorescence, shown in blue). Magnification is 630 x. A = overlay of chlorophyll fluorescence and MitoTracker Green-mediated fluorescence; B = overlay of chlorophyll fluorescence and dsRED-mediated fluorescence.

The confocal laser images in Figure 3.3.5 show the chlorophyll fluorescence of chloroplasts in blue, the stained mitochondria in green and the dsRED-mediated fluorescence of the fusion protein in red. Care was taken that the green fluorescence of the MitoTracker Green dye was not visible in the red channel detecting the fluorescence of the dsRED protein and *vice versa* (see Materials and Methods). The mitochondrial stain shown in Figure 3.3.5A, almost

perfectly co-localizes with the dsRED fluorescence shown in Figure 3.3.5B, indicating that the N-terminal domain of At*GDH* targets proteins to mitochondria *in vivo*.

4 DISCUSSION.

4.1 A novel pathway in the chloroplast of *Nicotiana tabacum* aiming to increase the CO_2 concentration in the vicinity of Rubisco.

In this thesis, a novel pathway has been proposed aiming to suppress the CO_2 loss resulting from photorespiration in C_3 plants. Most of our crops, such as wheat, rice, soybean or potato are classified as C_3 plants as the first product of atmospheric CO_2 fixation is the 3-carbon compound 3-phosphoglycerate (3-PGA), which is produced in the Calvin cycle by Rubisco (the only enzyme capable of net carbon assimilation) in the chloroplast stroma (Häusler *et al.*, 2002). However, Rubisco also fixes O_2 and produces 2-phosphoglycolate which can not enter the Calvin cycle. The competition of O_2 with CO_2 at the active site of Rubisco (Chen and Spreitzer, 1992; Jordan and Ogren, 1984) results in a loss of up to 50 % of the carbon fixed in a process known as photorespiration (Ogren, 1984) (details of the pathway are described in 1.2). Despite of some evidence that photorespiration may play a protective role when excess energy is present (Andrews and Lorimer, 1987; Kozaki and Takeba, 1996), it is mainly a wasteful process since for every O_2 reacting with RuBP the equivalent of 2 NADPH are utilized (to re-assimilate the PGA and ammonia formed) (Maroco *et al.*, 2000).

The proposed novel pathway will concentrate CO_2 in the vicinity of Rubisco. Rubisco favours CO_2 over O_2 by a factor of up to 100, but the concentration of O_2 in the atmosphere is much higher than that of CO_2 (Sharkey, 2001). As a result, about one molecule of O_2 is fixed by Rubisco for every three molecules of CO_2. So by increasing the concentration of CO_2, the pathway will suppress the wasteful photorespiration pathway in C_3 plants. C_3 plants will benefit from the proposed pathway in two ways: (1) glycolate does not enter the photorespiratory pathway and thus the energy loss is avoided (2) the alternative pathway increases the CO_2 concentration inside the chloroplast and, by this, reduces the formation of novel glycolate. The importance of photorespiration for plant growth and yield has been shown by several experiments where the atmospheric CO_2 concentration has been artificially raised in greenhouse experiments. Drastic increases in the performance of several crop species have been observed already when the CO_2 concentration is doubled (Arp *et al.*, 1998; Kimball, 1983). However, this approach is not applicable to the huge areas used for agricultural production. On the other hand, the proposed pathway increases the concentration of CO_2 inside the chloroplast thus it will be applicable for agricultural production.

The following chapter will discuss the various mechanisms that have been developed in plants during evolution to supply elevated concentrations of CO_2 at the site of Rubisco in order to suppress photorespiration resulting in an enhanced photosynthetic efficiency. Plants displaying C_4-metabolism release CO_2 at high rates in the vicinity of Rubisco and thereby substantially increase the ratio of RubP carboxylation to oxygenation (Leegood, 1997; Leegood, 2002). C_4 plants have employed enzymes already present in their C_3 ancestors, but changed the degree of expression as well as the localisation on a subcellular and cell-type specific level. By separating primary and secondary carbon fixation in two different tissues, they drastically increase the local CO_2 concentration at the site of Rubisco activity (details of C_4 pathway has been described in chapter 1.1.2). CAM plants possess a CO_2-concentrating mechanism similar to that of C_4 plants. The initial CO_2 fixation occurs at night when the stomata open, the resulting C_4 acids are accumulated as malate in large vacuoles, which is decarboxylated in the ensuing light period behind the stomata closure (details of CAM pathway has been described in chapter 1.1.3). Many aquatic photosynthesizers also have developed a variety of CO_2-concentrating mechanisms (CCMs) in order to acclimatize themselves to the limiting and variable CO_2 concentrations in water. Some of them show similar CO_2 concentrating mechanism as in C_4 photosynthesis. The best studied aquatic photosynthesizer is *Hydrilla verticillata.* C_4-like photosynthesis is induced in *H. verticillata* at very limiting CO_2 concentrations caused by high levels of irradiance and temperature (Salvucci and Bowes, 1981). The structural features of *H. verticillata* show that it lacks the Kranz anatomy characteristics of terrestrial C_4 species (Reiskind *et al*., 1997). This result shows that the Kranz anatomy is not obligatory for C_4 type photosynthesis. In the pathway proposed in this thesis, an approach has been taken to concentrate CO_2 in the vicinity of Rubisco where Kranz anatomy is not required. So this pathway can also work in current C_3 plants without changing its anatomy.

In the photorespiration, the first products of the oxygenase reaction of Rubisco are one molecule of phosphoglycolate and one molecule of phosphoglycerate. Phosphoglycerate is used by the Calvin cycle whereas phosphoglycolate is converted into glycolate by an enzyme present in the chloroplast of C_3 plants. Glycolate is then transported to the peroxisomes where it oxidised into glyoxylate in a reaction catalysed by glycolate oxidase. This enzyme is oxygen dependent and produces H_2O_2 which is readily hydrolysed by a catalase present in the peroxisomes (1.2). The proposed novel pathway (3.1) is to convert glycolate into glycerate inside the chloroplast. The aim of the novel pathway is not to completely switch off the

photorespiratory pathway but the proposed mechanism will compete with the existing photorespiratory pathway and will reduce photorespiratory CO_2 loss by modifying the metabolic pathways of the products resulting from the Rubsico oxygenase activity. This will be achieved by installing the bacterial glycerate pathway inside the chloroplast. Bacteria like *E.coli* are capable of growing on glycolate as the sole carbon source. Three enzymes, glycolate dehydrogenase (GDH), glyoxylate carboligase (GCL) and tartronic semialdehyde reductase (TSR) are involved in this pathway (details in section 3.1). A similar pathway is also applied as a photorespiratory cycle in some green algae and cyanobacteria. The idea of the present work comes from the bacterial glycerate pathway.

In the last chapter, the mechanism of proposed pathway by which it will suppress the photorespiration has been described. However, it is still a general question whether any CO_2 concentrating mechanism would work in C_3 plants. Badger and Spalding (2000) suggested that C_4 photosynthesis has at least 7 main characteristics that are essential for its CO_2 concentrating mechanism. In the following chapter it will be discussed whether the glycerate pathway would be compatible with these prerequisites.

(1). C_4 photosynthesis requires an active, photosynthetically-driven, CO_2 capture system. In C_4 plants this role is played by PEP carboxylase that is highly expressed specifically in mesophyll cells (Stockhaus *et al*., 1997). The proposed pathway does not require such a system because it will use the CO_2 capturing system existing in C_3 plants. All reaction steps up to the formation of glycolate are identical to the photosynthesis/photorespiration as described for C_3 plants.

(2). C_4 photosynthesis requires extra energy to perform. The proposed pathway does not require extra energy. Plants benefit from the C_4 pathway under photorespiratory conditions (high light intensity and high temperature). In photorespiratory conditions a lot of extra energy is produced from the light reaction of photosynthesis. Use of this extra energy also helps to protect plants from photoinhibition (Kozaki and Takeba, 1996). The proposed pathway will only work under photorespiratory conditions and not constitutively because its activity will depend on the amount of glycolate available. However, the novel pathway will produce extra energy. One molecule of NADH is produce during the conversion of glycolate to glycerate. On the other hand, one molecule of NADH is used by Tartronic semialdehyde reductase. Since two molecules of glyoxylate are required to produce one molecule of tartronic semialdehyde, two molecules of NADH will be produced. On the other hand only one molecule of NAD(P)H will be reduced. So one molecule extra NADH will be produced in

the pathway. Unfortunately, the conditions are already reduced in chloroplasts under photorespiratory conditions. It is known that the excess reducing power converts in plant by some other pathway. For example in *Euglena gracilis,* excess NADPH from the light reactions of photosynthesis is transferred to the mitochondrium by the malate-oxaloacetate shuttle and used for the reduction of glyoxylate to glycolate which is known as oxaloacetate/malate shuttle (Yokota *et al*., 1985b). So the excess NADH might not be harmful for the plants. However, It is not possible to conclude at this stage that this extra reducing power will have damaging effect for plant or not.

(3). An intermediate pool of captured CO_2 is found in C_4 photosynthesis because oxaloacetate is highly reactive and does not accumulate to high concentrations in C_4 plants (Leegood, 2002). Generally oxaloacetate is converted to C_4 acids, such as malate and aspartate, which act as transient stores of fixed CO_2 (Hatch *et al*., 1971). In the proposed pathway no oxaloacetate is formed, so no intermediate pool of captured CO_2 is required. Instead, the CO_2 is directly available at the location of Rubisco activity and can be refixed without being transported as an organic compound.

(4). A mechanism is required in a C_4 pathway to release CO_2 from the intermediate pool. In C_4 plants this role is taken by specific enzymes decarboxylating C_4 acids in the bundle-sheath (Leegood, 2002). The novel pathway provides a mechanism to release CO_2 in the vicinity of Rubisco based on GCL activity. In the decarboxylation reaction that is catalyzed by GCL, one molecule of CO_2 is released for each two molecules of glycolate formed by the oxygenase activity of Rubisco. Because this reaction takes place inside the chloroplast, so the released CO_2 will compete with O_2 in the active site of Rubisco. By this way the oxygenase activity of Rubisco will be reduced.

(5). A C_4 pathway needs a compartment in which it concentrates CO_2 around Rubisco. In most of the C_4 plants the photosynthetic cells within the leaf are organized in two concentric cylinders known as Kranz anatomy (details 1.1.2). The thick wall of bundle sheath cells is a major barrier to the diffusion of solutes and gases. In C_4 plants CO_2 is concentrated in the bundle sheath. The diffusion of CO_2 in C_3 plants is determined by leaf anatomy, liquid path lengths and membrane properties (Evans and Von Caemmerer, 1996). C_3 leaves have large intercellular airspaces and chloroplasts are appressed to cell wall exposed to intercellular airspace, thus greatly increasing internal CO_2 diffusion. Von Caemmerer and Furbank (2003) compared the CO_2 diffusion in C_3 plants and C_4 plants utilizing a mathematical model and analyzed the possibility of introducing single cell C_4 photosynthesis and concluded that, “A single-cell C_4 system with the current C_3 diffusion characteristics is clearly not an efficient

CO_2 concentrating mechanism with its high leakiness and energy requirements. Nevertheless, the model has demonstrated that by introducing a C_4 system in C_3 plants, it may be possible to reduce the drop in pCO_2 (partial pressure of CO_2) between intercellular airspace and chloroplast. Introducing a C_4 pathway into C_3 cells may therefore be useful in ameliorating internal CO_2 diffusion limitations particularly at low intercellular pCO_2. In C_3 leaves the largest reductions in pCO_2 from intercellular airspace to chloroplasts occur at high light, in which the ATP supply is not limiting and considerations of energy efficiency may be of secondary importance. The model shows that this is particularly effective at lower intercellular pCO_2. Such a system may therefore be of benefit in water-limited conditions when stomata are closed and low intercellular pCO_2 increases photorespiration. It is unlikely that this approach will lead to increased leaf CO_2 assimilation rates under low irradiance because of the increased ATP requirement, which may be an important consideration in crop situations, where lower canopy leaves are light limited" (Von Caemmerer and Furbank, 2003). All the calculations valid for the transfer of a C_4-like pathway to C_3 plants are also applicable for the pathway proposed in this study. There is one major difference: No extra-energy is required-instead it produces energy. Therefore, it will be as effective in lower canopy as higher canopy in CO_2 limiting condition. This makes the glycolate oxidation inside the chloroplast especially suitbale for field applications.

(6). C_4 plants developed systems to reduce the leakage of CO_2 from the site of CO_2 elevation (Leegood, 2002). The C_4 pathway reduces the leakage in three ways (Leegood, 2002). (1) The C_4 stucture provides a long liquid diffusion pathway from the bundle sheath organelles to the intercellular spaces surrounding the mesophyll cells in some C_4 species. (2) The thickened wall of the bundle sheath reduces its permeability to CO_2. (3) Absence of the carbonic anhydrase in bundle sheath. The proposed pathway lacks such a system. This problem is neither solved by a C_4-like pathway nor by the pathway proposed in this study. Therefore, the positive effects of CO_2 concentration can never be as extensive as for a true C_4 pathway.

(7).The affinity of Rubisco for CO_2 in C_4 plants is lower compared the Rubisco of C_3 plants (The Km of Rubisco in C_4 plants ranges between 28-60 μM, in C_3 plants it ranges between 13-26 μM). A reduced affinity of Rubisco for CO_2 is associated with an increased catalytic turnover. So in C_3 pathways the catalytic turnover of Rubisco is lower than in C_4 pathways. However, the significance of this catalytic turnover is an open question. It is not clear whether photosynthesis is limited by the turnover rate of Rubisco and especially whether this is relevant under photorespiratory conditions where the proposed pathway is active.

In addition to the 7 characteristics described above, there are some other specific requirements of a CO_2 concentration mechanism related to C_4 photosynthesis. For example, C_3 plants also lack many transporters that are present in C_4 plants. Thus, it is necessary to introduce specific transporters in order to engineer an efficient C_4 like pathway in C_3 plants (Leegood, 2002). After considering all the above mentioned aspects, Leegood (2002) has concluded, "leaving aside all the argument about whether or not it is desirable to engineer C_4 photosynthesis into C_3 plants, it seems unlikely that attempts to introduce single cell CO_2-concentrating mechanisms will be successful without also introducing some of the structural characteristics of C_4 photosynthesis, that is, a compartment in which CO_2 could be concentrated." The proposed pathway does not require any transporters since there are no metabolic movements across membranes or in between cells. All the metabolites required for the proposed pathway are present in one single organelle, the chloroplast. However, whether and to which extent the missing compartmentation will interfere with the potentially beneficial effects of glycolate oxidation inside the chloroplast will be analysed after completion of a functional pathway inside a plant.

After considering all the above mentioned factors it seems that the proposed pathway is more suitable and has a better chance to suppress photorespiration in C_3 plants than introducing a C_4 pathway in C_3 plants. Moreover, it seems easier to introduce the proposed novel pathway into plants since only three enzymes are required for this pathway.

4.2 The strategy to establish the proposed pathway inside the chloroplast of C_3 plants.

The aim of the present thesis is to create transgenic plant containing all the genes necessary for the proposed pathway. Two strategies have been taken in order to transfer the coding sequences of the enzymes that are required to establish the novel pathway into the C_3 plant, tobacco. The first strategy is to transfer all the required genes into the plants by plastidial transformation. The second strategy is to transfer all the required genes into plants by nuclear transformation using chloroplast targeting sequence.

4.2.1 Creation of transgenic plant by plastidial transformation of an operon containing all genes required for the proposed pathway.

There are many advantages to create transgenic plants by plastidial transformation compared to nuclear transformation. Bock and Hagemann (2000) suggested 6 major advantages of transplasmic plants over classical transgenic plants:

1. High levels of transgene expression and foreign protein accumulation.
The transgene expression and foreign protein accumulation is much higher upon expression of a foreign gene in the plastid compartment compared to nucleocytoplasmic transgene expression. The higher expression may be caused by the polyploidy of the plastid genetic system with up to 10000 copies of the ptDNA per cell (Bendich, 1987). The higher accumulation of the foreign protein may be due to the high stability of foreign proteins in plastids (Staub and Maliga, 1993). Bock and Hagemann (2000) also suggested that the higher stability of the foreign proteins in the plastid is probably the cause of poor recognition of the plastid protein degration machinery.
2. Exact tuning of the expression level of transgene.
According to Bock and Hagemann (2000), transgene regulation in plastid can be regulated at three levels: (1) transcriptionally by the promoter choice (2) post-transcriptonally by the choice of the 3´ untranslated regions and (3) translationally by the choice of the shine-Dalgarno sequence directing translation initiation. With specific combinations of these three elements, one should be able to adjust any desired expression level of a transgene. Moreover, all nuclear tools for the regulation of transgene expression can also be employed for controlling gene expression in plastids. On the other hand, sophisticated tools for the regulation of transgene activity after nuclear transformation are also available.
3. Expression of (biosynthesis) pathway as operon.
It is possible to introduce several transgenes into a plant with a single transformation vector construct. Unlike in the nucleo-cytoplasmic compartment, polycistronic mRNAs can be efficiently translated in plastid, thereby allowing the simultaneous expression of several transgenes driven by a single promoter and stabilized by a sigle 3` untranslated region (Bock and Hagemann, 2000; Staub and Maliga, 1995). This, together with the prokaryotic nature of the chloroplast gene expression system gives the opportunity of expressing entire bacterial operons (Bock and Hagemann, 2000). Exactly such a system has been employed in this study. A vector was constructed allowing the simultaneous expression of all polypeptides necessary for the establishment of the proposed pathway. All 5 genes that are required to establish the

proposed pathway were amplified using the PCR method. Shine dalgarno sequences were added upstream of the *TSR* and *GCL* gene in order to allow translation of these open reading frames in the chloroplast of transgenic plants. The plastidial transformation was done in the lab of Proffesor Ralph Bock, University of Münster, Germany. Southern blot analysis showed that many transgenic plants loose part of the transgenes. Variable sizes of transgenes with much smaller size of the operon containing *GCL, TSR* and *GDH* genes have been detected by southernblot. Many of these plants also showed drastic phenotypic (e.g. Smaller leaf, no full expanded leaf etc.) syndromes (data not shown). The integration of foreign DNA sequences into the plastid genome appears to occur through homologous recombination (Bock and Hagemann, 2000). So it is possible that some homologous sequences of the transgenes are present in the chloroplast genome of tobacco. The homologous region of the transgenes may be excised from the operon by homologous recombination. Another possibility can be that the products of some transgenes in the operon are toxic to the plastid. So plastids somehow avoid the integration of that part of the operon. At this moment it is not clear why the operon loose part of the transgenes in the plastid of some of the transgenic plants. However, southern blot with the DNA of the few transgenic plants indicate the integration of the whole operon (Figure 3.2.1). These transgenic plants are flowering at this stage. Expression of the transgenes and activity of the enzymes encoded by the transgenes will be determined in next generation. However, although it seem very reasonable and simple – until now no pathway has been established in a chloroplast by over expression of a polycistronic transgene (to the best of my knowledge)

4. Absence of position effects in plastids.

Unlike the nuclear transformation, transgene integration into the plastid genome seems to occur exclusively via homologous recombination, facilitating the targeting of foreign genes to a specific location in the plastid DNA. So there is no positioning effect that found in transgenes expression in the plastid (Bock and Hagemann, 2000). Moreover, there is no epigenetic effect known in plastids whereas nuclear transformation experiments in plants have frequently been observed to suffer from epigenetic effects that cause low level of transgene expressions. In this study, strong position effects were observed after nuclear transformation of *TSR* and *GCL* gene into tobacco plant. Transgene expression varied by a factor of 5-50 comparing individual lines and transgene expression was sometimes lost in descendants from lines that showed high expression in the previous generation (data not shown).

5. Containment.

In most of the crop plants, chloroplasts are maternally inherited (Birky, 1995). In contrast to nuclear transgenes, plastid transgenes are excluded from distribution by the pollen of transgenic plants. So plastidial transformation experiments in plants minimizes the ecological risks associated with transgenic plants. This problem is not of major significance during the establishment of the pathway. However, the principle has been submitted for patent protection in collaboration with BAYER Cropscience (International Patent Application PCT/EP 03/05398) and is thought to be established in crops as soon as it has been shown to be functional. Therefore, ecological questions and problems of consumer concerns are always also relevant for this kind of work.

4.2.2 Generation of transgenic plant by nuclear transformation.

The second strategy of the present work was to create transgenic plants containing all the genes by nuclear transformation. The first enzyme of the proposed novel pathway is glycolate dehydrogenase. Bacterial glycolate dehydrogenase is encoded by the *glc* operon that consists of 6 open reading frames, with three of them being necesaary for activity. It is a time consuming and laborious process to create transgenic plants with each open reading frame and then bring them together (3.2). Moreover, bacterial glycolate dehydrogenase is a protein complex. So it is possible that it might not assemble correctly inside the chloroplast from single subunits. Considering all these problems, it was decided that first *TSR* and *GCL* should be transformed into plants because these enzymes are encoded by a single open reading frame. Then the transgenic plants (expressing *TSR* and *GCL* genes) will be transformed with the operon encoding the bacterial *GDH* by plastidial transformation. Alternatively a glycolate dehydrogenase encoded by a single open reading frame will be transformed into the transgenic plants expressing *TSR* and *GCL* gene by nuclear transformation.

Before transforming *GCL* and *TSR* genes into plants, first both genes were cloned into a prokaryotic expression vector. Expression of the genes and the enzymatic activity of the proteins were determined in bacteria. The chapter below will discuss the expression and enzymatic activity in bacteria, as well as, the creation of transgenic plants containing *TSR* and *GCL* genes.

4.2.2.1 Expression and activities of GCL and TSR proteins in bacteria.

In order to detect the expression of the genes in future experiments, the His-tag coding sequence is translationally fused to the genes. Due to the cloning strategy, 2 more additional amino acids are added between the C-terminal part of the proteins (TSR and GCL) and the His-tag. Enzymatic assays have been performed *in vitro* to assure that these additional amino acids do not interfere with the enzymatic activity. The *TSR* gene was cloned in parallel without being fused to a His-tag. The results from the enzymatic assays with and without His-tagged TSR proteins showed no significant difference (data not shown) proving that the additional amino acids fused to the C-terminal part of the TSR protein do not interfere with its activity. Crude extracts from the induced bacterial culture containing TSR and GCL protein has been used for the enzymatic assay. The enzymatic activity was measured spectophotometrically and based on the reduction of NADH. Initially, high backgrounds were found in the enzymatic assays for both TSR and GCL proteins (3.1.3 and 3.1.6). The background is much reduced but not abolished when an ultracentrifugation step was added before the crude extracts were subjected to enzymatic assays (data not shown). Even if the substrates are omitted from the reactions still some reduction of NADH can be observed (Figure 3.1.4). This reduction is probably resulting from other reductases and their substrates present in the crude extracts rather than TSR and GCL enzymes (3.1.3 and 3.1.6). When the crude extracts were omitted from the reaction mixture no reduction of NADH was observed (Figure 3.1.4). In order to minimize the background activity, the proteins (TSR and GCL) were also purified by Ni-NTA column chromatography. The purification step has been done at room temperature as well as at 4°C. Unfortunately, in both cases, the proteins (TSR and GCL) loose much of their activity during the purification step for unknown reasons. There can be several reasons for the reduced activity of the purified protein. It is known that GCL is a dimeric protein (Cromartie and Walsh, 1976) and TSR is a tetrameric (Ijau *et al*., 2000) protein. So it is possible that the enzymes somehow disassemble during the purification and can't reassemble properly. Moreover, the proteins were eluted from the column using 300 mM imidazol + 300 mM KCl and the high concentration of salt also can denature or disassemble the proteins causing reduced activity. GCL and TSR enzymes also required several co-factors (Badour and Waygood, 1971; van der Drift and de Windt, 1983) and GCL enzymes also required metal ion Mg^{+2}. In the enzymatic assay the co-factors and metal ions were supplied. So at this stage the exact reason for the reduced activity of the purified proteins is not clear.

However, crude extracts of induced bacterial cultures containing both proteins showed much higher activity compared to crude extracts from non-induced bacterial cultures as well as from crude extract of induced bacterial culture containing empty vector (Figure 3.1.2 and Figure 3.1.4). Results from the enzymatic assays proved that both enzymes (TSR and GCL) are active *in vitro* and that the His-tag fusion is not inhibiting their activity. So it is expected that the enzymes will also be active *in planta.*

4.2.2.2 Expression of GCL and TSR genes in transgenic tobacco plants.

TSR and *GCL* genes were cloned in single plant expression vectors separately as well as both genes were cloned together in one plant expression vector. Plant cells are commonly transformed with two or more tandemly arranged genes but orientation affects their expression. Padidam and Cao (2001) demonstrated that when two genes are oriented head to tail (→ →), the expression of the downstream gene is reduced by 80% compared to the upstream gene. When two genes are oriented tail to tail (→ ←) the expression of the upstream gene in reduced by 53% by the expression of the downstream gene. If the orientation of the genes are head to head (← →) then there is no interference of expression. The authors argue that the transcriptional interference of the genes is a result of RNA polymerase read through and/or antisense RNA production. However, Paddidam and Cao also demonstrated that the transcriptional interference also can be eliminated by inserting a transcription blocker (TB) sequence or a sequence from λ phage (Padidam and Cao, 2001). In order to eliminate the transcriptional interference in the present study, a transcriptional blocker, SAR (Scaffold attachment region), has been used between the coding sequence of *TSR* and *GCL* genes.

The construct containing *TSR* and *GCL* genes was transformed into plants by *Agrobacterium* mediated transformation. The regenerants were selected in MS medium containing kanamycin. The expression of genes was detected by western blotting. The enzymatic activity of GCL was measured *in vivo*. Among the transformants overexpressing a given foreign gene, varying protein amounts (Figure 3.1.5) as well as activity of its encoded enzyme was observed. In nuclear transformation experiments of higher plants, the transforming DNA integrates predominantly by nonhomologous recombination, resulting in a population of transgenic lines with different copy numbers of the transgene and different expression levels depending on the genomic context at the integration site (Bock and Hagemann, 2000). Several other factors, such as translational and post-translational regulation, epigenetics or gene

silencing mechanism, can affect the protein amount as well as the activity of an enzyme encoded by a transgene (Fojtova *et al*., 2003). As for the present study, the exact reasons for the variations in levels of accumulated foreign proteins as well as their enzyme activities in transformed tobacco plants remained to be elucidated. Different susceptibility of respective genes to co-suppression might partially contribute to the differences in detection rates of different foreign proteins.

4.2.2.3 Phenotypic effects of the transgenic plants expressing GCL and TSR protein.

After the generation of roots, the regenerants were transferred into soil and were grown in a phytochamber. The light intensity in the phytochamber is around 150 µmol m^{-2} s^{-1} and the plants were grown in ambient air. Three weeks later, the plants were transferred to the green house where the light intensity is around 300 µmol m^{-2} s^{-1}. Already in the phytochamber or even in sterile culture, some of the plant started to exhibit chlorototic phenotype. All the upper leaves of the transgenic plants became chlorotic whereas the first 2 or 3 leaves are not affected by chlorosis even later in development (Figure 3.1.9). It seems that the chlorotic effect is developmentally regulated. The leaf veins of the chlorotic plants are always green. Those plants that showed severe chlorotic (Figure 3.1.7C) effect died before flowering whereas those showing less chlorotic effects (Figure 3.1.7B) survived. Seeds from the less chlorotic plants were collected. Next generation of the chlorotic plants also showed the similar phenotype. Experiments with transgenic plants containing single genes (either *TSR* or *GCL*) showed that the expression of the *GCL* gene is responsible for the phenotypic effects. However, the chlorotic effect varied in between individual plants and correlated with the level of *GCL* expression**.** There are two possibilities for the chlorotic effect of the transgenic plants expressing *GCL* gene: (1) Rubisco transit peptide might interfere with the import of necessary proteins because of the high amount of GCL protein expressed in the nucleus of transgenic plants and exported to the chloroplast or (2) the activity of the GCL enzyme causes metabolic changes in the chloroplast of transgenic plants that damage the chlorophyll. The first possibility is improbable since transgenic plants expressing a similar level of the *TSR* gene did not show any chlorotic effect (3.1.9). One reason of the chlorotic effect in the transgenic plants can be that the GCL enzyme interferes in the glycolate-glyoxylate shuttle present between the chloroplast and peroxisomes of higher plants. Tolbert *et al*. (1970) demonstrated that a NADPH-glyoxylate reductase enzyme is present in the chloroplasts of higher plants which convert glyoxylate to glycolate. From the chloroplast the glycolate moves to the peroxisomes and is oxidized to glyoxylate. A part of the glyoxylate returns to the chloroplast

and is used to produce glycolate and complete the glycolate-glyoxylate shuttle. The glycolate-glyoxylate shuttle between the two particles provides a means for disposing of excess reducing power (NADPH) generated during photosynthesis in the chloroplast. So it is possible that GCL enzyme uses the glyoxylate present in the chloroplast and converts it into tartronic semialdehyde which stops the glycolate-glyoxylate shuttle. Moreover, GCL does not use any co-factor to conduct this reaction, so the excess reducing power in the chloroplast might cause the chlorotic effect found in transgenic plant. However, it is unlikely since transgenic plants containing both *TSR* and *GCL* also showed the same chlorotic phenotype. TSR enzyme reduced tartronic semialdehyde and used NADH. It should be noted that it was not possible to measure TSR activity *in vivo* since the protein is membrane bound and precipitated with cell debris. So one can not rule out the possibility that plants loose its ability to dispose the excess reducing power in the presence of the GCL protein causing the chlorotic effect. Recently one of the colleagues in our lab, Krishnaveni Thiruveedhi, transformed a coding sequence of AtGDH (this enzyme has been characterized in the present work and will be discussed in a later chapter) into the chlorotic transgenic plants expressing *TSR* and *GCL* genes. It seems that the transgenic plants recover from the chlorotic effect after transformation with the coding sequence of the glycolate dehydrogenase enzyme. So it is possible that AtGDH converts sufficient substrate for the glycolate-glyoxylate shuttle as well as for GCL enzyme. However, the expression of the foreign gene (*AtGDH*) in transgenic plants has not been determined yet. At this stage the exact reason for this chlorotic effect is unclear. Further studies are required to answer this question unequivocally.

4.3 Characterization of a glycolate dehydrogenase in the mitochondria of *Arabidopsis thaliana*.

The purpose of the present thesis is to introduce all genes necessary to establish the proposed novel pathway inside the chloroplast of C_3 plants. In order to fulfill the objective, coding sequences for three enzymes (GCL, TSR and GDH) have to be transformed into tobacco plants. Transgenic plants have been successfully generated that are overexpressing *TSR* and *GCL* genes in the present work. If the coding sequence of the third enzyme, the glycolate oxydising activity, can be introduced into these transgenic plants all the required genes would be present in a single plant. The problem with the nuclear transformation of the coding sequence of Glycolate dehydrogenase (GDH) enzyme has been described before. Because of the above mentioned problem, an alternative to the *E. coli* glycolate dehydrogenase enzyme

was desirable in order to establish the proposed pathway inside the chloroplast of tobacco plants by nuclear transformation.

The alternatives to the *E. coli* glycolate dehydrogenase are shown in Table 4.1:

Table 4.1. Different glycolate oxidizing enzymes present in higher plants and animals.

Enzyme	Activity
Glycolate oxidase (GO; EC 1.1.3.15)	oxygen dependent peroxisomal plant photorespiration
Glyoxylate oxidoreductase (GOR; EC 1.1.1.26/79)	NAD/NADP dependent cloned from human source equilibrium unclear
glycolate dehydrogenase and D-lactate dehydrogenase homologue in *Arabidopsis*	functions are unknown

The main characteristics of the above mentioned enzymes, their advantages and disadvantages are shortly described below:

1. The plant glycolate oxidase (GO) enzyme that converts glycolate to glyoxylate is located in the peroxisome. The plant glycolate oxidase is an oxygen dependent enzyme and produces H_2O_2 which is rapidly hydrolised by a catalase present in the peroxisome of the plant. Such a catalase is not reported yet in the chloroplast of the plant. So the introduction of higher plant glycolate oxidase in the chloroplast of the tobacco plant will produce H_2O_2 that can have a very damaging effect. So this possibility was excluded from the present work.
2. Human glyoxylate reductase (HGR) converts glyoxylate to glycolate. The equilibrium of this reaction is unclear. HGR was cloned from human liver cDNA and expressed in an identical way as described before for *AtGDH*. Enzymatic assays in crude extracts revealed that the enzyme readily catalysed the reduction of glyoxylate to glycolate but not the inverse reaction (data not shown). Therefore it was decided that this enzyme is not suitable for the present work.

3. Sequence analysis of the *Arabidopsis* genome revealed an open reading frame (At5g06580) with significant homology to the subunit D of *Escherichia coli* glycolate oxidase. The function of this open reading frame was unknown.

In order to clarify the question whether the enzyme encoded by this open reading frame is really active as a glycolate dehydrogenase, cDNA was cloned from *Arabidopsis* mRNA and overexpressed in bacteria. Several results argue in favor of AtGDH being a glycolate dehydrogenase. The amplified PCR product was cloned and expressed in bacteria. The expression of the open reading frame was determined by westernbloting. The Enzymatic assay was performed with crude extracts from induced bacterial culture because due to some unknown reason the enzyme lost most of its activity during the purification as seen in the case of TSR and GCL enzymes (see above for a detailed discussion). Results from the enzymatic assays showed that indeed AtGDH converts glycolate to glyoxylate in an oxygen-independent manner. Enzymes that convert glycolate to glyoxylate in plants have been grouped into two main classes (Frederick *et al*., 1973). One that is found in higher plants is oxygen dependent and located in the peroxisomes as detailed before. Moreover, this enzyme oxidises L(+)-lactate preferentially over D(-)- lactate. The enzymatic activity of higher plants glycolate oxidases is not inhibited by cyanide. On the other hand, the second class of glycolate oxidising enzymes are found in the mitochondrion of algae. In contrast to the first class, the first electron acceptor for most green algal enzymes seems to be a so far unidentified organic compound that can be replaced by DCIP *in vitro* (Nelson and Tolbert, 1970). Moreover, the algal mitochondrial glycolate oxidases catalyze the oxidation of D(-)- lactate preferentially over L(+)-lactate. The activity of these enzymes is inhibited by cyanide and the enzyme is located in the mitochondria. Beside the peroxisomal and the mitochondrial glycolate oxidoreductases, glycolate dehydrogenase activity has also been described for as well algal as higher plant chloroplasts (Goyal, 2002; Goyal and Tolbert, 1996).

Results from the enzymatic assays show that AtGDH resembles the algal glycolate dehydrogenase. AtGDH shares enzymatic properties with its algal counterparts like the specificity for substrates and co-factors as well as the sensitivity to inhibitors. This clearly discriminates the enzyme from the so far described peroxisomal glycolate oxidases of higher plants and no sequence homology is found to this class of enzymes (data not shown). The complementation analysis shows that *AtGDH* is capable of complementing bacterial mutants that are deficient in glycolate oxidation dependent on organic co-factors. *AtGDH* can replace

any of the three subunits of *E. coli* glycolate dehydrogenase. However, in the present it was not tested whether the *Arabidopsis* enzyme also restores growth in mutants where all three subunits have been deleted simultaneously. Therefore, it is not possible to formally exclude that *At*GDH can only replace any individual subunit of *Ec*GO but not the complete enzyme and forms active complexes with the remaining subunits. This seems improbable because the enzymatic activity can be measured in crude extracts of overexpressing wild-type *E. coli* strains that show only a very low background glycolate dehydrogenase activity in the absence of *At*GDH. In order to understand the subcellular localisation of AtGDH, the sequence was analyzed using the TargetP algorithm (Emanuelsson *et al.*, 2000). The sequence analysis identified high scores both for a putative chloroplast transit sequence of 56 amino acids and a putative mitochondrial target sequence of 30 amino acids. The N-terminal domain of *AtGDH* encoding the first 77 amino acids was translationally fused to green fluorescent protein (gfp) and transformed in BY-2 cells indicated that the protein may also be localized in plastids or in mitochondria (data not shown). There is much evidence that dual targeting of a protein is possible (Babiychuk *et al*., 2003; Chew *et al*., 2003; Creissen *et al*., 1995; Goggin *et al*., 2003; Small *et al*., 1998). Recently, Chew *et al.* (2003) characterized the targeting signal of pea glutathione reductase. They showed that the same glutathione reductase of pea is located both in mitochondria and chloroplasts. However, the data from the present work were not clear enough to conclude that the protein definitely is targeted to both chloroplast and mitochondrion. In order to be sure about the localization, the same N-terminal domain of *AtGDH* was translationally fused to red fluorescent protein (rfp). Protoplasts were isolated from the transgenic *Arabidopsis* plants and stained with Mito Tracker dye. The recombinant protein clearly co-localized with mitochondria that were identified using the MitoTracker dye (Figure 3.3.5). Although computer predictions also identified a high score for a chloroplast transit signal, fluorescence of the overexpressed enzyme was only occasionally found in leaf chloroplasts probably due to mistargeting (data not shown). Cytochemical analyses provided evidence that the mitochondrial glycolate dehydrogenases of *Chlamydomonas* is located in between the inner and the outer membrane (Beezley *et al*., 1976) and we are currently generating antibodies to *At*GDH in order to determine the targeting of *At*GDH within the mitochondrion.

The crucial question is which can be the possible role of a glycolate dehydrogenase present in the mitochondria of a higher plant. There are several possibilities which can explain the presence of glycolate dehydrogenase in the mitochondrion of *Arabidopsis*. The first and the

most probable possibility is that the glycolate dehydrogenase reported in the present work may be reminiscent of the algal glycolate dehydrogenase. In many green algal species, glycolate dehydrogenase is present in mitochondria where it produces glyoxylate from glycolate. The glyoxylate is further metabolized to glycine in the mitochondrion and afterwards by different pathways to glycerate, serine or related compounds (Igamberdiev and Lea, 2002; Winkler and Stabenau, 1992). This pathway is part of the algal photorespiration. So is it possible that a second photorespiratory pathway is present in the mitochondrion of higher plants? It is not clear that the *Arabidopsis* glycolate dehydrogenase reported in the present work is playing the same role as their algal counterpart since there is no evidence that any enzyme converting glyoxylate to glycine is present in the mitochondrion of *Arabidopsis*. Moreover, mutations in peroxisomal photorespiration usually lead to lethal phenotypes that can only be rescued by non-photorespiratory growth conditions (Somerville, 1984). So it seems improbable that a second photorespiratory pathway is present in higher plants. On the other hand, the available data indicate that the activity of the mitochondrial glycolate dehydrogenase in algae is inadequate under photorespiratory conditions and algae are capable of excreting glycolate to a large extent (Colman *et al*., 1974; Stabenau, 1992). So it is possible that a second alternative photorespiratory pathway is present in the plant that is insufficient to complement mutations in peroxisomal photorespiration.

A second possible function of AtGDH can be that it acts as a lactate dehydrogenase *in vivo*. Lactate dehydrogenases are present in plants and involved in anaerobic energy production. But anoxic conditions in plants have only been described for roots and seedlings and the enzymes involved only use L-lactate as a substrate (Drew, 1997). However, enzymatic assays with both L-lactate and D-lactate show that AtGDH is preferentially using D-lactate as its substrate. Moreover, the transcript abundance tested by Real-Time PCR indicates that *AtGDH* is found in all tested organs, but that the accumulation is almost double in leaves compared to roots and leaves hardly ever face anoxic conditions. So it seems very improbable that the AtGDH is functioning as lactate dehydrogenase in plants.

Another possible function of AtGDH might be the involvement in a glycolate/glyoxylate shuttle as described for the alga *Euglena gracilis* (Yokota *et al*., 1985a; Yokota and Kitaoka, 1979). The shuttle operates in the mitochondrium of *E. gracilis* and eliminates the excess energy formed under photorespiratory conditions. In Euglena, excess NADPH from the light reaction is transported to the mitochondrium by the malate-oxaloacetate shuttle. The NADPH

is used for the reduction of glyoxylate to glycolate. Glyoxylate is in turn recycled by glycolate dehydrogenase and the electrons are transferred into the respiratory electron transport chain and used for ATP synthesis.

Goyal and Tolbert (1996), reported the presence of a glycolate dehydrogenase enzyme in the chloroplast of *Dunaliella* and spinach that is associated with the photosynthetic electron transport system. They proposed that this may be a way to recycle carbon from glycolate while regenerating energy under extreme environments. There is also evidence of glyoxylate reductase activity in the chloroplast of higher plants and *Chlamydomonas* mitochondria (Givan and Kleczkowski, 1992; Yokota and Kitaoka, 1979), but such an enzyme has not been described for higher plant mitochondria until now.

Although data from this present work clearly demonstrated the presence of a glycolate dehydrogenase enzyme in the mitochondrion of *Arabidopsis*, the exact role of this enzyme is not clear yet. The available data favor the hypothesis of an ancient algal photorespiratory system in higher plants.

4.4 Outlook.

The aim of the present thesis is to create transgenic plants containing all genes necessary to complete the conversion of photorespiratory glycolate to glycerate inside the chloroplast. In the present work, transgenic plants have been created by plastidial transformation containing all genes required for the pathway. Transgenic plants expressing *TSR* and *GCL* have been created by nuclear transformation. Recently, the *AtGDH* coding sequence has been transformed into the chlorotic transgenic plants expressing *TSR* and *GCL* genes. So there are also transgenic plants available now containing all the necessary genes after nuclear transformation with chloroplast targeting sequences. So the immediate future work should be to check the expression of the genes and measure the activity of the enzymes *in planta*. In the present work, GCL activity *in planta* has been measured. It will also be interesting to check TSR, AtGDH and GDH activity *in planta.* One possibility to check the functional pathway would be to feed ^{14}C-glycolate to the transgenic plants and measure the labeled glycerate. Another possibility would be to measure the activity of the enzymes from enriched chloroplasts of transgenic plant. Photosynthetic metabolites will need to be measured in order to determine the metabolic activity changes in transgenic plants. The crucial question is does

this pathway improve the CO_2 fixation in transgenic plants? To answer this question, photosynthetic parameters of the transgenic plants should be measured. The transgenic plants will be grown together with control plants in photorespiratory conditions (high light intensity, high temperature and dry conditions) and the ability of the plants to stand unfavorable conditions will be tested. Somerville and Ogren (1982) have created mutants with deficiencies in enzymes of the photorespiratory pathway. Photosynthesis and growth are normal in these mutants under non-respiratory conditions (high CO_2 and low O_2 concentration), but plants died in ambient air. It would be very interesting to cross transgenic plants containing the proposed pathway with the photorespiratory mutants and see if the plants can survive under photorespiratory conditions.

5 LIST OF ABBREVIATIONS.

Abbreviation	Full form
Amp/Ampr	ampicillin/ampicillin resistance
APS	ammonium persulfate
AtGDH	*Arabidopsis thaliana* glycolate dehydrogenase
ATP	adenosine triphosphate
bla	gene for β-lactamase
bps	base pairs
BSA	bovine serum albumin
BSC	bundle sheath cell
C2-cycle	photorespiratory cycle (2 Carbon cycle)
C3-cycle	benson calvin cycle (3 Carbon cycle)
C4-cycle	C4-like CO_2 assimilation pathway
CA	carbonic anhydrase
CAT	catalase
CAM	crassulacean acid metabolism
CaMV	cauliflower mosaic virus
Carb	carbenicillin
cDNA	complementary DNA
CoA	coenzyme A
cv.	cultivar
DMSO	dimethyl sulfoxide
DNA	deoxyribonucleic acid
dNTP	deoxyribonucleoside triphosphate
DTT	dithiothreitol
EDTA	ethylene diamine tetraacetic acid
G3P	glyceraldehyde-3-phosphate
GCL	glyoxylate carboxyligase
GDC	glycine decarboxylase
GDH	glycolate dehydrogenase
gfp	green fluorescent protein
GGAT	glutamate:glyoxylate aminotransferase
GK	glycerate kinase
*Glc*D	coding sequence for the D subunit of glycolate oxidase in *E. coli*
*Glc*E	coding sequence for the E subunit of glycolate oxidase in *E. coli*
*Glc*F	coding sequence for the F subunit of glycolate oxidase in *E. coli*
GO	glycolate oxidase
GOGAT	glutamate:glyoxylate aminotransferase
GOX	glycolate oxidase
GS	glutamine synthetase
h	hour
Hepes	N-2-hydroxyethylpiperazine-N´-2-ethanesulfonic acid
kb	kilobase pair
kD	kilodalton
Km	michaelis constant
HCO_3^-	bicarbonate
HPR	hydroxypyruvate reductase

Abbreviation	Full form
IPTG	isopropyl-β-D-thiogalactoside
Kan	kanamycin
LB medium	Luria Bertani medium
MC	mesophyll cell
ME	malic enzyme
min	minute
MOPS	3-(N-morpholino) propane sulfonic acid
mRNA	messenger RNA
N. tabacum	*Nicotiana tabatum*
NAD-ME	NAD-malic enzyme
NAD+/NADH	nicotinamide adenine dinucleotide (oxidized/reduced form)
NADP+/NADPH	nicotinamide adenine dinucleotide phosphate (oxidized/reduced form)
NCBI	national center for biotechnology information
OAA	oxalo acetic acid
OD	optical density
PCK	phosphoenolpyruvate carboxykinase
pCO_2	partial pressure of CO_2
PCR	polymerase chain reaction
PCR-cycle	photosynthetic carbon reduction cycle
PEPC	phosphoenolpyruvate carboxylase
PEP-CK	phosphoenolpyruvate carboxykinase
PG	phosphoglycolate
PGA	phosphoglycerate
PGP	phosphoglycolate phosphatase
PPDK	pyruvate-orthophosphate dikinase
ptDNA	plastidial DNA
PYR	pyruvate
rfp	red fluorescent protein
Rif	rifampicin
RNA	ribonucleic acid
RP	ribulose phosphate
rpm	rotation per minute
RT	room temperature
RT	reverse transcriptase
RT-PCR	reverse transcriptase-polymerase chain reaction
Rubisco	ribulose 1,5 bisphosphate carboxylase/oxygenase
RuBP	ribulose 1, 5 bisphosphate
SDS-PAGE	sodium dodecyl sulphate-polyacrylamide gel electrophoresis
sec	second
SGAT	serine:glutamate aminotransferase
SS	serine synthase
TEMED	N, N, N´, N´-tetramethyl ethylene diamine
TSR	tartronic semialdehyde reductase
U	unit
UV	ultraviolet
vol.	volume
v/v	volume per volume
w/v	weight per volume

6 LIST OF FIGURES AND TABLES.

6.1 List of Figures.

6.2 List of Tables.

7 LITERATURE.

Altschul, S. F., Madden, T. L., Schaffer, A. A., Zhang, J., Zhang, Z., Miller, W., and Lipman, D. J. (1997). Gapped BLAST and PSI-BLAST: a new generation of protein database search programs. Nucleic Acids Res *25*, 3389-3402.

Andrews, T., and Lorimer, G. (1987). RUBISCO: structure, mechanisms and prospects for improvement. Academic press, New York, The biochemistry of plants *10*, 131-218.

Arp, W. J., Van Mierlo, J. E. M., Berendse, F., and Snijders, W. (1998). Interactions between elevated CO_2 concentration, nitrogen and water: Effects on growth and water use of six perennial plant species. Plant Cell Env *21*, 1-11.

Ausubel, F. M., Brent, R., and Kingston, R. E. (1994). Current Protocols in Molecular Biology. Wiley Interscience, New York.

Babiychuk, E., Muller, F., Eubel, H., Braun, H. P., Frentzen, M., and Kushnir, S. (2003). Arabidopsis phosphatidylglycerophosphate synthase 1 is essential for chloroplast differentiation, but is dispensable for mitochondrial function. Plant J *33*, 899-909.

Badger, M. R., and Spalding, M. H. (2000). CO_2 acquisition, concentration and fixation in cyanobacteria and algae. Photosynthesis: Physiology and Metabolism *9*, 369-397.

Badour, S. S., and Waygood, E. R. (1971). Glyoxylate carboxy-lyase activity in the unicellular green alga *Gloeomonas sp*. Biochim Biophys Acta *242*, 493-499.

Beezley, B. B., Gruber, P. J., and Frederick, S. E. (1976). Cytochemical localization of glycolate dehydrogenase in mitochondria of *Chlamydomonas reinhardi*. Plant Physiol *58*, 315-319.

Bendich, A. (1987). Why do chloroplasts and mitochondria contain so many copies of their genome? BioEssays *6*, 279-282.

Besford, R. (1990). The greenhouse effects on the acclimation of tomato plants growing in high carbon dioxide relative to changes in Calvin cycle enzymes. J Plant Phys *136*, 458–463.

Birky, C. J. (1995). Uniparental inheritance of mitochondrial and chloroplast genes: mechanisms and evolution. Proc Natl Acad Sci USA *92*, 11331-11338.

Bock, R. (2001). Transgenic plastids in basic research and plant biotechnology. J Mol Biol *312*, 425-438.

Bock, R., and Hagemann, R. (2000). Extranuclear inheritance: Plastid genetics: manipulation of plastid genomes and biotechnological applications. Prog Bot *61*, 76-90.

Bowes, G., Ogren, W., and Hageman, R. (1971). Phosphoglycolate production catalysed by Ribulose diphosphate carboxylase. Biochem Biophys Res Commun *45*, 716-722.

Bradford, M. M. (1976). A Rapid and sensitive method for the quantitation of microgram quantities of protein utilizing the principle of protein-dye binding. Anal Biochem *72*, 248-254.

Brown, R. H., and Bouton, J. H. (1993). Physiology and genetics of interspecific hybrids between photosynthetic types. Annu Rev Plant Physiol Plant Mol Biol *44*, 435-456.

Buchanan, B. B., Gruissem, W., and Jones, R. L. (2000). Biochemistry & Molecular Biology of plants. American Society of Plant Physiologists, Rockville, Maryland, 625.

Burnell, J. N., and Hatch, M. D. (1988). Photosynthesis in phosphoenolpyruvate carboxykinase-type C_4 plants: pathways of C4 acid decarboxylation in bundle sheath cells of *Urochloa panicoides*. Arch Biochem Biophys *260*, 187-199.

Casati, P., Lara, M. V., and Andreo, C. S. (2000). Induction of a C_4-like mechanism of CO_2 fixation in Egeria densa, a submersed aquatic species. Plant Physiol *123*, 1611-1622.

Chang, Y. Y., Wang, A. Y., and Cronan, J. E., Jr. (1993). Molecular cloning, DNA sequencing, and biochemical analyses of Escherichia coli glyoxylate carboligase. An enzyme of the acetohydroxy acid synthase-pyruvate oxidase family. J Biol Chem *268*, 3911-3919.

Chen, K., Hu, G., Kreutgen, N., and Lenz, F. (1997). The effect of CO_2 concentration on strawberries. I. Plant growth analysis. J Appl Bot *71*, 168–172.

Chen, Z., and Spreitzer, R. (1992). How various factors influence the CO_2/O_2 specificity of ribulose-1,5 bisphosphate carboxylase/oxygenase. Photosynthesis Res *31*, 157–164.

Chew, O., Rudhe, C., Glaser, E., and Whelan, J. (2003). Characterization of the targeting signal of dual-targeted pea glutathione reductase. Plant Mol Biol *53*, 341-356.

Clough, S., and Bent, A. (1998). Floral Dip: a simplified method for Agrobacterium-mediated transformation of *Arabidopsis thaliana*. Plant J *16*, 735-743.

Colman, B., Miller, A. G., and Grodzinski, B. (1974). A study on the control of glycolate excretion in *Chlorella pyrenoidosa*. Plant Physiol *53*, 395-397.

Creissen, G., Reynolds, H., Xue, Y., and Mullineaux, P. (1995). Simultaneous targeting of pea glutathione reductase and of a bacterial fusion protein to chloroplasts and mitochondria in transgenic tobacco. Plant J *8*, 167-175.

Cromartie, T. H., and Walsh, C. T. (1976). *Escherichia coli* glyoxylate carboligase. J Biol Chem *251*, 329-333.

Cushman, J. C., and Bohnert, H. J. (1997). Molecular Genetics of Crassulacean Acid Metabolism. Plant Physiol *113*, 667-676.

Dai, Z., Ku, M., and Edwards, G. E. (1993). C_4 Photosynthesis (The CO_2-Concentrating Mechanism and Photorespiration). Plant Physiol *103*, 83-90.

Drew, M. (1997). Oxygen deficiency and root metabolism: Injury and acclimation under hypoxia and anoxia. Annu Rev Plant Physiol Plant Mol Biol *48*, 223-250.

Dym, O., and Eisenberg, D. (2001). Sequence-structure analysis of FAD-containing proteins. Protein Sci *10*, 1712-1728.

Edwards, G. E., and Walker, D. A. (1983). C_3, C_4: mechanisms and cellular and environmental regulation of photosynthesis. Blackwell Scientific, Oxford.

Ehleringer, J. R., Sage, R. F., Flanagan, L. B., and Pearcy, R. W. (1991). Climate change and the evolution of C_4 photosynthesis. Trends Ecol Evolution *6*, 95-99.

Emanuelsson, O., Nielsen, H., Brunak, S., and von Heijne, G. (2000). Predicting Subcellular Localization of Proteins Based on their N-terminal Amino Acid Sequence. J Mol Biol *300*, 1005-1016.

Evans, J. R., and Von Caemmerer, S. (1996). Carbon Dioxide diffusion inside leaves. Plant Physiol *110*, 339-346.

Fojtova, M., Van Houdt, H., Depicker, A., and Kovarik, A. (2003). Epigenetic Switch from Posttranscriptional to Transcriptional Silencing Is Correlated with Promoter Hypermethylation. Plant Physiol *133*, 1240-1250.

Frederick, S. E., Gruber, P. J., and Tolbert, N. E. (1973). The occurence of glycolate dehydrogenase and glycolate oxidase in green plants: An evolutionary survey. Plant Physiol *52*, 318-323.

Furbank, R. T., and Taylor, W. C. (1995). Regulation of photosynthesis in C3 and C4 plants: A molecular approach. Plant Cell *7*, 797-807.

Furumoto, T., Hata, S., and Izui, K. (1999). cDNA cloning and characterization of maize phosphoenolpyruvate carboxykinase, a bundle sheath cell-specific enzyme. Plant Mol Biol *41*, 301-311.

Gerbaud, A., and Andre, M. (1987). An evaluation of the recycling in measurements of photorespiration. Plant Physiol *83*, 933-937.

Givan, C. V., and Kleczkowski, L. A. (1992). The enzymic reduction of glyoxylate and hydroxypyruvate in leaves of higher plants. Plant Physiol *100*, 552-556.

Goggin, D. E., Lipscombe, R., Fedorova, E., Millar, A. H., Mann, A., Atkins, C. A., and Smith, P. M. (2003). Dual intracellular localization and targeting of aminoimidazole ribonucleotide synthetase in cowpea. Plant Physiol *131*, 1033-1041.

Gotto, A. M., and Kornberg, H. L. (1961). The metabolism of C_2 compounds in micro-organisms. 7. Preparation and properties of crystalline tartronic semialdehyde reductase. Biochem J *81*, 273-284.

Goyal, A. (2002). Glycolate metabolism in algal chloroplasts: inhibition by salicylhydroxamic acid (SHAM). Physiol Plant *116*, 264-270.

Goyal, A., and Tolbert, N. E. (1996). Association of glycolate oxidation with photosynthetic electron transport in plant and algal chloroplasts. Proc Natl Acad Sci USA *93*, 3319-3324.

Gutheil, W. G. (1998). A sensitive equilibrium-based assay for D-lactate using D-lactate dehydrogenase: application to penicillin-binding protein/DD-carboxypeptidase activity assays. Anal Biochem *259*, 62-67.

Hanahan, D. (1983). Studies on transformation of *Escherichia coli* with plasmids. J Mol Biol *166*, 557-580.

Hansen, R. W., and Hayashi, J. A. (1962). Glycolate Metabolism in *Escherichia coli*. J Bacteriol *83*, 679-687.

Hatch, M., Osmond, C., and Slatyer, R. (1971). Photosynthesis and photorespiration. New York: Wiley-Interscience.

Hatch, M. D. (1987). C_4 photosynthesis: a unique blend of modified biochemistry, anatomy and ultrastructure. Biochim Biophys Acta *895*, 81-106.

Hatch, M. D. (1992). C_4 Photosynthesis: an Unlikely Process Full of Surprises. Plant Cell Physiol *33*, 333-342.

Hatch, M. D., Kagawa, T., and Craig, S. (1975). Subdivision of C_4 pathway species based on differing C_4 acid decarboxylating systems and ultrastructural features. Aust J Plant Physiol *2*, 111-128.

Häusler, R. E., Hirsch, H. J., Kreuzaler, F., and Peterhänsel, C. (2002). Overexpression of C_4-cycle enzymes in transgenic C_3 plants: a biotechnological approach to improve C_3-photosynthesis. J Exp Bot *53*, 591-607.

He, D., and Edwards, G. E. (1996). Estimation of diffusive resistance of bundle sheath cells to CO_2 from modeling of C_4 photosynthesis. Photosynthesis Res *49*, 195-208.

Heldt, H.-W. (1997). Plant Biochemistry & Molecular Biology. Oxford University Press, New York.

Horsch, R. B., Fry, J. E., Hoffmann, N. L., Eichholtz, D., Rogers, S. G., and Fraley, R. T. (1985). A simple and general method for transferring genes into plants. Science *227*, 1229-1231.

Igamberdiev, A. U., and Lea, P. J. (2002). The role of peroxisomes in the integration of metabolism and evolutionary diversity of photosynthetic organisms. Phytochem *60*, 651-674.

Igarashi, D., Miwa, T., Seki, M., Kobayashi, M., Kato, T., Tabata, S., Shinozaki, K., and Ohsumi, C. (2003). Identification of photorespiratory glutamate:glyoxylate aminotransferase (GGAT) gene in *Arabidopsis*. Plant J *33*, 975-987.

Ijau, R. K., Herndon, C. A., and Hawes, J. W. (2000). Novel beta-hydroxyacid dehydrogenases in *Escherichia coli* and *Haemophilus infuenzae.* J Biol Chem *275*, 38780-38786.

Ireland, R., and Lea, P. (1998). The enzymes of glutamine, glutamate, asparagine and aspartate metabolism. In: Plant amino acids. Edited by Singh BK, Academic Press, New York, 49-109.

Jach, G., Binot, E., Frings, S., Luxa, K., and Schell, J. (2001). Use of red fluorescent protein from Discosoma sp. (dsRED) as a reporter for plant gene expression. Plant J *28*, 483-491.

Jenkins, C. L. D., Furbank, R. T., and M.D., H. (1989). Mechanism of C_4 photosynthesis. A model describing the inorganic carbon pool in bundle sheath cells. Plant Physiol *91*, 1372-1381.

Jordan, D., and Ogren, W. (1984). The CO_2/O_2 specificity of ribulose 1,5-bisphosphate carboxylase/oxygenase. Dependence on ribulose bisphosphate concentration, pH and temperature. Planta *161*, 308–313.

Keys, A. (1986). Rubisco: its role in photorespiration. Phil Trans Royal Soc *313*, 325-336.

Kimball, B. A. (1983). Carbon dioxide and agricultural yield: an assemblage and analysis of 430 prior observations [Effect on crop yields of the increasing global atmospheric carbon dioxide concentration, growth, production includes some woody plants]. Agronomy J Sept/Oct, 779-788.

Kohn, L. D., and Jakoby, W. B. (1968). Tartaric acid metabolism. 3. The formation of glyceric acid. J Biol Chem *243*, 2465-2471.

Koncz, C., and Schell, J. (1986). The promoter of TL-DNA gene 5 controls the tissue-specific expression of chimaeric genes carried by a novel type of *Agrobacterium* binary vector. Mol Gen Genet *204*, 383-396.

Kornberg, H. L., and Sadler, J.R., (1961). The Metabolism of C2-Compounds in Microorganisms. Biochem J *81*, 503-513.

Kozaki, A., and Takeba, G. (1996). Photorespiration protects C_3 plants from photooxidation. Nature *384*, 557-560.

Ku, M. S., Agarie, S., Nomura, M., Fukayama, H., Tsuchida, H., Ono, K., Hirose, S., Toki, S., Miyao, M., and Matsuoka, M. (1999). High-level expression of maize phosphoenolpyruvate carboxylase in transgenic rice plants. Nat Biotechnol *17*, 76-80.

Ku, M. S., Kano-Murakami, Y., and Matsuoka, M. (1996). Evolution and expression of C_4 photosynthesis genes. Plant Physiol *111*, 949-957.

Laemmli, U. K. (1970). Cleavage of structural proteins during the assembly of the head of bacteriophage T4. Nature *227*, 680-685.

Leegood, R. C. (1997). The regulation of C_4 photosynthesis. Adv Bot Res *26*, 251-316.

Leegood, R. C. (2002). C_4 photosynthesis: principles of CO_2 concentration and prospects for its introduction into C_3 plants. J Exp Bot *53*, 581-590.

Leegood, R. C., Lea, P. J., Adcock, M. D., and Häusler, R. E. (1995). The regulation and control of photorespiration. J Exp Bot *46*, 1397-1414.

Lord, J. M. (1972). Glycolate oxidoreductase in *Escherichia coli*. Biochim Biophys Acta *267*, 227-237.

Maliga, P., Sz-Breznovits, A., and Marton, L. (1973). Streptomycin-resistant plants from callus culture of haploid tobacco. Nature New Biol *244*, 29-30.

Maroco, J. P., Ku, M. S. B., and Edwards, G. E. (2000). Utilization of O_2 in the metabolic optimization of C_4 photosynthesis. Plant Cell Env *23*, 115-121.

Matsuoka, M., Furbank, R. T., Fukayama, H., and Miyao, M. (2001). Molecular engineering of C_4 photosynthesis. Annu Rev Plant Physiol Plant Mol Biol *52*, 297-314.

Meuer, S., Wittwer, K., and Nakagawara, K. (2001). Rapid Cycler Real-Time PCR. Methods and applications Springer -Berlin, Heidelberg.

Migge, A., Carryol, E., Kunz, C., Hirel, B., Foch, H., and Becker, T. (1997). Expression of the tobacco genes encoding plastidic glutamamine synthetase or ferrodoxin- dependent glutamate synthetase doesn't depend on the rate of nitrate reduction and is unaffected by suppression of photorespiration. J Exp Bot *48*, 1175-1184.

Miller, J. H. (1972). Experiments in Molecular Genetics (New York, Cold Spring Harbor Laboratory Press).

Nelson, E. B., and Tolbert, N. E. (1970). Glycolate dehydrogenase in green algae. Arch Biochem Biophys *141*, 102-110.

Nelson, T., and Langdale, J. A. (1992). Developmental genetics of C_4 photosynthesis. Annu Rev Plant Physiol Plant Mol Biol *43*, 25-47.

Normile, D. (1999). Genetic engineers aim to soup up crop photosynthesis. Science *283*, 314-316.

Ogren, W. L. (1984). Photorespiration pathways regulation and modification. Annu Rev Plant Physiol *35*, 415-442.

Osmond, B., Badger, M., Maxwell, K., Björkman, O., and Leegood, R. C. (1997). Too many photons: Photorespiration, photoinhibition and photooxidation. Trends Plant Sci *4*, 119-123.

Padidam, M., and Cao, Y. (2001). Elimination of transcriptional interference between tandem genes in plant cells. Biotechniques *31*, 328-330.

Pellicer, M. T., Badia, J., Aguilar, J., and Baldoma, L. (1996). *glc* locus of *Escherichia coli*: characterization of genes encoding the subunits of glycolate oxidase and the *glc* regulator protein. J Bacteriol *178*, 2051-2059.

Rademacher, T., Häusler, R. E., Hirsch, H. J., Zhang, L., Lipka, V., Weier, D., Kreuzaler, F., and Peterhänsel, C. (2002). An engineered phosphoenolpyruvate carboxylase redirects carbon and nitrogen flow in transgenic potato plants. Plant J *32*, 25-39.

Reiskind, J. B., Madsen, T. V., Van Ginkel, L. C., and Bowes, G. (1997). Evidence that inducible C-4-type photosynthesis is a chloroplastic CO_2-concentrating mechanism in *Hydrilla*, a submersed monocot. Plant Cell Env *20*, 211-220.

Sage, R. F. (2001). Environmental and evolutionary preconditions for the origin and diversification of the C_4 photosynthetic syndrome. Plant Biol *3*, 202-213.

Saiki, R. K., Gelfand, D. H., Stoffel, S., Scharf, S. J., Higuchi, R., Horn, G. T., Mullis, K. B., and Erlich, H. A. (1988). Primer-directed enzymatic amplification of DNA with a thermostable DNA polymerase. Science *239*, 487-491.

Sambrook, J., and Russel, D. W. (2002). Molecular Cloning - A Laboratory Mannual, Vol 1-3, 3 edn Cold Spring Habour, New York, Cold Spring Habour Laboratory Press.

Sanger, F., Nicklen, S., and Coulson, A. R. (1977). DNA sequencing with chain-termination inhibitors. Proc Natl Acad Sci USA *74*, 5463-5467.

Sharkey, T. D. (2001). Photorespiration. Encyclopedia of Life Sciences, 1-5.

Sheen, J. (1999). C_4 gene expression. Annu Rev Plant Physiol Plant Mol Biol *50*, 187-217.

Small, I., Wintz, H., Akashi, K., and Mireau, H. (1998). Two birds with one stone: genes that encode products targeted to two or more compartments. Plant Mol Biol *38*, 265-277.

Somerville, C. R. (1984). The analysis of photosynthetic carbon dioxide fixation and photorespiration by mutant selection. Oxford Surveys of Plant Mol Cell Biol *1*, 103-131.

Somerville, C. R., and Ogren, W. L. (1982). Genetic modification of photorespiration. Trends Biochem Sci *7*, 171-174.

Stabenau, H. (1992). Evolution of peroxisomes in green algae. In Phylogenetic changes in peroxisomes of algae. Phylogeny of plant peroxisomes, (ed H Stabenau), pp 63-79 Oldenburg: University of Oldenburg.

Staub, J., and Maliga, P. (1993). Accumulation of D1 polypeptide in tobacco plastids is regulated via the untranslated region of the psbA mRNA. EMBO J *12*, 601-606.

Staub, J., and Maliga, P. (1995). Expression of a chimeric *uidA* gene indicates that polycistronic mRNAs are efficiently translated in tobacco plastids. Plant J *7*, 845-848.

Stockhaus, J., Schlue, U., Koczor, M., Chitty, J. A., Taylor, W. C., and Westhoff, P. (1997). The Promoter of the Gene Encoding the C_4 Form of Phosphoenolpyruvate Carboxylase Directs Mesophyll-Specific Expression in Transgenic C_4 *Flaveria spp*. Plant Cell *9*, 479-489.

Teramura, A. H., Sullivan, J. H., and Ziska, L. H. (1990). Interaction of elevated ultraviolet-B radiation and CO_2 on productivity and photosynthetic characteristics in wheat, rice and soybean. Plant Physiol *94*, 470-475.

Tolbert, N. E., Yamazaki, R. K., and Oeser, A. (1970). Localization and properties of hydroxypyruvate and glyoxylate reductases in spinach leaf particles. J Biol Chem *245*, 5129-5136.

van der Drift, C., and de Windt, F. E. (1983). Glyoxylate conversion by *Hyphomicrobium* species grown on allantoin as nitrogen source. Antonie Leeuwenhoek *49*, 167-172.

von Caemmerer, S., and Furbank, R. T. (1999). Modeling C_4 photosynthesis. In biology of C_4 photosynthesis (eds RF Sage and RK Monson), Academic press, New York, 173-211.

von Caemmerer, S., and Furbank, R. T. (2003). The C_4 pathway: an efficient CO_2 pump. Photosynth Res *77*, 191-207.

Voznesenskaya, E. V., Franceschi, V. R., Kiirats, O., Freitag, H., and Edwards, G. E. (2001). Kranz anatomy is not essential for terrestrial C_4 plant photosynthesis. Nature *414*, 543-546.

Walker, R., Acheson, R., Técsi, L., and Leegood, R. (1997). Phosphoenolpyruvate carboxylase in C_4 plants, its role and regulation. Aust J Plant Physiol *24*.

Wilson, T. (1993). Strategies to protect crop plants against viruses: pathogen-derived resistance blossoms. Proc Natl Acad Sci USA *90*, 3134-3141.

Winkler, U., and Stabenau, H. (1992). Metabolism of glycolate in mitochondria and peroxisomes of green algae. In Phylogenetic changes in peroxisomes of algae Phylogeny of plant peroxisomes, (ed H Stabenau), pp 80-91 Oldenburg: University of Oldenburg.

Yokota, A., Haga, S., and Kitaoka, S. (1985a). Purification and some properties of glyoxylate reductase (NADP+) and its functional location in mitochondria in *Euglena gracilis Z.* Biochem J *227*, 211-216.

Yokota, A., and Kitaoka, S. (1979). Occurrence and operation of the glycollate-glyoxylate shuttle in mitochondria of *Euglena gracilis Z.* Biochem J *184*, 189-192.

Yokota, A., Kitaoka, S., Miura, K., and Wadano, A. (1985b). Reactivity of glyoxylate with hydrogen perioxide and simulation of the glycolate pathway of C_3 plants and Euglena. Planta *165*, 59-67.

Zelitch, I. (1989). Selection and characterization of tobacco plants with novel O_2-resistant photosynthesis. Plant Physiol *90*, 1457-1464.

Zhu, X.-G., Portis, A. R., and Long, S. P. (2004). Would transformation of C_3 crop plants with foreign Rubisco increase productivity? A computational analysis extrapolating from kinetic properties to canopy photosynthesis. Plant Cell Env *27*, 155-165.

8 ACKNOWLEDGEMENTS.

Firstly, I thank Professor Dr. Fritz M. Kreuzaler for availing me an opportunity to work as a student in his laboratory. I am also very thankful for his friendship and hospitality. I am greatly indebted to my supervisor Dr. Christoph Peterhänsel for his unlimited dedication and commitment towards this work. The critical reading, discussion and correction of this manuscript by him made it possible for me to present this manuscript in its present form.

I am also grateful to Professor Dr. U. Priefer for her readiness to be the second advisor of this thesis.

I also take this opportunity to thank Sonja for her skillful technical assistance. Special thanks to Silke, Rainer, Markus, Sascha, and Rashad for their friendship and help during this work.

I would wish to express my special thanks to Dr. H. J. Hirsch, Peter, Sabine, Teresa, Tanja, Krisna, Anna and other members of Botany Institute for their kindness and cooperation.

Many thanks also to Prof. Dr. Ralph Bock and Dr. Stephanie Ruf for their excellent support on chloroplast transformation and to Dr. Maria Pellicer for providing me with bacterial strains. Dr. Thomas Rademacher kindly helped me during my work on the confocal laser microscope. Dr. Nikolaus Schlaich and Nicolas Sauerbrunn introduced me into the art of *Arabidopsis* cultivation. Dr. Veronica Maurino worked out chloroplast import assays with *At*GDH that helped me a lot to understand the possible localization of this protein.

Declaration / Erklärung

Herewith I declare that I have written this PhD thesis myself, using only the referenced literature.

Hiermit versichere ich, dass ich die vorliegende Doktorarbeit selbstständig verfasst und keine anderen als die angebenen Hilfsmittel und Quellen verwendet habe.

Aachen, February 2004

Curriculum vitae

PERSONAL PROFILE:

Full Name	:	**Md.Rafijul Bari**
First Name	:	**Rafijul**
Family Name	:	**Bari**
Father's Name	:	**A.K.M Safiul Bari**
Date of Birth	:	**06.02.1971**
Gender	:	**Male**
Nationality	:	**Bangladeshi**

ACADEMICS:

Years	**Degrees obtained**	**Name of the Institutes**	**Grades obtained**	**Country**
2000-2004	Ph.D	RWTH Aachen University	yet to be completed	Germany
1998-2000	Master of Science (M.Sc) in Molecular Biology	Katholieke Universiteit Leuven (KUL)	A	Belgium
1988-1992	Bachelor of Science (B.Sc) in Agriculture	Bangladesh Agricultural University (BAU)	2nd class	Bangladesh
1986-1988	H.S.C	Govt. Bangla College	First division	Bangladesh
1980-1986	S.S.C	Alfadanga High School	First division	Bangladesh
1975-1980	Primary school	Deauli Primary School	None	Bagladesh